

# Approximating Blocking Rates in UMTS Radio Networks

Diplomarbeit

vorgelegt von Franziska Ryll

Matrikel-Nr.: 19 88 98

bei Prof. Dr. Martin Grötschel

*Technische Universität Berlin*  
*Fakultät II: Mathematik und Naturwissenschaften*  
*Institut für Mathematik*  
*Studiengang Wirtschaftsmathematik*

April 2006



Die selbständige und eigenhändige Anfertigung versichere ich an Eides statt.

Berlin, den 06.04.2006



# Acknowledgements

I am deeply grateful to Hans-Florian Geerdes for the productive support throughout my whole time at ZIB. Moreover, I thank Dr. Andreas Eisenblätter for his constructive advices. Both were good reviewers and gave helpful suggestions. I acknowledge the great working conditions at ZIB. In this connection, I am indebted to Prof. Dr. Martin Grötschel giving me the opportunity to develop my diploma thesis in such a professional surrounding. I thank Holger van Bargaen for supporting me in topics concerning the Central Limit Theorem. Furthermore, I am grateful to my family and Sören for their encouragement and support.



# Contents

<b>1</b>	<b>Introduction</b>	<b>1</b>
<b>2</b>	<b>Preliminaries</b>	<b>5</b>
2.1	Basics of Wireless Communications . . . . .	5
2.2	Cellular Mobile Radio Networks . . . . .	6
2.3	Radio Network Planning . . . . .	7
2.4	Specifics of UMTS . . . . .	8
2.4.1	CDMA . . . . .	8
2.4.2	Interference in CDMA Systems . . . . .	12
2.4.3	Blocking in UMTS . . . . .	14
2.5	General Mathematical Model . . . . .	15
2.5.1	Static View . . . . .	15
2.5.2	Input Data and Assumptions . . . . .	16
2.5.3	CIR Constraints and Blocking . . . . .	18
<b>3</b>	<b>Existing Methods</b>	<b>21</b>
3.1	System of Equations . . . . .	21
3.1.1	Snapshot Based Derivation . . . . .	22
3.1.2	Expected Coupling . . . . .	24
3.1.3	Approximating Blocking . . . . .	25
3.2	Monte Carlo Simulation . . . . .	27
3.3	Shortcomings . . . . .	28
<b>4</b>	<b>The Blocking Rate as Expected Value</b>	<b>31</b>
4.1	Constant User Load . . . . .	32
4.1.1	Preliminaries . . . . .	32
4.1.2	Uplink . . . . .	34
4.1.3	Downlink . . . . .	35
4.1.4	Extension . . . . .	38
4.2	Variable User Load . . . . .	40
4.2.1	Preliminaries . . . . .	40

---

4.2.2	Uplink . . . . .	40
4.2.3	Downlink . . . . .	42
4.3	The Effect of Coupling . . . . .	44
4.4	The Assumption of a Normal Distribution . . . . .	45
4.4.1	The Central Limit Theorem . . . . .	45
4.4.2	Transformation . . . . .	46
4.4.3	Proof . . . . .	48
4.4.4	Discussion . . . . .	53
<b>5</b>	<b>Power Knapsack</b>	<b>55</b>
5.1	Snapshot Based Derivation . . . . .	56
5.1.1	Downlink . . . . .	56
5.1.2	Uplink . . . . .	58
5.2	The Expected Power Knapsack . . . . .	60
5.2.1	Downlink . . . . .	61
5.2.2	Uplink . . . . .	62
<b>6</b>	<b>Comparison of both Methods</b>	<b>65</b>
6.1	Uplink . . . . .	65
6.2	Downlink . . . . .	66
<b>7</b>	<b>Computational Results</b>	<b>69</b>
7.1	Implementation . . . . .	69
7.2	Test Cases . . . . .	70
7.3	Validation . . . . .	71
7.3.1	One Cell . . . . .	71
7.3.2	Two Cells . . . . .	73
7.4	Results . . . . .	76
7.4.1	Running Time . . . . .	80
7.5	Conclusions . . . . .	82
<b>8</b>	<b>Summary and Outlook</b>	<b>85</b>
<b>A</b>	<b>Notation</b>	<b>87</b>
<b>B</b>	<b>Further Results</b>	<b>91</b>
<b>C</b>	<b>Zusammenfassung</b>	<b>111</b>
	<b>List of Figures</b>	<b>115</b>
	<b>Bibliography</b>	<b>118</b>

# 1 Introduction

The first nationwide mobile telecommunications system was installed in Germany in 1958. Until then, regional systems covered only small areas, like cities or communities, and a customer could not use his mobile radio unit in another region than his serving one [5]. Still in the beginning of the 1980s, mobile communications were not widespread because the fees and prices for terminal equipment were too high for many people. With the liberalization of the telecommunications market and the introduction of a unified standard for digital cellular mobile radio systems in 1992 [2], mobile communications developed to a mass market in the 1990s [22]. This introduced standard is called the *Global System for Mobile Communications* (GSM). GSM is said to belong to the second generation of mobile phone technology following the first generation of analog radio networks [5].

Although the transmission of data is possible in GSM besides speech telephony, the system is inadequate for various applications that require higher bit rates [22]. This is one reason why the *Universal Mobile Telecommunications System* (UMTS) was developed. UMTS is a third generation cellular mobile phone technology, which is deployed commercially in Germany since 2004 [24]. With UMTS, it is possible to transmit at variable data rates of up to 384 kbit/s [2]. This is 40 times faster than the connection speed GSM offers [23]. Therefore, a variety of new services is available like multimedia applications or video transmissions. Furthermore, UMTS systems are more resistant against failure than second generation radio networks. For example, connections break off less often when a mobile user moves.

The providers of mobile communications want to offer a system that covers a large area with high quality services and acceptable prices to their customers. For this reason, it is important to design efficient radio networks. One fundamental topic in radio network planning is the *capacity* of a radio network. Ideally, a sufficient amount of radio resources has to be provided for all users to establish a connection. However, in practice this is not always possible. Due to the limitation of radio resources a mobile user might not be served. The rejection of a customer who wants to establish a new connection

to the radio network is called *blocking*. One of the goals when designing a radio network is that the ratio of rejected mobiles – called the *blocking rate* – does not exceed a certain threshold.

In UMTS, the multi user access scheme *Code Division Multiple Access* (CDMA) is employed in the radio interface, the interface between the user and the radio network. Because of this technology, the capacity of the radio network is not fixed and therefore not known exactly during the planning phase. The capacity depends on the current interference situation in the radio network which in turn depends among others on the number and position of simultaneous mobiles and the kinds of services they use. For this reason, in the case of UMTS, we speak of “*soft capacity*” [5]. This special characteristic of UMTS systems makes it difficult to determine the maximum number of users the radio network is able to carry. Consequently, it turns out to be complicated to predict the average blocking rate of the radio network reliably.

Various methods have been proposed to assess the consumption of resources in a UMTS radio network, which must be known in order to determine the blocking rate of the system. There is a trade-off between accuracy and efficiency in all of these models. Their inadequacies led to the necessity of an improved method for the calculation of the blocking rate of a UMTS radio network. One such method is introduced in this diploma thesis.

The thesis develops and analyzes a model to efficiently approximate the average blocking rate of a UMTS radio network. In doing so, we consider a moment during the periods, when the average expected amount of traffic is highest. One such period is called the *busy hour*. The presented method is based on a stochastic estimation of the average interference in the system. With this model, it is possible to predict the average blocking rate of a configured radio network quickly during the planning phase. Shortcomings in the radio network design can thus be detected easily.

## Outline

Chapter 2 presents a short survey of UMTS and its radio technology. Among others, cellular radio networks are introduced, as well as the multi user access technique CDMA. Furthermore, blocking is discussed in more detail and the difficulties of assessing the blocking rate of UMTS radio networks are described. A common mathematical model is given that represents a UMTS radio network in a static way. All these topics are summarized from comprehensive literature studies.

In Chapter 3, established methods to determine the average blocking rate of a UMTS radio network are introduced. In one approach, a system of equations is set up to compute the average blocking rate. This approach can

---

be used in two ways. One way of using this method is very time consuming while the other one leads to unacceptable estimation errors. The extensive version is a numerical method known as *Monte Carlo simulation*. The basic principle of this popular method is explained briefly. The inadequacies of these approaches are the motivation to propose another model that reduces their shortcomings.

The next three chapters cover a new method to approximate the blocking rate of a UMTS radio network. This method is based on the expected coupling approach presented in the preceding chapter. The new model is introduced in two different ways in Chapter 4 and in Chapter 5. In both cases, the expected value of the average blocking rate is computed. In doing so, the interference of other radio cells is estimated by constant values while the interference of the own radio cell is modeled stochastically. Chapter 6 shows analytically that the results of both approaches are equal.

The results of extensive computational tests are presented and analyzed in Chapter 7. These results are compared to outputs of Monte Carlo simulation. Finally, in Chapter 8, a summary of the entire thesis and an outlook are given.



## 2 Preliminaries

This chapter introduces necessary preliminaries for this thesis brought together from several literary sources. A short overview of the technical basics of general cellular radio networks is given as well as the specifics of the UMTS technology. Moreover, a common mathematical model for the explained features is shown.

The chapter is organized as follows. First, some basics of wireless communications are mentioned. Then, characteristics of cellular radio networks are pointed out. At the same time, basic notation is introduced. Afterwards, the tasks and purposes of radio network planning are highlighted. In the next section, the particularities of UMTS are discussed. We deal with the access scheme CDMA and the consequences for the system caused by this technology. Furthermore, the resulting difficulties for the computation of the blocking rate are revealed. Finally, a static mathematical model which is the basis for the considerations in this thesis is given. Whenever we use the term “network” throughout this thesis, a radio network is actually meant.

### 2.1 Basics of Wireless Communications

A communications system conveys messages. These messages originate in an information source and are transmitted to a destination. Basically, there are three components in the communications pipe: the *transmitter*, the *channel* and the *receiver* [12], as shown in Figure 2.1. The transmitter and the receiver are distant of each other. The physical manifestation of a message is a *signal* [14].

The transmitter adapts the signal of the information source such that it can be transmitted over the channel. In wireless communications systems, the transmission medium delivering the signal from the transmitter to the receiver is a *radio channel*. During transmission in space, the channel is impaired by *interference* and *noise*. Interference originates from other sources occupying the same frequency band. Noise is generated by electronic devices

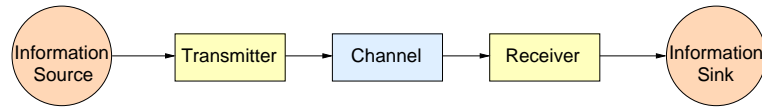


Figure 2.1: Block diagram of a communications system, based on [12, p. 4]

at the receiver. Finally, the receiver creates an estimate of the original signal out of the received information-bearing signal. An exact reproduction is not possible because of the mentioned influences on the radio channel (cf. [12]).

The frequency range occupied by the energy of a signal is denoted by the *bandwidth* of the signal. The bandwidth of the communications system is the frequency range the radio channel is able to transmit. The *power spectrum* of a signal describes the distribution of the signal's power along the digital frequency range [14]. The power spectrum can be understood as a function of frequency. Then the integral over the entire bandwidth represents the average power of the signal [12]. The power of *narrowband* signals is concentrated on a relative small bandwidth. In contrast, *wideband* signals have a wide bandwidth.

## 2.2 Cellular Mobile Radio Networks

A cellular radio network consists of a set of *base stations* which are set up in the terrain. At each base station, one or more *antennas* are installed. The electromagnetic signals they emit are conveyed in space and are attenuated on their way to the receiver. The complete attenuation on the radio channel is called *path loss*. The higher the distance from the transmitter is, the weaker is the power of the receiving signal at a specific position. However, this power has to be sufficiently high in order to establish a connection to the radio network. Because the maximum power of an antenna is restricted this leads to a regional confinement of the radio signal range. The complete area is divided into so-called *cells* or *sectors* (cf. [2]). Users (*mobile stations*) in one sector are served by a certain base station antenna. This is usually the one that provides the strongest signal in this region. This antenna is called the *best server*. Mostly, cells are coherent areas which overlap partly [22]. In Figure 2.2, the cellular structure of a UMTS radio network is shown. Besides the cells, the figure depicts the locations where the antennas could be set up (red points) and the installed antennas (black arrows).

Cellular systems for mobile telecommunications are organized centrally.

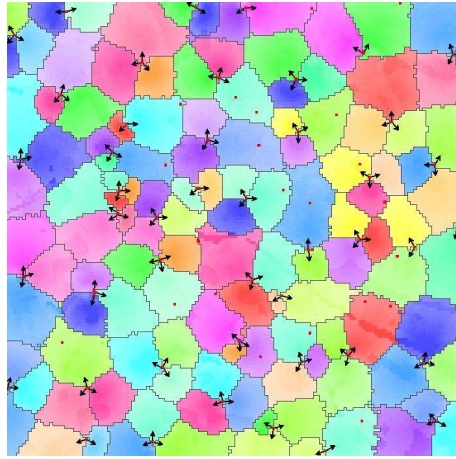


Figure 2.2: Cells in a UMTS radio network

That is, users are not linked directly to each other but to central radio stations [5]. These connections can be seen as point-to-point connections [12]. Links of a base station antenna to exactly one mobile are denoted by *dedicated channels*. In contrast, *common channels* are used by all mobiles of one cell [2]. There are two directions of communication in radio networks. In the *downlink* direction, the base station antenna transmits signals to the mobile station. The reverse direction is called *uplink* (cf. [23]).

The *capacity* of a cell denotes the maximum number of users the associated antenna can serve without exceeding its available resources. If the capacity of an antenna is exhausted, users trying to establish a new connection are left unserved. They are *blocked*.

## 2.3 Radio Network Planning

The purpose of radio network planning is to create a radio network with good performance for the expected demand at low costs. There are various indicators to estimate the performance of a configured radio network. One such indicator is the quality of a service. Another important criterion is the size of the *coverage area*. This is the area where the signal can be received with sufficient strength to establish a connection. The *blocking rate* of a network also represents a measure for the performance of a network design. Usually, this value should lie below 2% in an acceptable radio network [23] such that high availability of good quality service is ensured (cf. [16]).

The problem of radio network planning occurs in different forms. In the so-called “*Green Field Planning*”, a complete radio network shall be designed from scratch. Nowadays, this is not relevant practically since base stations and antennas are already installed in large regions. More interesting are the problems of *Site Selection* and *Network Tuning*. In the first one, a subset of existing sites is chosen where UMTS antennas are set up. In the second task, the quality of an existing radio network shall be improved by changing the configuration of the antennas, e. g. their height, their azimuth angle in the horizontal plane or their tilt angle in the vertical plane.

As much users as possible shall be provided with high quality services. At the same time, the arising expenses for the deployment and maintenance of the network shall be as low as possible. That is, with a minimum amount of radio resources the network design which handles the expected traffic best in terms of the given requirements shall be conceived. In order to solve this problem several optimization models are proposed. In [6] for example, an approach for optimizing antenna tilts is introduced. With the method presented in this thesis for quickly assessing the blocking rate of a UMTS radio network, it is possible to refine such models. One could, e. g. insert an additional constraint concerning the maximum allowed blocking rate of the cells in order to improve the quality of the results.

## 2.4 Specifics of UMTS

This section describes the specific particularities of UMTS radio networks. Due to its new access scheme, called *CDMA*, interference plays a major role in the design of UMTS radio networks. This in turn leads to problems when assessing the blocking rates of the cells in the network. These topics are handled successively in the following.

### 2.4.1 CDMA

In mobile communications systems, all mobiles in a sector use a common physical resource to transmit and receive signals. This transmitting medium is a frequency band in the radio spectrum [16]. The simultaneous access of all users to it (*multi-user access*) has to be controlled in order to avoid a loss of information [5].

In the technology GSM, users are separated by *Frequency Division Multiple Access* (FDMA) and *Time Division Multiple Access* (TDMA). In FDMA systems, the available spectrum is subdivided into several frequency bands which are used simultaneously. Each band can be interpreted as a physical

channel which is assigned to exactly one user. TDMA means that a frequency channel is split up into disjoint time slots. In doing so, every mobile conveys signals in different periods of time (cf. [22]).

The access technique used in UMTS is *Code Division Multiple Access* (CDMA). In contrast to FDMA and TDMA, the complete frequency band is available for the total duration of the connection to every mobile. Due to the simultaneous use of the radio spectrum by all mobiles, various signals arrive at the receiver. From those, it has to separate the desired one. This is done by assigning a unique code sequence to each link (cf. [22, 23]). Figure 2.3 visualizes the operating mode of this access technique.

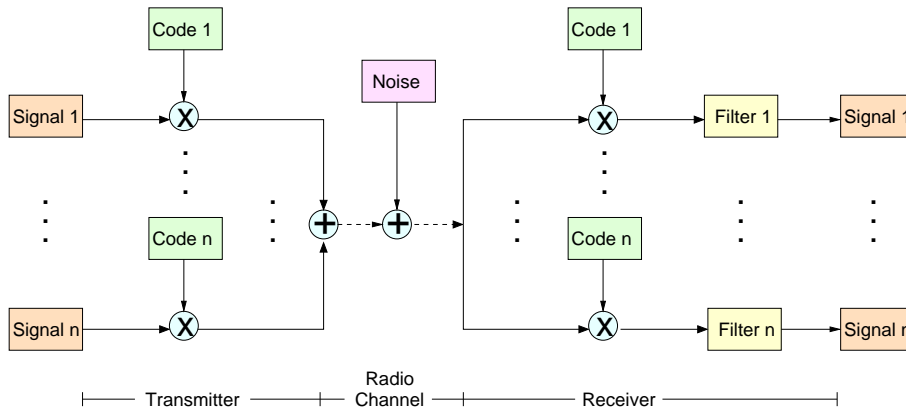


Figure 2.3: Operating mode of Code Division Multiplex

Besides separation between the links, the code sequences are used to spread the narrowband radio signals to wideband signals for the transmission across the wireless channel. That is, the energy which was concentrated on a narrow frequency range is then spread to a wider bandwidth. For this reason, CDMA systems are commonly called *spread spectrum* systems. The spread spectrum technique deployed in UMTS is *Direct Sequence-CDMA* (DS-CDMA). That is, the user data stream is multiplied by a specific code sequence whose bit rate is by a multiple higher than the user bit rate. In doing so, the resulting bit sequence has a higher bandwidth and a lower power spectrum than the original stream. The signal is said to be *spread*. Figure 2.4 illustrates the spreading operation.

At the receiver, the arriving data stream contains additionally spread bit sequences from other users and other interfering signals. This stream is multiplied with exactly the same code sequence used in the spreading operation. This *despreading* process restores the lower bandwidth and the higher power

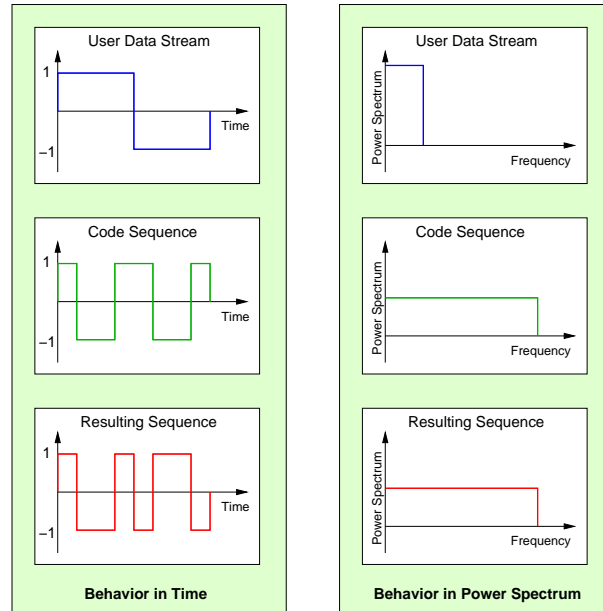


Figure 2.4: Wideband spreading, based on [5, p. 221]

spectrum of the original user bit stream. At the same time, the power spectrum of interfering narrowband signals, such as thermal noise, is decreased because they are spread now. Narrowband means that the bandwidth is significantly smaller than that of the spread user signal. The wideband signals from other users remain wideband, and thus their power spectrum remains low. Hence, the power spectrum of the desired signal is increased relative to the power spectrum of the interfering signals. Afterwards, the resulting product is filtered with a filter adapted to the current signal [2]. The whole operation at the receiver in case of narrowband interference is depicted in Figure 2.5.

The property of CDMA to reduce interferences, especially those originating from other simultaneously proceeding calls, is fundamental in order to reuse the available frequencies over geographically close distances. Ideally, the codes of the different users are perfectly orthogonal such that they are independent and the different physical channels do not disturb each other. A more detailed description of code spreading can be found in [5, 23, 13].

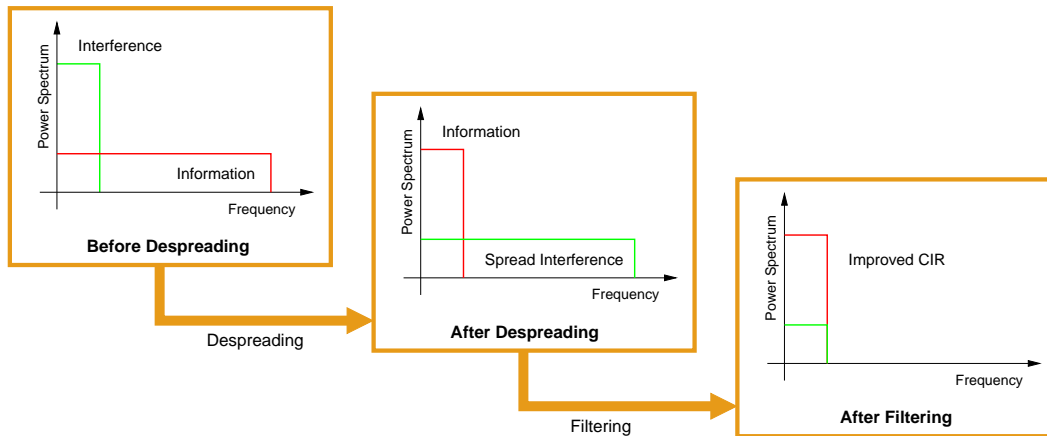


Figure 2.5: Interference attenuation in CDMA, based on [5, p. 222]

## WCDMA

The most widely adopted radio interface for third generation systems is *WCDMA* (Wideband-DS-CDMA). This radio interface is used in UMTS in Europe and Asia. In WCDMA, the bandwidth is around 5 MHz (cf. [13]). In the uplink direction, the spreading codes of different mobiles are quasi-orthogonal. That is, the disturbances from other physical channels do not disappear but are very small. In the downlink, the code sequences that a base station antenna uses to convey messages to its associated mobiles are perfectly orthogonal if the sequences belong to the same code family. However, this property is partly lost due to reflection and scattering of the radio waves on their way to the receiver. The codes of different cells are quasi-orthogonal (cf. [23]).

In UMTS radio networks, each base station antenna emits a special signal with constant power, called *pilot signal*. A mobile station connects to that antenna from which it receives the strongest pilot signal [6]. Since several base stations are using the same frequency band in WCDMA systems, it is possible that one mobile is connected to up to three serving antennas at a time if the received radio signals offer a comparable strength. The received information from each physical channel are combined appropriately. This usually happens when the user is located at the border or overlapping area between some cells. Then besides the connection to the best server, a connection to one or more neighboring base station antennas is established. The mobile is said to be in *soft handover* in this moment. If this feature was

not available, the mobile station at the cell border would have to transmit and receive at high power because of the large distance to the base station. This would cause a high amount of interference to the associated cell as well as to the neighboring ones. Thus, the link quality in these sectors would be downgraded (cf. Section 2.4.2). Due to the additional link(s), the transmit powers of both, the mobile and the best server, can be decreased. Hence, the arising interference is weakened. Moreover, the probability of the connection being interrupted when the user moves between the cells is almost eliminated (cf. [23, 5]).

### 2.4.2 Interference in CDMA Systems

Interference is received power from other transmitters than the desired one that radiate energy in the same frequency band. That is, interference is an unmeant contribution to the received power that complicates the detection of the desired signal (cf. [23]). The higher the amount of interference is, the more difficult is it to filter out the desired radio signal properly.

In CDMA systems, all mobiles in one cell use the same frequency spectrum simultaneously as described in Section 2.4.1. Hence, they cause interference, denoted by *intra-cell interference*. Furthermore, the same frequency channels are available to several base station antennas in the network [5]. Therefore, all mobiles from those cells use the same frequency band at the same time, too. These impairments originating from other sectors are called *inter-cell interference*. Consequently, there is a high amount of interference in radio networks using the CDMA technology. In the uplink direction, the signals from other mobile stations overlay the own radio waves. In the downlink, interference is produced by other base stations [23]. Both directions do not interfere because either two different frequency bands are used (*FDD: Frequency Division Duplex*) or receiving and transmitting happen at different moments in time (*TDD: Time Division Duplex*) [22].

The strength of the interfering signals depends among others on the distance between receiver and disturbing transmitter due to the propagation characteristics of radio waves. That is, the spatial constellation between the users influences the amount of interference each link receives. Typically, the interferers in the own cell are located much closer than those of other sectors. For this reason, the power of the intra-cell interference is usually higher than that of the inter-cell interference. Another influence on the strength of the interfering signal is the power with which the disturber transmits data (cf. [23]).

Every kind of interference causes a modification of the radio signal during propagation. Possibly, this could lead to an incorrect detection at the

receiver. The stronger the wanted signal  $C$  (carrier) and the smaller the interference power  $I$ , the lower is the error rate. Therefore, the *Carrier to Interference Ratio (CIR)*  $C/I$  must exceed a specific threshold, called the *CIR target*. The following inequality must hold:

$$\frac{\text{Strength of Desired Signal}}{\sum \text{Strength of Interfering Signals} + \text{Noise}} \geq \text{CIR target.} \quad (2.1)$$

Besides the interference caused by the system, there are natural impairments like the thermal noise at the receiver, which is always present (cf. [23]). Also emissions of other external sources like radars or industrial equipment have to be considered [16]. The influence of such factors is included in the term “Noise” in the inequality.

For the required CIR target to be maintained in spite of the high amount of disturbance, interference control is crucial in UMTS radio networks. A receiver is able to tolerate a specific maximum level of interference power to which each user contributes [2]. If this level is exceeded the desired signal is buried among the interfering signals after despreading. For this reason, a complex *power control* is applied to dedicated links in UMTS radio networks. The power control minimizes the interference in the system by adjusting the transmission powers as low as possible. On the other hand, it ensures an adequate signal quality at the receiver according to the CIR target (cf. [16]). If the interference situation in the network changes the CIR target has to be adapted to the actual circumstances by the power control mechanisms [5]. Furthermore, the power control equalizes signal variation due to dynamical phenomena called *shadowing* and *fading*.

In UMTS systems, many users share the same frequency spectrum simultaneously. Therefore, the value of the CIR at the receiver is smaller than one since the power of the desired signal is usually weaker than the sum of the powers of the other signals [23]. The CIR target is also much smaller than one. Due to the ability of CDMA systems to appreciably reduce the interference power proportional to the power of the desired signal (cf. Section 2.4.1), the required power density is higher than the interference power density after despreading. In UMTS radio networks, the signal power can thus be lower than the power of the interference and the receiver can still detect the desired signal.

The CIR target depends mainly on the requested service. A higher threshold has to be achieved when it is transmitted at a higher data rate [23]. Moreover, the user’s velocity influences the CIR target. The faster he moves the faster changes the fading situation of its link. For high speeds, the variances are too fast to be made up by power control. In order to guarantee the quality of a connection even in this case, the CIR target to meet is higher.

Since uplink and downlink are usually asymmetrically loaded [16], the target values for uplink and downlink differ.

### 2.4.3 Blocking in UMTS

If all channels in the radio network are occupied it is impossible to establish a connection. In this situation, a new arriving call would be refused or *blocked*. In UMTS radio networks, the *admission control* handles all new incoming traffic. This control admits a new request to the system only if this would not overload the network and if the necessary resources are available. The admission control belongs to a variety of functions which ensure that the radio interface load does not exceed predefined thresholds. They are grouped under the so-called *congestion control* which in turn belongs to the *Radio Resource Management*. Besides admission control, the congestion control contains the *load control* which is responsible to bring the system into a feasible situation when it is overloaded. The Radio Resource Management includes among others the power control as well as the handover control (cf. [16]).

The capacity of a CDMA cell mainly depends on the orthogonality and number of the used spreading codes. When having perfectly orthogonal code sequences the different dedicated channels do not influence each other. In this case, the capacity of a sector is determined by the number of orthogonal codes. However, as pointed out in Section 2.4.1, the codes are *not* perfectly orthogonal in UMTS radio networks. For this reason, interference is the factor determining the capacity of a UMTS cell. UMTS networks are said to be interference limited (cf. [23]). Every new accepted link – in the whole network as well as in one arbitrary cell – causes a degradation of the quality of all other existent connections in the same frequency band since each CIR decreases. In the case that one CIR drops below the according CIR target, power control triggers the appropriate transmitter to raise its emitted energy. This in turn increases the interference power on all other connections in the frequency band which possibly causes other transmitters to emit with more power and so on (cf. [5]). The transmission and reception powers of the base station antennas are limited due to the installed hardware. If the available radio resources are exhausted, no more users can be served. Then new requests are rejected.

When a user tries to establish a completely new connection to the radio network and is refused by a base station antenna due to the explained reasons, he is *blocked*. A similar situation appears if an active mobile moves from one cell to another one having no radio resources available. Then it may happen that the connection is broken off. We speak of a *dropped call*. Since often users estimate such an experience more negative than a blocked request some

channels are reserved especially for handover by the radio network operators (cf. [23]). Therefore, we will not consider dropped calls in this diploma thesis.

Besides rejecting new arrivals it is possible that the link quality for some mobiles of circuit-switched services is downgraded. Circuit-switched services are real-time traffic services like speech telephony or video transmissions. In contrast, packet-switched services are services which can be carried out delayed such as sending e-mails. Furthermore, it may happen that a desired link is blocked even though there are radio resources available in order to guarantee the quality of the entire system [5]. In this diploma thesis, we address blocking only in the case of exceeded cell powers leading to a rejected user request.

In second generation mobile communications systems like GSM, the capacity of a cell can be specified during the planning phase. The common use of the frequency band is controlled by assigning a specific frequency channel and time slot to each user (cf. Section 2.4.1). To every base station antenna, a certain number of channels and slots is associated. From that, the maximum number of simultaneous links can be derived. If a new arrival finds them all occupied, then it is blocked (cf. [5]). In UMTS radio networks, the number of simultaneous users is restricted by their mutual interference at the receiver [22]. In contrast to second generation cellular systems, each cell has a varying capacity which mainly depends on the current interference situation. Therefore, it is called *soft capacity* [5]. The difficulty is that it is not known exactly beforehand but can only be estimated. Thus, the capacity in CDMA systems is not deterministic but a stochastic value.

## 2.5 General Mathematical Model

In the current section, we set up a mathematical model of a UMTS radio network. The presented approach is the basis for the further considerations in this thesis. First, we briefly explain the essential simplifications of the generated model compared to a UMTS radio network in reality. Afterwards, the input data is explained as well as the central assumptions. Finally, formulas for the CIR targets and powers of the antennas are derived.

### 2.5.1 Static View

The proposed model is an abstraction of the real processes in a UMTS radio network. That is, the properties of the modeled system are covered which are essential for our purpose while other features are ignored. In this manner, the complexity of the original system is reduced in order to be able to better

understand and analyze it. Nevertheless, the represented properties have to be modeled as precise as necessary to obtain reasonable study results which can be applied to the original system. Hence, a trade-off between accuracy and simplicity has to be found.

Actually, a UMTS radio network is a *dynamic* system. That is, the state of the network changes steadily. Due to moving mobiles and successively incoming service requests the interference situation varies in the complete network. The power control effects the transmit powers to change according to the new CIR targets, which can be updated every 10 ms [2]. Other dynamic features are, e. g. the handovers of the existent links from one cell to another [16] or blocking as explained in Section 2.4.3.

However, we consider this dynamic radio network in a *static* way. That is, users are located at fixed positions instead of moving in the area. The different arriving times of the requests are not taken into account, rather the whole traffic demand is present at once. Furthermore, the changing CIR targets at a receiver are modeled each by one constant, average value. The same applies to the interference in the radio network and the transmission and reception powers. Consequently, we just consider the UMTS radio network at one instance in time. Moreover, we ignore the possibility of soft handover and assume, that each mobile station is linked to exactly one antenna, namely the one with the strongest pilot signal.

## 2.5.2 Input Data and Assumptions

We consider a *planning area*  $A \neq \emptyset$ . This region is embedded into the two dimensional plane for a fixed height or into the three dimensional space with variable heights for each point. The dimension of the area is denoted by  $d \in \{2, 3\}$ . In order to discretize the planning region, it is subdivided into a finite set of *pixels*. Each pixel marks a  $d$ -dimensional location in the area. In the planning area  $A$ , a UMTS radio network with a set  $\mathcal{N}$  of antennas is installed. The best server area of an antenna  $i \in \mathcal{N}$  is denoted by  $A_i \subset A$ . The users in the network are represented by a set  $\mathcal{M}$  of mobile stations. The set  $\mathcal{M}_i \subset \mathcal{M}$  denotes the users served by antenna  $i \in \mathcal{N}$ . Furthermore, a set  $S$  of available services is considered. All these sets are finite. Their cardinality is a natural number, that is,  $|A| \in \mathbb{N}$ ,  $|\mathcal{N}| \in \mathbb{N}$ ,  $|\mathcal{M}| \in \mathbb{N}$  and  $|S| \in \mathbb{N}$ .

The mobile users  $\mathcal{M}$  are given by a *traffic snapshot*. This is a static realization of the average user demand obtained on basis of spatial average traffic load distributions. A traffic snapshot gives detailed information on the position, mobility, and service of each user. The average spatial traffic distribution of a service  $s \in S$  is denoted by  $T_s : A \rightarrow \mathbb{R}_+$ . For a position

$p \in A$ ,  $T_s(p)$  is the average traffic intensity of the service  $s$  at one instance in time. Figure 2.6 illustrates the average spatial traffic distribution for one service.



Figure 2.6: Average traffic distribution for one service

The number of users and their locations is a random variable. It is a common assumption that the average user distribution in one pixel follows a Poisson distribution. In general, the Poisson distribution is a discrete probability distribution which “arises in a variety of situations in which it is desired to count the number of occurrences of some phenomenon in an interval of time or space” [20, p. 199]. Usually, the number of *possible* successes is large while the probability for *one* success is small [15]. Both features apply in our case. The pixels in the planning area are small compared to the size of the entire region. For this reason, the number of pixels is high while the average traffic intensity in one pixel is very low. The expected number of users in a pixel is always much smaller than one. Thus, the probability for one user being located at a pixel is low. Consequently, the Poisson distribution is an adequate characterization of the spatial user distribution.

The user intensities in non-overlapping areas are assumed to be independent. The sum of independent Poisson distributed random variables is again a Poisson distributed random variable whose parameter is the sum of the parameters of the original random variables [15]. Hence, for each sequence

$(A_n)_{n \in \mathbb{N}}$ ,  $A_n \subset A$ , of pairwise disjoint sets following equation applies:

$$T_s\left(\bigcup_n A_n\right) = \sum_n T_s(A_n). \quad (2.2)$$

Furthermore,  $T_s(\emptyset) = 0$  holds. These properties show that  $T_s$  is a measure on  $A$  [9]. Actually, it is a counting measure which maps to a region the expected number of users in it. This measure is finite, that is,  $T_s(A) < \infty$  since we only consider situations in which the traffic intensity in the entire planning area is finite.

We assume that the number of users for each service  $s \in S$  in a certain region  $\tilde{A} \subseteq A$  is proportional to the size of the region  $\lambda^d(\tilde{A})$ . The measure  $\lambda^d$  is the  $d$ -dimensional *Lebesgue-Measure*. We assume that there exists a user density  $f_s : A \rightarrow \mathbb{R}_+$  for each service  $s \in S$ . The expected number of users of service  $s$  in area  $\tilde{A}$  is thus expressed by

$$T_s(\tilde{A}) = \int_{p \in \tilde{A}} f_s(p) dp. \quad (2.3)$$

### 2.5.3 CIR Constraints and Blocking

At first, we derive the complete CIR constraints for the uplink and downlink direction. The average CIR targets for a mobile station  $m \in \mathcal{M}$  are denoted by  $\mu_m^\uparrow$  for uplink and  $\mu_m^\downarrow$  for downlink. Furthermore, there are *transmit activity factors*  $\alpha_m^\uparrow$  and  $\alpha_m^\downarrow$  for every mobile indicating the average ratio of time it is transmitting data on the radio channel. In speech conversations, for example, every user speaks on average 50% of the time. The CIR inequality has to be satisfied in active periods only. At other instances in time, there is no data transmission. For this reason, we assign a transmit activity factor of one to the desired mobile. We do not know if the signals of other users are currently in an active period or not. Therefore, we apply the transmit activity factors to the other signals in (2.1) in order to consider the *average* interference power. Finally,  $\gamma_{mi}^\uparrow$  in uplink and  $\gamma_{im}^\downarrow$  in downlink are the *attenuation factors* for mobile station  $m \in \mathcal{M}$  and base station antenna  $i \in \mathcal{N}$ . Apart from the path loss between the mobile and the antenna, additional losses and gains are included dependent on the cabling, hardware, and user equipment.

In the uplink direction, the transmission power of a mobile  $m \in \mathcal{M}$  is denoted by  $p_m^\uparrow$ . Then the strength of the desired signal at base station antenna  $i \in \mathcal{N}$  is  $\gamma_{mi}^\uparrow p_m^\uparrow$ . The received background noise at antenna  $i$  is marked by  $\eta_i$ . With these conventions, the basic CIR target inequality (2.1)

for the uplink transmission from mobile  $m$  to antenna  $i$  reads as:

$$\frac{\gamma_{mi}^\uparrow p_m^\uparrow}{\sum_{n \neq m} \gamma_{ni}^\uparrow \alpha_n^\uparrow p_n^\uparrow + \eta_i} \geq \mu_m^\uparrow. \quad (2.4)$$

Several base stations use the same frequency band (cf. Section 2.4.1). In this model, we assume that all base stations use the same frequency spectrum. Hence, *all* users in the area convey information in the same frequency band at the same time. All these transmissions are received with varying strength by each base station antenna. For mobile stations using another frequency band in reality, the attenuation factor is appropriately low. The *average total reception power* at antenna  $i \in \mathcal{N}$  is thus given by

$$\bar{p}_i^\uparrow := \sum_{m \in \mathcal{M}} \gamma_{mi}^\uparrow \alpha_m^\uparrow p_m^\uparrow + \eta_i. \quad (2.5)$$

As mentioned previously, it is not known for a link whether it is active or not. For this reason, we take the transmit activity factors of the mobiles into account and obtain the *average power*. Using the last equation, (2.4) simplifies to

$$\frac{\gamma_{mi}^\uparrow p_m^\uparrow}{\bar{p}_i^\uparrow - \gamma_{mi}^\uparrow \alpha_m^\uparrow p_m^\uparrow} \geq \mu_m^\uparrow. \quad (2.6)$$

In the downlink direction, the pilot and common channels are included, whose power we denote by  $p_i^{(c)}$  at base station antenna  $i \in \mathcal{N}$ . This value is assumed to be constant. Furthermore,  $p_{im}^\downarrow$  is the strength of the signal from antenna  $i$  to mobile  $m$  and  $\bar{\omega}_m \in [0, 1]$  is an environment dependent *orthogonality factor*. The signals an antenna transmits to its associated mobiles partly lose their orthogonality due to multipath propagation (cf. Section 2.4.1). If  $\bar{\omega}_m = 0$  holds, the signals are perfectly orthogonal and  $\bar{\omega}_m = 1$  means no orthogonality. The *average total transmission power* of antenna  $i$  is defined by

$$\bar{p}_i^\downarrow := \sum_{m \in \mathcal{M}_i} \alpha_m^\downarrow p_{im}^\downarrow + p_i^{(c)}. \quad (2.7)$$

We denote by  $\eta_m$  the noise at mobile  $m$ . Then the CIR constraint in downlink satisfies following inequality:

$$\frac{\gamma_{im}^\downarrow p_{im}^\downarrow}{\gamma_{im}^\downarrow \bar{\omega}_m (\bar{p}_i^\downarrow - \alpha_m^\downarrow p_{im}^\downarrow) + \sum_{j \neq i} \gamma_{jm}^\downarrow \bar{p}_j^\downarrow + \eta_m} \geq \mu_m^\downarrow. \quad (2.8)$$

The transmission power of a base station antenna is restricted. Typically, a UMTS antenna cannot emit more than 20 W. In addition, there are limits

on the average load of a cell. These load limits lie significantly below 100 % since it is important to have a buffer to compensate for dynamic effects. The *downlink load* is defined as the ratio of the current transmission power to the maximum possible output power. Usually, the limit of the downlink load lies at 70 %. The *uplink load* is given by  $1 - \frac{1}{\text{noise rise}}$ . The *noise rise* is the ratio of the total received power at a base station antenna to the noise power. The uplink load should not rise above 50 %. We denote by  $\Pi_i^{\max\downarrow}$  the maximum possible transmission power and by  $p_i^{\max\uparrow}$  and  $p_i^{\max\downarrow}$  the maximum allowed reception and transmission power of a base station antenna  $i \in \mathcal{N}$ . The latter can be derived by resolving

$$1 - \frac{\eta_i}{p_i^{\max\uparrow}} = \text{load limit}^\uparrow \quad \text{and} \quad \frac{p_i^{\max\downarrow}}{\Pi_i^{\max\downarrow}} = \text{load limit}^\downarrow.$$

Throughout this thesis, we mean with “maximum total power” the maximum allowed total power  $p_i^{\max\uparrow}$  and  $p_i^{\max\downarrow}$ , respectively.

The following inequalities express that on average all users in cell  $i$  are served and thus no blocking occurs:

$$\bar{p}_i^\uparrow \leq p_i^{\max\uparrow} \quad \text{and} \quad \bar{p}_i^\downarrow \leq p_i^{\max\downarrow}. \quad (2.9)$$

Using equations (2.5) and (2.7), this can be transformed into

$$\sum_{m \in \mathcal{M}} \gamma_{mi}^\uparrow \alpha_m^\uparrow p_m^\uparrow \leq p_i^{\max\uparrow} - \eta_i \quad \text{and} \quad \sum_{m \in \mathcal{M}_i} \alpha_m^\downarrow p_{im}^\downarrow \leq p_i^{\max\downarrow} - p_i^{(c)}. \quad (2.10)$$

## 3 Existing Methods

In this chapter, we discuss established methods to assess the average blocking rate of a base station antenna in a UMTS radio network. First, we introduce an approach to approximate the blocking rate based on a system of equations. This system can be set up for one traffic snapshot as described in the first part of the following section. In order to obtain statistically reliable results, such equation systems have to be solved for a large number of snapshots. Since the computational complexity of this procedure is too high to be applicable in some situations, the basic idea of this approach is generalized on the basis of average traffic load distributions. This idea is explained afterwards. This method speeds up calculation radically. In exchange, it causes a significant underestimation of the blocking rate of a cell in a region under around 5%. In the next section, the so-called *Monte Carlo simulation* on traffic snapshots is described briefly. This is a popular method but this approach is very extensive and time consuming. The snapshot based system of equations is also a Monte Carlo simulation. The last section summarizes the shortcomings of the formerly presented methods.

The notation can be found in Appendix A. Throughout this thesis, we assume perfect power control on dedicated channels. That is, the CIR targets are met at equality. Moreover, no user is in soft handover, and effects of shadow fading are neglected. Uplink and downlink are considered independently.

### 3.1 System of Equations

In this section, the ideas from [6] are introduced briefly. A system of equations is set up for uplink and downlink respectively describing the average transmission and reception powers of the antennas in the radio network. These results are then used to assess the blocking rate of each cell.

First, the equations are derived based on a traffic snapshot and then generalized on the basis of stochastic average load. Afterwards, we point

out how the blocking rate is calculated in both cases. This model is the basic principle of the method we develop in the next chapters. Throughout this thesis, the indices  $i$  and  $j$  will be used for base station antennas. The subscript  $i$  denotes the cell whose blocking rate we wish to determine. A vector with elements  $v_j$  is denoted in bold font  $\mathbf{v}$ . Moreover,  $\text{diag}(\mathbf{v})$  marks a diagonal matrix having the same dimension as  $\mathbf{v}$  and the components of  $\mathbf{v}$  on the main diagonal.

### 3.1.1 Snapshot Based Derivation

We consider a set  $\mathcal{M}$  of mobile stations given by a traffic snapshot. Following assumptions are made in this model for the time being:

- (i) limitations of transmission powers and noise rise are neglected and
- (ii) all users are served.

These restrictions are important for the derivation of the equations. Later, they will be abolished when blocking is modeled.

#### Uplink

In the uplink direction, we start from equation (2.5), which describes the average reception power of antenna  $i$ , written as

$$\bar{p}_i^\uparrow = \sum_{m \in \mathcal{M}_i} \gamma_{mi}^\uparrow \alpha_m^\uparrow p_m^\uparrow + \sum_{j \neq i} \sum_{m \in \mathcal{M}_j} \gamma_{mi}^\uparrow \alpha_m^\uparrow p_m^\uparrow + \eta_i. \quad (3.1)$$

In this way, it can be recognized that the total reception power at an antenna consists of three parts: one portion for the interference from the own and from the other cells respectively and the noise exterior to the system. For the uplink CIR target to be maintained by transmission from mobile station  $m \in \mathcal{M}$  to antenna  $i \in \mathcal{N}$ , inequality (2.6) must hold. As stated in the beginning, we assume that equality applies. When converting this equation properly and defining the *uplink user load* of a mobile  $m$  as

$$l_m^\uparrow := \frac{\alpha_m^\uparrow \mu_m^\uparrow}{1 + \alpha_m^\uparrow \mu_m^\uparrow}, \quad (3.2)$$

the *uplink coupling factors* result in

$$C_{ij}^\uparrow := \sum_{m \in \mathcal{M}_j} \frac{\gamma_{mi}^\uparrow}{\gamma_{mj}^\uparrow} l_m^\uparrow. \quad (3.3)$$

Consequently, with (3.1) and (3.3), the uplink transmission power of base station antenna  $i$  reads as

$$\bar{p}_i^\uparrow = C_{ii}^\uparrow \bar{p}_i^\uparrow + \sum_{j \neq i} C_{ij}^\uparrow \bar{p}_j^\uparrow + \eta_i. \quad (3.4)$$

We call the matrix

$$C^\uparrow := (C_{ij}^\uparrow)_{1 \leq i, j \leq |\mathcal{N}|}$$

the *uplink cell load coupling matrix* (uplink coupling matrix). The components of  $C^\uparrow$  can be interpreted in following way. The diagonal entry  $C_{ii}^\uparrow$  measures the contribution from the intra-cell interference to the total received power. The value  $C_{ij}^\uparrow$  scales the inter-cell interference contribution from antenna  $j \neq i$ . The desired system of equations arises from (3.4):

$$\bar{\mathbf{p}}^\uparrow = C^\uparrow \bar{\mathbf{p}}^\uparrow + \boldsymbol{\eta}^\uparrow. \quad (3.5)$$

The solution of this system is the vector with the uplink reception powers at each base station antenna.

## Downlink

The same approach is applied in the downlink case. The total average output power of base station antenna  $i \in \mathcal{N}$  is defined by (2.7). The CIR constraint is given by (2.8). Again, the assumption of perfect power control holds and the constraint is an equation. The *downlink user load* reads as

$$l_m^\downarrow := \frac{\alpha_m^\downarrow \mu_m^\downarrow}{1 + \bar{\omega}_m \alpha_m^\downarrow \mu_m^\downarrow}. \quad (3.6)$$

We use it to introduce the *downlink coupling factors*

$$C_{ii}^\downarrow := \sum_{m \in \mathcal{M}_i} \bar{\omega}_m l_m^\downarrow \quad \text{and} \quad C_{ij}^\downarrow := \sum_{m \in \mathcal{M}_i} \frac{\gamma_{jm}^\downarrow}{\gamma_{im}^\downarrow} l_m^\downarrow \quad (j \neq i) \quad (3.7)$$

for antennas  $i$  and  $j$ , as well as the *traffic noise power* of sector  $i$

$$p_i^{(\eta)} := \sum_{m \in \mathcal{M}_i} \frac{\eta_m}{\gamma_{im}^\downarrow} l_m^\downarrow. \quad (3.8)$$

The meaning of the coupling factors  $C_{ij}^\downarrow$  is the following. The diagonal entry  $C_{ii}^\downarrow$  represents the contribution from the intra-cell interference to the total transmission power. The value  $C_{ij}^\downarrow$  specifies the portion of transmission power

allocated on overcoming the inter-cell interference from antenna  $j \neq i$ . The item  $p_i^{(\eta)}$  expresses the fraction of transmission power spent on overcoming the noise at the mobiles if there was no intra-system interference. For the transmission power at antenna  $i$  we obtain

$$\bar{p}_i^\downarrow = C_{ii}^\downarrow \bar{p}_i^\downarrow + \sum_{j \neq i} C_{ij}^\downarrow \bar{p}_j^\downarrow + p_i^{(\eta)} + p_i^{(c)}. \quad (3.9)$$

The matrix

$$C^\downarrow := (C_{ij}^\downarrow)_{1 \leq i, j \leq |\mathcal{N}|}$$

is called the *downlink cell load coupling matrix* (downlink coupling matrix). Equation (3.9) for each base station antenna yields the following system of equations

$$\bar{\mathbf{p}}^\downarrow = C^\downarrow \bar{\mathbf{p}}^\downarrow + \mathbf{p}^{(\eta)} + \mathbf{p}^{(c)}. \quad (3.10)$$

The solution of this system is the downlink transmission power for every cell.

### 3.1.2 Expected Coupling

The coupling matrices  $C^\uparrow$  and  $C^\downarrow$  are stochastic. They depend on the positions and services of the active mobiles. We assume the user distribution in the planning area to be known (cf. Section 2.5.2). The matrix entries defined in (3.3) and (3.7) are linear compositions. For this reasons, it is possible to determine the expected values of the load coupling matrices, denoted by  $\bar{C}^\uparrow$  and  $\bar{C}^\downarrow$ . Then, the equation systems (3.5) and (3.10) can be set up with these expected values.

For a clearer presentation, it is implied, that we have representative CIR targets  $\mu_s^\uparrow$ ,  $\mu_s^\downarrow$  and transmit activity factors  $\alpha_s^\uparrow$ ,  $\alpha_s^\downarrow$  in both directions for each service  $s \in S$ . Furthermore,  $\eta_p$  is the noise and  $\bar{\omega}_p$  the orthogonality factor at a mobile in position  $p$ . The attenuation factors between a base station antenna  $i$  and a user located in  $p$  are denoted by  $\gamma_{pi}^\uparrow$  in uplink and  $\gamma_{ip}^\downarrow$  in downlink.

The definitions of the user load (3.2) and (3.6) are substituted by

$$l_p^\uparrow := \sum_{s \in S} \frac{\alpha_s^\uparrow \mu_s^\uparrow}{1 + \alpha_s^\uparrow \mu_s^\uparrow} T_s(p) \quad \text{and} \quad l_p^\downarrow := \sum_{s \in S} \frac{\alpha_s^\downarrow \mu_s^\downarrow}{1 + \bar{\omega}_p \alpha_s^\downarrow \mu_s^\downarrow} T_s(p). \quad (3.11)$$

Remember, that  $T_s(p)$  is the expected value of the traffic intensity for service  $s$  at location  $p$ . The other factors in the above definitions are constants. Thus,  $l_p^\uparrow$  and  $l_p^\downarrow$  are the expected values of  $l_m^\uparrow$  and  $l_m^\downarrow$  at location  $p$ . We derive the

entries of the expected uplink coupling matrix by

$$\bar{C}_{ii}^\uparrow := \int_{p \in A_i} l_p^\uparrow dp, \quad \bar{C}_{ij}^\uparrow := \int_{p \in A_j} \frac{\gamma_{ip}^\uparrow}{\gamma_{jp}^\uparrow} l_p^\uparrow dp. \quad (3.12)$$

The components of the expected downlink coupling matrix and traffic noise power read as

$$\bar{C}_{ii}^\downarrow := \int_{p \in A_i} \bar{\omega}_p l_p^\downarrow dp, \quad \bar{C}_{ij}^\downarrow := \int_{p \in A_i} \frac{\gamma_{jp}^\downarrow}{\gamma_{ip}^\downarrow} l_p^\downarrow dp, \quad \bar{p}_i^{(\eta)} := \int_{p \in A_i} \frac{\eta_p}{\gamma_{ip}^\downarrow} l_p^\downarrow dp. \quad (3.13)$$

### 3.1.3 Approximating Blocking

Until now, the system of linear equations introduced in the former sections ignores the effects due to load control which is triggered if the power of a cell would exceed its limit (cf. Section 2.4.3). To mimic load control, the approach from [7] is adopted to reduce the load in saturated cells. In this proposed model, it is not necessary to distinguish whether a user is rejected or whether the service quality of other users is downgraded. Following two properties characterize a proper load control:

- (i) *Admissibility*: After load control has been applied, all antenna power values are feasible, that is, (2.10) holds.
- (ii) *Greediness*: Users are only rejected by a cell if it cannot serve them without rising above its *own* capacity. That is, an antenna does not reject users to ease the situation of its neighboring cell.

Furthermore, we assume that a base station antenna is able to serve all its users up to a certain fraction of their resource demands. This is realized by scaling the relative user load ( (3.2) and (3.6) or (3.11) ) in the according cell by a value  $\lambda$  between 0 and 1. In doing so, only as little load as necessary is withdrawn. The blocking rate is then  $1 - \lambda$ . However, in realistic settings, the assumption of *compressible* user demand is not valid. The obtained scaling vectors can be used as a guideline for determining how many mobiles need to be refused.

A *complementarity condition* has to hold for the resulting power and scaling vectors in order to achieve the above two properties. In general, in a complementarity condition one or several subgroups of inequalities are comprised. In each group at least one of these inequalities should be met at equality [4]. In our case, it claims that if user demand in a cell is reduced, then the cell power is equal to its maximum allowed value.

The in the following described procedure can be applied to both kinds of equation system: the one derived by snapshot analysis and the one obtained on the basis of stochastic average load. For this reason, we simply use the notation we introduced in Section 3.1.1 for the traffic noise power vector as well as for the coupling matrices. The power vector obtained by this scaling procedure is denoted by  $\tilde{\mathbf{p}}^\uparrow$  and  $\tilde{\mathbf{p}}^\downarrow$ , respectively. The approach using the expected coupling matrices yields an approximation of the expected blocking rate. We explain the method for the downlink direction first since this is the easier one. The approach in uplink is more complex because scaling is applied to columns instead of rows.

### Downlink

In the downlink direction, the rows of the load coupling matrix have to be scaled, that is,

$$\tilde{\mathbf{p}}^\downarrow = \text{diag}(\lambda^\downarrow) \cdot C^\downarrow \cdot \tilde{\mathbf{p}}^\downarrow + \text{diag}(\lambda^\downarrow) \cdot \mathbf{p}^{(\eta)} + \mathbf{p}^{(c)}. \quad (3.14a)$$

Due to the linear definitions of the matrix entries and the entries of the traffic noise power vector, scaling the user load is equal to scaling the load coupling matrix and the traffic noise power. The complementarity condition is expressed by

$$\lambda_i^\downarrow < 1 \implies \tilde{p}_i^\downarrow = p_i^{\max\downarrow}. \quad (3.14b)$$

The scaling vector  $\lambda$  and the corresponding transmit power estimates are obtained by following recursion formula provided that  $0 < p_i^{(c)} \leq p_i^{\max\downarrow}$  and  $\sum_j C_{ij}^\downarrow > 0$  for all  $i$ :

With the initial settings

$$\begin{aligned} \lambda_i^0 &= 1 \\ \tilde{p}_i^0 &= p_i^{(c)}, \end{aligned}$$

the update step is given by

$$\begin{aligned} \lambda_i^{t+1} &= \min \left\{ \lambda_i^t, \frac{p_i^{\max\downarrow} - p_i^{(c)}}{C_{ii}^\downarrow p_i^{\max\downarrow} + \sum_{j \neq i} C_{ij}^\downarrow \tilde{p}_j^t + p_i^{(\eta)}} \right\} \\ \tilde{p}_i^{t+1} &= \frac{1}{1 - \lambda_i^{t+1} C_{ii}^\downarrow} \left[ p_i^{(c)} + \lambda_i^{t+1} \left( \sum_{j \neq i} C_{ij}^\downarrow \tilde{p}_j^t + p_i^{(\eta)} \right) \right]. \end{aligned} \quad (3.15)$$

The resulting sequences have the properties

$$\begin{aligned} 1 &= \lambda_i^0 \geq \lambda_i^1 \geq \lambda_i^2 \geq \dots \geq 0, \\ p_i^{(c)} &= \tilde{p}_i^0 \leq \tilde{p}_i^1 \leq \tilde{p}_i^2 \leq \dots \leq p_i^{\max\downarrow}, \end{aligned}$$

and

$$\lambda_i^t < 1 \implies \tilde{p}_i^t = p_i^{\max \downarrow}.$$

The sequences  $(\lambda_i^s)_{s \geq 0}$  and  $(\tilde{p}_i^s)_{s \geq 0}$  converge since they are component-wise monotonous and bounded. Their limiting values represent a complementary solution to (3.14), that is, a feasible solution to (3.14a) that fulfills the complementarity condition (3.14b). This solution is unique.

### Uplink

In the uplink case, the columns of the load coupling matrix are scaled:

$$\tilde{\mathbf{p}}^\uparrow = C^\uparrow \cdot \text{diag}(\lambda^\uparrow) \cdot \tilde{\mathbf{p}}^\uparrow + \eta^\uparrow. \quad (3.16a)$$

The complementarity condition looks as follows

$$\begin{aligned} 0 < \lambda_i^\uparrow < 1 &\implies \tilde{p}_i^\uparrow = p_i^{\max \uparrow} \\ \tilde{p}_i^\uparrow > p_i^{\max \uparrow} &\implies \lambda_i^\uparrow = 0. \end{aligned} \quad (3.16b)$$

One method to determine a complementary solution to (3.16) is to express the problem as a so-called *extended linear complementarity problem*. Essentially, this is a linear feasibility problem where in addition at least one complementarity condition is given [4]. The purpose of this thesis is not to describe the technique to solve this problem. Therefore, the interested reader is referred to [7]. The important point is that the problem is solvable. In contrast to the downlink direction, the solutions to (3.16) are not unique.

## 3.2 Monte Carlo Simulation

A popular method to assess the average blocking rates of the cells in a UMTS radio network is the so-called *Monte Carlo simulation*. This is a numerical method providing an approximate solution to the treated mathematical problem by executing a large number of statistical experiments. The results of every trial are collected. In the end, they are averaged (cf. [10]). The Monte Carlo Simulation is based on the *Law of Large Numbers* [17]. This theorem states, that the arithmetic mean of  $n$  mutually independent, identically distributed random variables converges to the common expected value of these variables as  $n$  goes to infinity if this expected value exists. Several formulations of this law specify convergence in different ways [11].

In our case, one traffic snapshot is evaluated in each sample experiment. Realistic CIR targets and attenuation factors of the mobile stations are determined and thus their individual capacity demands. Depending on this data,

the power levels of all active connections in the system are calculated. The input and output powers are assigned to every antenna in the radio network according to (2.5) and (2.7). If these powers exceed the maximum values one or more connections are dropped until the capacity constraints (2.10) are fulfilled. In this way, the blocking rate of every cell can be assessed. There are various methods to evaluate the radio network performance based on one traffic snapshot. Besides static or dynamic simulations of the system (cf. [21]) a snapshot based set of equations can be solved as described in the Sections 3.1.1 and 3.1.3.

The results of several independent snapshot analyses are combined to obtain statistically significant results. In this connection, we want to know how precise the estimated solution is for a certain number of trials, called the *sample size*. For this reason, the *confidence interval* is determined. This is a numerical interval covering the true value of the wanted unknown with a specified probability. That is, we find a value  $\delta > 0$  such that

$$\mathbb{P}(x \in [\bar{x} - \delta, \bar{x} + \delta]) = 1 - \alpha \quad (3.17)$$

for a given *confidence level*  $1 - \alpha$ . The value  $x$  denotes the true value of the blocking rate and  $\bar{x}$  is the solution obtained by the Monte Carlo simulation. For techniques to assess the interval  $[\bar{x} - \delta, \bar{x} + \delta]$  refer to [17, 10].

Usually, the sample size is very large if one wants to ensure statistical accuracy. Hundreds or even thousands of snapshots have to be analyzed to achieve statistically significant results [6]. For this reason, this method is very time-consuming and extensive. This procedural problem gets even worse if an evaluation of the network load shall be used within a local search procedure where it has to be executed several times. Consequently, the Monte Carlo simulation achieves accurate results at the expense of a high complexity that limits the applicability of this method.

### 3.3 Shortcomings

The problem of the snapshot based model was already highlighted in Section 3.2. The computational effort of this method is just too high for some purposes. In order to reduce this complexity, the approach using the expected cell load coupling matrix is applied. This is much less time consuming. However, this method produces estimation errors in the power values and the blocking rate. These errors are particularly significant for the blocking rate since the tolerable values are very small. We aim at designing radio networks with blocking rates lower than 2%. Due to this low limit of tolerance, the expected coupling approach should be improved for our purpose.

Figure 3.1 illustrates this effect schematically in case of a network with a single base station antenna for the downlink direction. Figure 3.1(a) shows the blocking rate of the cell and Figure 3.1(b) the power of the antenna depending on the average number of users in the cell. The green curve in each picture represents the results of the expected coupling approach from Section 3.1.2. The red one shows the exact values which can be described analytically for this simple case. The exact values can be understood as the expected values of the power and the blocking rate, respectively. That is, the power or blocking rate of all possible snapshot situations is weighted by the probability for the according traffic snapshot to occur and summed up.

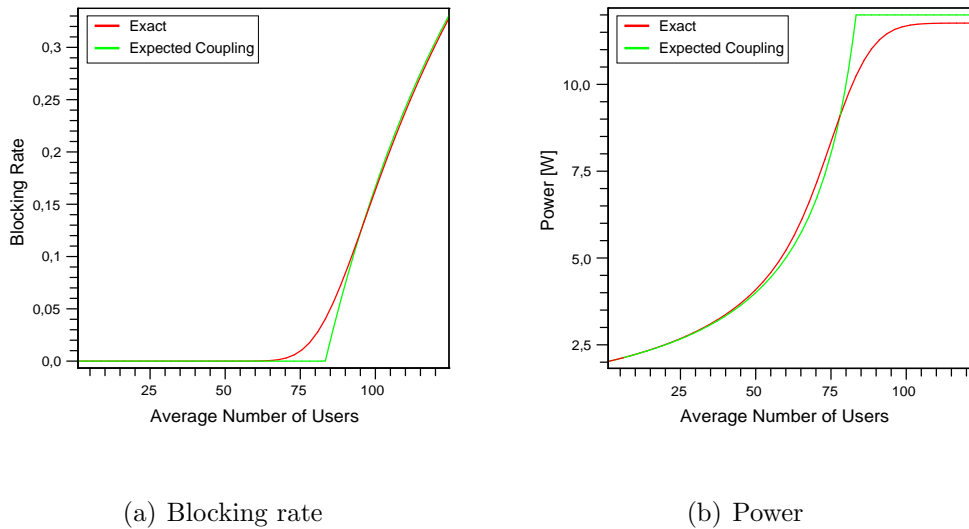


Figure 3.1: Power and blocking rate in downlink for an isolated cell

In Figure 3.1(a), it is remarkable that the blocking rate obtained by the expected coupling approach is zero up to a certain point. Then the curve has an abrupt, steep rise. At this inflection point, the scaling factor computed according to (3.15) is smaller than one for the first time. By contrast, the exact blocking rate rises much earlier. This value is already greater than zero if in one traffic snapshot situation blocking occurs in the cell. Such effects of randomness are ignored by using average traffic load distributions. This statistical data specifies the expected amount of traffic in the radio network. Possible variations from this expected value are not taken into account.

Figure 3.1(b) depicts that the expected coupling method tends to underestimate the power in the low region under around 9 W. The reason is that the power is a convex, monotonically increasing function of the average user intensity. Snapshot situations with more users than expected increase the

power of a base station antenna above average. In the concerned region of average user density, the number of users is distributed almost symmetrically around its expected value. That is, traffic situations with more users than expected are as possible as those with less users than expected. Therefore, the expected power value of all possible traffic snapshots is higher than that obtained by the expected coupling method. In the higher region from shortly below the maximum power, the expected coupling approach overestimates the power. This is due to the fact that the maximum power is not exactly met in reality. If there is more than one antenna in the radio network this overestimation of the other antennas' powers leads to an overestimation of the blocking rate in the considered cell in this high region.

In conclusion, there are methods to determine the average blocking rate almost exactly with high computational effort on the one hand. On the other hand, we have a model that has an acceptable complexity but whose results need to be improved for our purpose. Such improvements are developed and analyzed in the rest of this thesis.

## 4 The Blocking Rate as Expected Value

The goal of this diploma thesis is to develop a mathematical model to efficiently approximate the blocking rates of the cells in a UMTS radio network. Efficiently in this case means that the new method shall have about the speed of the expected coupling approach of the former chapter and about the accuracy of Monte Carlo simulation. In this chapter, we propose a new model to solve this task.

The basis for the following considerations is the expected coupling approach introduced in Section 3.1.2 and the computation of the blocking rate given in Section 3.1.3. We aim at reducing the inaccuracies of this method with regard to the blocking rate (cf. Section 3.3). These inaccuracies are due to the fact that the expected coupling approach neglects effects of randomness. These effects can be taken into account by approximating the blocking rate of a cell by its expected value. This is the idea of the model presented in this chapter. We determine the expected value of the average blocking rate depending on the intra-cell interference. In this model, we make two essential simplifications:

- (1) The mobile stations in the own cell are modeled independently of their locations, that is, we consider average users within the own sector.
- (2) We use constant estimates for the inter-cell interference.

For didactical reasons, we first address the case that all users in a sector have constant load  $l_m^\uparrow$  and  $l_m^\downarrow$ , respectively. In this case, the average blocking rate of an antenna can be expressed depending on the number of users in the cell. In the next step, we examine the situation in which the user load within the sector varies. In this case, the discrete approach is not suitable. Instead, we compute the expected value of the blocking rate depending on the main-diagonal entry of the load coupling matrix. We assume that this random variable follows a normal distribution. Afterwards, an enhancement

of the model is proposed, which possibly improves the estimates of the inter-cell interference. Finally, we discuss the assumption that the main-diagonal matrix entry is normally distributed.

## 4.1 Constant User Load

The sketch of modeling the intra-cell interference stochastically is descriptive in the case that all users in the cell have equal load  $l_m^\uparrow, l_m^\downarrow$ . We are able to model the intra-cell interference depending on the number of users in the sector. Thus, it is possible to specify the capacity of a cell explicitly and to compute the expected value of the average blocking rate depending on this capacity. In reality, the case of constant user load could be achieved if all mobile stations in the cell request the same service, have the same velocity, user equipment, and orthogonality factor. Of course, such a setting is not realistic. However, it serves to introduce the model in an easy way.

This section is organized as follows. First, we give the basic formula of the expected value of the average blocking rate. Moreover, we define the basic variables capacity and average blocking rate of a sector. Then, the capacity of a cell is computed in uplink and downlink. In the downlink direction, a refinement is shown since the inter-cell interference power also depends on the number of users in the own sector. Afterwards, we extend the model to the case that the user load within a cell is not constant but its variation is small. In the following, we denote the constant user load in cell  $i$  by  $l_i^\uparrow$  and  $l_i^\downarrow$ , respectively. The number of users in sector  $i$  is expressed by  $n \in \mathbb{N}$ .

### 4.1.1 Preliminaries

The average blocking rate at base station antenna  $i$  is denoted by  $\bar{b}_i^\uparrow$  in uplink and  $\bar{b}_i^\downarrow$  in the downlink direction. The common formulas for the expected value of the average blocking rate of the sector depending on the user number  $n$  are given by

$$\mathbb{E}[\bar{b}_i^\uparrow] = \sum_{n=0}^{\infty} \bar{b}_i^\uparrow(n) \mathbb{P}(n) \quad \text{and} \quad \mathbb{E}[\bar{b}_i^\downarrow] = \sum_{n=0}^{\infty} \bar{b}_i^\downarrow(n) \mathbb{P}(n). \quad (4.1)$$

Here,  $\mathbb{P}(n)$  denotes the probability of exactly  $n$  mobiles being located in cell  $i$ . We assume that the traffic intensity for one service in a cell is a random variable that follows a Poisson distribution with parameter  $T_i$  (cf. Section 2.5.2). Knowing the average traffic intensity  $T_p$  of the available service in location  $p$

we can define the expected number of users in cell  $i$  by

$$T_i := \int_{p \in A_i} T_p \, dp. \quad (4.2)$$

This follows from equation (2.2), which states the additivity of the counting measure  $T$ . The probability for  $n$  users in sector  $i$  is given by

$$\mathbb{P}_{T_i}(n) = e^{-T_i} \frac{(T_i)^n}{n!}, \quad n \in \mathbb{N}. \quad (4.3)$$

The capacity of a cell is the maximum number of users the base station antenna is able to serve without exceeding its power limit. For cell  $i$ , the uplink and downlink capacity is expressed by

$$\begin{aligned} \bar{n}_i^{\max\uparrow} &:= \max\{n \in \mathbb{N} : \bar{p}_i^\uparrow(n) \leq p_i^{\max\uparrow}\} \quad \text{and} \\ \bar{n}_i^{\max\downarrow} &:= \max\{n \in \mathbb{N} : \bar{p}_i^\downarrow(n) \leq p_i^{\max\downarrow}\}. \end{aligned} \quad (4.4)$$

Generally, the blocking rate of an antenna is described by the ratio of rejected users to the total number of users. Therefore, the average blocking rates in uplink and downlink are given by

$$\begin{aligned} \bar{b}_i^\uparrow(n) &:= \begin{cases} 0 & \text{for } n \leq \bar{n}_i^{\max\uparrow} \\ \frac{n - \bar{n}_i^{\max\uparrow}}{n} & \text{for } n > \bar{n}_i^{\max\uparrow}, \end{cases} \\ \bar{b}_i^\downarrow(n) &:= \begin{cases} 0 & \text{for } n \leq \bar{n}_i^{\max\downarrow} \\ \frac{n - \bar{n}_i^{\max\downarrow}}{n} & \text{for } n > \bar{n}_i^{\max\downarrow}. \end{cases} \end{aligned} \quad (4.5)$$

If  $\bar{n}_i^{\max\uparrow}$  and  $\bar{n}_i^{\max\downarrow}$  were the exact capacities of cell  $i$ , these formulas would express the exact blocking rates. Since we approximate the capacities of the antennas we deal exclusively with average blocking rates. Using equations (4.3) and (4.5), the expected values of the blocking rates (4.1) read as

$$\begin{aligned} \mathbb{E}[\bar{b}_i^\uparrow] &= \sum_{n=\bar{n}_i^{\max\uparrow}+1}^{\infty} \frac{n - \bar{n}_i^{\max\uparrow}}{n} \mathbb{P}_{T_i}(n), \\ \mathbb{E}[\bar{b}_i^\downarrow] &= \sum_{n=\bar{n}_i^{\max\downarrow}+1}^{\infty} \frac{n - \bar{n}_i^{\max\downarrow}}{n} \mathbb{P}_{T_i}(n). \end{aligned} \quad (4.6)$$

Hence, we approximate the capacities of the base station antennas in uplink ( $\bar{\mathbf{n}}^{\max\uparrow}$ ) and downlink ( $\bar{\mathbf{n}}^{\max\downarrow}$ ) in the following.

### 4.1.2 Uplink

Due to assumption (1), the main diagonal entry of the load coupling matrix depends merely on the number of users in the sector. That is,

$$C_{ii}^\uparrow(n) = n l_i^\uparrow. \quad (4.7)$$

Because the number of users in the cell is Poisson distributed,  $C_{ii}^\uparrow$  follows a scaled Poisson distribution with scaling factor  $l_i^\uparrow$ . Since  $C_{ii}^\uparrow$  depends on the user intensity  $n$ , the power  $\bar{p}_i^\uparrow$  depends on  $n$ , too. Substituting  $C_{ii}^\uparrow$  according to (4.7), the equation for the reception power at base station antenna  $i$  reads as

$$\bar{p}_i^\uparrow(n) = n l_i^\uparrow \bar{p}_i^\uparrow(n) + \sum_{j \neq i} \tilde{C}_{ij}^\uparrow \tilde{p}_j^\uparrow + \eta_i. \quad (4.8)$$

The power values  $\tilde{C}_{ij}^\uparrow$  for  $j \neq i$  are defined by

$$\tilde{C}_{ij}^\uparrow := \bar{C}_{ij}^\uparrow \lambda_j^\uparrow.$$

The values  $\tilde{p}_j^\uparrow$  are the solutions of the equation system (3.16) using the expected coupling matrix. According to assumption (2), we estimate the inter-cell interference by average values. In doing so, we use  $\tilde{C}_{ij}^\uparrow$  instead of  $\bar{C}_{ij}^\uparrow$  in order to express the realistic behavior of antenna  $j$ . Cell  $j$  only serves the fraction of users that does not exceed its available radio resources. The other portion is blocked. We assume that

$$\sum_{j \neq i} \tilde{C}_{ij}^\uparrow \tilde{p}_j^\uparrow + \eta_i > 0.$$

For this reason, with (4.8) it holds that

$$\bar{p}_i^\uparrow(n) > n l_i^\uparrow \bar{p}_i^\uparrow(n).$$

This is equivalent to

$$1 - n l_i^\uparrow > 0. \quad (4.9)$$

In cell  $i$ , blocking happens if more than  $\bar{n}_i^{\max\uparrow}$  active users are in the sector. Then, the surplus will not be served. In this case, the total received power of the antenna is  $\bar{p}_i^\uparrow(\bar{n}_i^{\max\uparrow}) \leq p_i^{\max\uparrow}$ . Transforming (4.8), the average uplink power for  $n$  mobile stations in the cell satisfies the expression

$$\bar{p}_i^\uparrow(n) = \begin{cases} \frac{\sum_{j \neq i} \tilde{C}_{ij}^\uparrow \tilde{p}_j^\uparrow + \eta_i}{1 - n l_i^\uparrow} & \text{for } n \leq \bar{n}_i^{\max\uparrow} \\ \bar{p}_i^\uparrow(\bar{n}_i^{\max\uparrow}) & \text{for } n > \bar{n}_i^{\max\uparrow}. \end{cases} \quad (4.10)$$

Due to (4.9), this formula is well defined. In order to assess the capacity of the cell we use the above equation in definition (4.4) of  $\bar{n}_i^{\max\uparrow}$ . This results in

$$\bar{n}_i^{\max\uparrow} = \max \left\{ n \in \mathbb{N} : \frac{\sum_{j \neq i} \tilde{C}_{ij}^\uparrow \tilde{p}_j^\uparrow + \eta_i}{1 - n l_i^\uparrow} \leq p_i^{\max\uparrow} \right\}.$$

From the above equation,  $\bar{n}_i^{\max\uparrow}$  can be derived as

$$\bar{n}_i^{\max\uparrow} = \left\lfloor \frac{p_i^{\max\uparrow} - \sum_{j \neq i} \tilde{C}_{ij}^\uparrow \tilde{p}_j^\uparrow - \eta_i}{p_i^{\max\uparrow} l_i^\uparrow} \right\rfloor. \quad (4.11)$$

We round down the received value since the number of users in a cell is integral.

### 4.1.3 Downlink

Now, we follow the same considerations in downlink. In contrast to the uplink direction, the traffic noise power  $p_i^{(\eta)}$  has to be taken into account, but this issue is ignored for the time being. In addition to the constant user load  $l_i^\downarrow$ , we also assume a constant orthogonality factor in the whole cell area. We denote this unique orthogonality factor by  $\bar{\omega}_i$ . The main diagonal entry of the downlink coupling matrix in case of  $n$  users in sector  $i$  is given by

$$C_{ii}^\downarrow(n) = n \bar{\omega}_i l_i^\downarrow. \quad (4.12)$$

Therefore, the average transmission power of antenna  $i$  depending on the user intensity  $n$  in the cell reads as

$$\bar{p}_i^\downarrow(n) = n \bar{\omega}_i l_i^\downarrow \bar{p}_i^\downarrow(n) + \sum_{j \neq i} \tilde{C}_{ij}^\downarrow \tilde{p}_j^\downarrow + p_i^{(c)}. \quad (4.13)$$

The scaled off-diagonal entries of the coupling matrix are defined as

$$\tilde{C}_{ij}^\downarrow := \lambda_i^\uparrow \bar{C}_{ij}^\downarrow.$$

The value  $\tilde{p}_j^\downarrow$  is the solution of the scaled, expected value based equation system (3.14). The values  $\bar{C}_{ij}^\downarrow$  estimate the fraction of the average total power at antenna  $i$  that is necessary to overcome the received power of other antennas at the mobiles in sector  $i$ . If some of them are blocked, these estimates are lower. We involve the scaling in order to take the blocking behavior of our own cell into account. Following expression is satisfied due to  $p_i^{(c)} > 0$ :

$$\sum_{j \neq i} \tilde{C}_{ij}^\downarrow \tilde{p}_j^\downarrow + p_i^{(c)} > 0.$$

Therefore, it holds that

$$\bar{p}_i^\downarrow(n) > n \bar{\omega}_i l_i^\downarrow \bar{p}_i^\downarrow(n).$$

This can be transformed into

$$1 - n \bar{\omega}_i l_i^\downarrow > 0. \quad (4.14)$$

If there are more users in the cell than  $\bar{n}_i^{\max\downarrow}$ , blocking happens such that the total transmission power does not exceed its limit. For this reason, equation (4.13) can be written as

$$\bar{p}_i^\downarrow(n) = \begin{cases} \frac{\sum_{j \neq i} \tilde{C}_{ij}^\downarrow \tilde{p}_j^\downarrow + p_i^{(c)}}{1 - n \bar{\omega}_i l_i^\downarrow} & \text{for } n \leq \bar{n}_i^{\max\downarrow} \\ \bar{p}_i^\downarrow(\bar{n}_i^{\max\downarrow}) & \text{for } n > \bar{n}_i^{\max\downarrow}. \end{cases}$$

Because of (4.14), this expression is well defined. Using the above formulation in the definition (4.4) of  $\bar{n}_i^{\max\downarrow}$ , we obtain

$$\bar{n}_i^{\max\downarrow} = \max \left\{ n \in \mathbb{N} : \frac{\sum_{j \neq i} \tilde{C}_{ij}^\downarrow \tilde{p}_j^\downarrow + p_i^{(c)}}{1 - n \bar{\omega}_i l_i^\downarrow} \leq p_i^{\max\uparrow} \right\}.$$

This can be transformed into

$$\bar{n}_i^{\max\downarrow} = \left\lfloor \frac{p_i^{\max\uparrow} - \sum_{j \neq i} \tilde{C}_{ij}^\downarrow \tilde{p}_j^\downarrow - p_i^{(c)}}{p_i^{\max\uparrow} \bar{\omega}_i l_i^\downarrow} \right\rfloor.$$

With this closed-form expression, we are able to calculate the quantity  $\bar{n}_i^{\max\downarrow}$  as well as the desired expected value of the average blocking rate according to (4.6).

### Refined Downlink

In the above approach, the contributions of other antennas to the interference in the own cell are not modeled stochastically. We use constant expected values. However, in downlink, it is possible to additionally vary the off-diagonal entries of the load coupling matrix  $C^\downarrow$  in order to obtain more precise results.

The coupling factors  $C_{ij}^\downarrow$  describe the fraction of total transmission power of antenna  $i$  spent on overcoming the interference originating in sector  $j$ . Each new request in cell  $i$  causes the transmission power of the antenna to its associated mobiles to increase. At the same time, this new user is affected by interference from other base station antennas. That is, the interference

power in sector  $i$  increases and the antenna has to raise the power to overcome this interference. Actually, the strength of the interference power depends on the location of the affected mobile. Users at the cell border are much more exposed to inter-cell interference than mobiles in the center of the sector. We do not consider the positions of the mobile stations in our own cell (condition (1)). Instead, we assume average users in the sector. Since the off-diagonal entries  $C_{ij}^\downarrow$  depend on the number of users in cell  $i$  we assume a proportional correlation between  $C_{ij}^\downarrow$  and the average number of users in sector  $i$ . In uplink, a similar approach is not possible because the inter-cell interference depends on the number of mobiles in the other cells, which we do not model stochastically.

Instead of (4.13), the total transmission power of antenna  $i$  is calculated as

$$\bar{p}_i^\downarrow(n) = n \bar{\omega}_i l_i^\downarrow \bar{p}_i^\downarrow(n_i) + n \sum_{j \neq i} \frac{\bar{C}_{ij}^\downarrow}{T_i} \tilde{p}_j^\downarrow + p_i^{(c)}$$

with  $T_i$  as defined in (4.2). The value  $\bar{C}_{ij}^\downarrow$  is an entry of the expected load coupling matrix. We assume the inter-cell interference to be uniformly distributed to all mobiles in sector  $i$ . Therefore, in place of being scaled, the off-diagonal entries of  $\bar{C}^\downarrow$  are normalized by the average user intensity in cell  $i$ . As in (4.13),  $\tilde{p}_j^\downarrow$  is the total transmission power of antenna  $j$  received by solving the equation system with the scaled, expected coupling matrix. The approximated transmission power of base station antenna  $i$  is thus:

$$\bar{p}_i^\downarrow(n) = \begin{cases} \frac{n \frac{1}{T_i} \sum_{j \neq i} \bar{C}_{ij}^\downarrow \tilde{p}_j^\downarrow + p_i^{(c)}}{1 - n \bar{\omega}_i l_i^\downarrow} & \text{for } n \leq \bar{n}_i^{\max \downarrow} \\ \bar{p}_i^\downarrow(\bar{n}_i^{\max \downarrow}) & \text{for } n > \bar{n}_i^{\max \downarrow}. \end{cases}$$

Then the approximated capacity of cell  $i$  is determined according to

$$\bar{n}_i^{\max \downarrow} = \left\lfloor \frac{p_i^{\max \downarrow} - p_i^{(c)}}{p_i^{\max \downarrow} \bar{\omega}_i l_i^\downarrow + \frac{1}{T_i} \sum_{j \neq i} \bar{C}_{ij}^\downarrow \tilde{p}_j^\downarrow} \right\rfloor.$$

### The Traffic Noise Power

The traffic noise power in downlink in cell  $i$  is modeled in analogy to the expected coupling approach. We estimate it by the expected value

$$\bar{p}_i^{(n)} := \int_{p \in A_i} \frac{\eta_p}{\gamma_{ip}^\downarrow} l_p^\downarrow dp.$$

The traffic noise power of an antenna depends on the number of mobiles in its best server area. The reason is the same as for the dependence of the

off-diagonal coupling matrix entries on the number of mobiles. The more users an antenna serves, the more power it has to spent on overcoming the noise at these mobiles. Therefore, we normalize the average noise power by the average user intensity in the cell and multiply this value with the user number  $n$ . Finally, the approximated total transmission power of antenna  $i$  for  $n$  mobiles in the cell results in

$$\bar{p}_i^\downarrow(n) = n \bar{\omega}_i l_i^\downarrow \bar{p}_i^\downarrow(n) + n_i \frac{1}{T_i} \left( \sum_{j \neq i} \bar{C}_{ij}^\downarrow \tilde{p}_j^\downarrow + \bar{p}_i^{(\eta)} \right) + p_i^{(c)}.$$

This can be transformed into

$$\bar{p}_i^\downarrow(n) = \begin{cases} \frac{n \frac{1}{T_i} (\sum_{j \neq i} \bar{C}_{ij}^\downarrow \tilde{p}_j^\downarrow + \bar{p}_i^{(\eta)}) + p_i^{(c)}}{1 - n \bar{\omega}_i l_i^\downarrow} & \text{for } n \leq \bar{n}_i^{\max \downarrow} \\ \bar{p}_i^\downarrow(\bar{n}_i^{\max \downarrow}) & \text{for } n > \bar{n}_i^{\max \downarrow}. \end{cases} \quad (4.15)$$

In analogy to the previous sections, the capacity of cell  $i$  is derived as

$$\bar{n}_i^{\max \downarrow} = \left\lfloor \frac{p_i^{\max \downarrow} - p_i^{(c)}}{p_i^{\max \downarrow} \bar{\omega}_i l_i^\downarrow + \frac{1}{T_i} (\sum_{j \neq i} \bar{C}_{ij}^\downarrow \tilde{p}_j^\downarrow + \bar{p}_i^{(\eta)})} \right\rfloor. \quad (4.16)$$

#### 4.1.4 Extension

The proposed discrete approach is valid in cases in which the variation of the user load  $l_m^\uparrow$  and  $l_m^\downarrow$ , respectively, within the sector is small such that it can be represented by its average value without being too unprecise. In reality, this situation could occur if all mobile stations in the cell request the same service but have each a different velocity, user equipment or orthogonality factor. We determine the average user load over all positions in the sector and assume it to be constant for every mobile station. That is, we transform this situation into the case with constant user load.

In mathematical models, it is common to classify the user mobility coarsely instead of considering speed as a continuous variable. One possible classification is to group the different mobility types according to the average velocity. E.g. the mobility type *pedestrian* has the speed 1 m/s. In the following,  $M$  denotes the set of mobility types.

#### Uplink

For every position  $p \in A_i$ , we compute the expected value of the user load. This yields

$$l_p^\uparrow = \sum_{m \in M} l_m^\uparrow T_p \mathbb{P}_p(m).$$

In this formula,  $T_p$  is the average traffic intensity in point  $p$ . The value  $\mathbb{P}_p(m)$  is the probability for the presence of a user having mobility type  $m$  at this location and  $l_m^\uparrow$  is the uplink user load for mobility type  $m$ . This user load is given by

$$l_m^\uparrow = \frac{\alpha_m^\uparrow \mu_m^\uparrow}{1 + \alpha_m^\uparrow \mu_m^\uparrow},$$

which is the same definition as (3.2) for the user load of a mobile station. The average uplink user load for a mobile in cell  $i$  reads as

$$l_i^\uparrow := \frac{1}{T_i} \int_{p \in A_i} l_p^\uparrow dp. \quad (4.17)$$

In fact, this is the main-diagonal entry of the expected cell load coupling matrix  $\bar{C}^\uparrow$  normalized by the average number of users in the according sector. The constant user load  $l_i^\uparrow$  is used in the equations (4.10) and (4.11) in order to derive a formula for the uplink capacity of cell  $i$ .

## Downlink

In analogy to the uplink, the expected value of the downlink user load in position  $p \in A_i$  is given by

$$l_p^\downarrow = \sum_{m \in M} l_m^\downarrow(p) T_p \mathbb{P}_p(m)$$

with  $T_p$  and  $\mathbb{P}_p(m)$  as explained before. The downlink user load for a user with mobility type  $m$  at location  $p$  reads as

$$l_m^\downarrow(p) = \frac{\alpha_m^\downarrow \mu_m^\downarrow}{1 + \bar{\omega}_p \alpha_m^\downarrow \mu_m^\downarrow}.$$

Besides the mobility type  $m$ , the user load depends on the point  $p$  because of the location-specific orthogonality factors  $\bar{\omega}_p$ . The average downlink user load for a mobile station served by base station antenna  $i$  is given by

$$l_i^\downarrow := \frac{1}{T_i} \int_{p \in A_i} \bar{\omega}_p l_p^\downarrow dp. \quad (4.18)$$

Again, this is the main-diagonal entry of the expected cell load coupling matrix  $\bar{C}^\downarrow$ , normalized by the average traffic intensity in cell  $i$ . We use  $l_i^\downarrow$  in the equations (4.15) and (4.16) to obtain the average capacity of the cell.

## 4.2 Variable User Load

In this section, we enhance the presented approach. In reality, the user load varies strongly due to different services, velocity, and so on. For this reason, computing the expected blocking rate according to (4.6) yields too unprecise results for our purpose. The assumption of the intra-cell interference being scaled Poisson distributed does not hold. Instead, we assume the main-diagonal entry of the coupling matrix to follow a normal distribution since this value is the sum of a large number of independent random variables. A detailed discussion of this assumption can be found in Section 4.4. As in the previous section, we first give the common formula for the expected value of the average blocking rate. Afterwards, the needed quantities are derived for the uplink and downlink direction. In the downlink, an enhancement is given in analogy to the case of constant user load.

### 4.2.1 Preliminaries

The underlying random variable is the main-diagonal entry of the cell load coupling matrix. This variable is continuous. For this reason, we compute the expected value of the average blocking rate according to

$$\mathbb{E}[\bar{b}_i^\uparrow] = \int_0^\infty \bar{b}_i^\uparrow(x) f_i^\uparrow(x) dx \quad \text{and} \quad \mathbb{E}[\bar{b}_i^\downarrow] = \int_0^\infty \bar{b}_i^\downarrow(x) f_i^\downarrow(x) dx. \quad (4.19)$$

The functions  $f_i^\uparrow$  and  $f_i^\downarrow$  denote the probability density functions of  $C_{ii}^\uparrow$  and  $C_{ii}^\downarrow$ , respectively. In this continuous case, it makes no sense to count the users in a cell and determine the average capacity as we did in the previous section. Each single user contribution is much too different to be represented reasonably by an average value. In order to compute the expected value according to (4.19), we derive formulas for the probability density functions  $f_i^\uparrow$  and  $f_i^\downarrow$  as well as for the average blocking rates  $\bar{b}_i^\uparrow$  and  $\bar{b}_i^\downarrow$  in the rest of this section.

### 4.2.2 Uplink

According to (3.3), the main-diagonal entry of the uplink cell load coupling matrix for antenna  $i$  is defined as

$$C_{ii}^\uparrow = \sum_{m \in \mathcal{M}_i} l_m^\uparrow.$$

We assume it to be normally distributed. Generally, it is reasonable to approximate the sum of many independent random variables with unknown

distribution by a normal distribution. As in the expected coupling approach, the expected value of  $C_{ii}^\uparrow$  can be calculated according to

$$\mathbb{E}[C_{ii}^\uparrow] = \int_{p \in A_i} \sum_{s \in S} \frac{\alpha_s^\uparrow \mu_s^\uparrow}{1 + \alpha_s^\uparrow \mu_s^\uparrow} T_s(p) dp. \quad (4.20)$$

Here,  $T_s(p)$  is the traffic intensity of service  $s$  in pixel  $p$ . The variance of the user intensity is equal to its expected value  $T_s(p)$  because the traffic intensity is assumed to be Poisson distributed. For the variance of  $C_{ii}^\uparrow$  thus holds

$$\mathbb{V}[C_{ii}^\uparrow] = \int_{p \in A_i} \sum_{s \in S} \left( \frac{\alpha_s^\uparrow \mu_s^\uparrow}{1 + \alpha_s^\uparrow \mu_s^\uparrow} \right)^2 T_s(p) dp. \quad (4.21)$$

No covariances have to be included because of the independence of the user numbers in each pixel and for each service. Knowing the expected value and variance of a normally distributed random variable allows for assessing its probability density function  $f_i^\uparrow$ .

The blocking rate  $\bar{b}_i^\uparrow$  in sector  $i$  can be determined by

$$\bar{b}_i^\uparrow(x) = 1 - \lambda_i^\uparrow(x). \quad (4.22)$$

The vector  $\lambda^\uparrow$  consists of the load scaling factors for each cell introduced in Section 3.1.3. In order to compute the whole vector and the according reception powers an extended linear complementarity problem has to be solved. In contrast, we now estimate the average load scaling factors and reception powers of the other antennas. Therefore, we simply have to solve the following equation for  $\lambda_i^\uparrow$  (cf. (3.16)):

$$p_i^{\max\uparrow} = C_{ii}^\uparrow \lambda_i^\uparrow p_i^{\max\uparrow} + \sum_{j \neq i} \tilde{C}_{ij}^\uparrow \tilde{p}_j^\uparrow + \eta_i.$$

Due to possible blocking in other cells, the scaled off-diagonal matrix entries  $\tilde{C}_{ij}^\uparrow$  are taken. Moreover, the average total reception power at antenna  $i$  is estimated by its maximum because otherwise  $\lambda_i^\uparrow = 1$  applies (cf. (3.16b)). In doing so, we simplify  $\bar{p}_i^\uparrow(\bar{n}_i^{\max\uparrow})$  to  $p_i^{\max\uparrow}$ . In conclusion, we obtain

$$\lambda_i^\uparrow(x) = \min \left\{ 1, \frac{p_i^{\max\uparrow} - \sum_{j \neq i} \tilde{C}_{ij}^\uparrow \tilde{p}_j^\uparrow - \eta_i}{x p_i^{\max\uparrow}} \right\} \quad (4.23)$$

for  $x \in (0, \infty)$ . Furthermore, we define  $\lambda_i^\uparrow(0) := 1$ .

### 4.2.3 Downlink

The main diagonal entry of the downlink cell load coupling matrix for an antenna  $i$  is given by

$$C_{ii}^\downarrow := \sum_{m \in \mathcal{M}_i} \bar{\omega}_m l_m^\downarrow.$$

We assume this random variable to follow a normal distribution. In analogy to the expected coupling approach, the expected value of  $C_{ii}^\downarrow$  is

$$\mathbb{E}[C_{ii}^\downarrow] = \int_{p \in A_i} \sum_{s \in S} \frac{\bar{\omega}_p \alpha_s^\downarrow \mu_s^\downarrow}{1 + \bar{\omega}_p \alpha_s^\downarrow \mu_s^\downarrow} T_s(p) dp.$$

Its variance satisfies

$$\mathbb{V}[C_{ii}^\downarrow] = \int_{p \in A_i} \sum_{s \in S} \left( \frac{\bar{\omega}_p \alpha_s^\downarrow \mu_s^\downarrow}{1 + \bar{\omega}_p \alpha_s^\downarrow \mu_s^\downarrow} \right)^2 T_s(p) dp$$

due to the independence of the traffic intensities in distinct locations and for different services. As in the uplink direction, the expected value and variance of  $C_{ii}^\downarrow$  are finite. With these values we can determine the probability density function  $f_i^\downarrow$  of  $C_{ii}^\downarrow$ .

The blocking rate at antenna  $i$  is expressed by

$$\bar{b}_i^\downarrow(x) = 1 - \lambda_i^\downarrow(x) \quad (4.24)$$

with  $\lambda^\downarrow$  being the downlink load scaling vector from Section 3.1.3. We estimate the average scaling factors and transmission powers of the other cells in the network. Furthermore, if  $\lambda_i^\downarrow < 1$ , then the transmission power at antenna  $i$  is assumed to meet  $p_i^{\max\downarrow}$  (cf. (3.14b)). For this reason, the following expression holds for  $\lambda_i^\downarrow < 1$ :

$$p_i^{\max\downarrow} = \lambda_i^\downarrow \left( C_{ii}^\downarrow p_i^{\max\downarrow} + \sum_{j \neq i} \bar{C}_{ij}^\downarrow \tilde{p}_j^\downarrow + \bar{p}_i^{(\eta)} \right) + p_i^{(c)}.$$

This yields

$$\lambda_i^\downarrow(x) = \min \left\{ 1, \frac{p_i^{\max\downarrow} - p_i^{(c)}}{x p_i^{\max\downarrow} + \sum_{j \neq i} \bar{C}_{ij}^\downarrow \tilde{p}_j^\downarrow + \bar{p}_i^{(\eta)}} \right\}$$

for  $x \in (0, \infty) \setminus \left\{ -\frac{1}{p_i^{\max\downarrow}} \left( \sum_{j \neq i} \bar{C}_{ij}^\downarrow \tilde{p}_j^\downarrow + \bar{p}_i^{(\eta)} \right) \right\}$ . For

$$x \in \left\{ 0, -\frac{1}{p_i^{\max\downarrow}} \left( \sum_{j \neq i} \bar{C}_{ij}^\downarrow \tilde{p}_j^\downarrow + \bar{p}_i^{(\eta)} \right) \right\},$$

we set  $\lambda_i^\downarrow(x) := 1$ .

In this approach, the random variable we actually consider is the user load  $l_m^\downarrow$  in each position of the own cell. Besides the main diagonal entries of the coupling matrix, it is also involved in the computation of the off-diagonal entries and the noise power. For this reason, we are able to refine the above approach similar to the case of constant user load by introducing the random variable

$$C_i^\downarrow := C_{ii}^\downarrow p_i^{\max\downarrow} + \sum_{j \neq i} C_{ij}^\downarrow \tilde{p}_j^\downarrow + p_i^{(\eta)}. \quad (4.25)$$

It is convenient to define

$$c_{im}^\downarrow := \bar{\omega}_m p_i^{\max\downarrow} + \sum_{j \neq i} \frac{\gamma_{jm}^\downarrow}{\gamma_{im}^\downarrow} \tilde{p}_j^\downarrow + \frac{\eta_m}{\gamma_{im}^\downarrow}$$

for a mobile station  $m$ . Then  $C_i^\downarrow$  can be written as

$$C_i^\downarrow = \sum_{m \in \mathcal{M}_i} c_{im}^\downarrow l_m^\downarrow.$$

We assume this random variable to be normally distributed as sum of many independent random variables. Its expected value and variance are

$$\begin{aligned} \mathbb{E}[C_i^\downarrow] &= \bar{C}_{ii}^\downarrow p_i^{\max\downarrow} + \sum_{j \neq i} \bar{C}_{ij}^\downarrow \tilde{p}_j^\downarrow + \bar{p}_i^{(\eta)}, \\ \mathbb{V}[C_i^\downarrow] &= \int_{p \in A_i} (c_{ip}^\downarrow)^2 \sum_{s \in S} \left( \frac{\alpha_s^\downarrow \mu_s^\downarrow}{1 + \bar{\omega}_p \alpha_s^\downarrow \mu_s^\downarrow} \right)^2 T_s(p) dp. \end{aligned} \quad (4.26)$$

Here,  $c_{ip}^\downarrow$  is defined as

$$c_{ip}^\downarrow := \bar{\omega}_p p_i^{\max\downarrow} + \sum_{j \neq i} \frac{\gamma_{jp}^\downarrow}{\gamma_{ip}^\downarrow} \tilde{p}_j^\downarrow + \frac{\eta_p}{\gamma_{ip}^\downarrow} \quad (4.27)$$

for a position  $p$ . The probability density function of  $C_i^\downarrow$  is denoted by  $f_i^\downarrow$ . Again, the expected blocking rate is determined according to (4.19) with  $\bar{b}_i^\downarrow$  given by (4.24). However, we compute  $\lambda_i^\downarrow$  by

$$\lambda_i^\downarrow(x) = \min \left\{ 1, \frac{p_i^{\max\downarrow} - p_i^{(c)}}{x} \right\} \quad (4.28)$$

for  $x \in (0, \infty)$ . We define  $\lambda_i^\downarrow(0) := 1$ .

### 4.3 The Effect of Coupling

In this section, we introduce an approach which possibly improves the estimates for the powers of the other base station antennas and thus the average blocking rate. We obtain these estimates by solving the equation system (3.14) and (3.16), respectively. By computing the expected value of the average blocking rate according to (4.1) or (4.19), only those situations are included in which the blocking rate of the cell is greater than zero. In the basic mathematical model, we equate this situation with the case that the power of the antenna in question is at its maximum (cf. (3.14b) and (3.16b)). In UMTS radio networks, the cells are coupled with each other (cf. Section 2.4). For this reason, setting the power of one base station antenna to its maximum causes other antennas to raise their power, too. So far, the estimates of the other antennas' powers are computed for the average situation in which the power of our antenna is eventually lower than its maximum. That is, the effect of coupling is not taken into account. Therefore, these estimates may be too low and thus the average blocking rate of our sector.

One possibility to consider the effect of coupling is to solve a modified equation system. In (3.14) and (3.16), respectively, we set the power of the own antenna to its maximum value. In this manner, we get an equation system with one variable less than before. In the uplink direction, it looks as follows:

$$\begin{aligned}\tilde{p}_k^\uparrow &= p_k^{\max\uparrow} \quad \text{for } k = i, \\ \tilde{p}_k^\uparrow &= \sum_{j \in \mathcal{N}} \tilde{C}_{kj}^\uparrow \tilde{p}_k^\uparrow + \eta_k \quad \text{for } k \neq i.\end{aligned}\tag{4.29}$$

For the downlink, we set up

$$\begin{aligned}\tilde{p}_k^\downarrow &= p_k^{\max\downarrow} \quad \text{for } k = i, \\ \tilde{p}_k^\downarrow &= \sum_{j \in \mathcal{N}} \tilde{C}_{kj}^\downarrow \tilde{p}_k^\downarrow + \tilde{p}_k^{(\eta)} + p_k^{(c)} \quad \text{for } k \neq i.\end{aligned}\tag{4.30}$$

Solving these equation systems results in powers for the other base station antennas, which are higher than before if they were not at their maximum and if the power of antenna  $i$  was not at its maximum. In fact, the assumption that  $\bar{p}_i^\uparrow(\bar{n}_i^{\max\uparrow}) = p_i^{\max\uparrow}$  and  $\bar{p}_i^\downarrow(\bar{n}_i^{\max\downarrow}) = p_i^{\max\downarrow}$ , respectively, does not apply in general (cf. Section 3.3). However, this estimation error may possibly be small in contrast to the estimation error we make if we do not consider the effect of coupling. This question is analyzed in Chapter 7.

## 4.4 The Assumption of a Normal Distribution

This section addresses the assumption of Section 4.2 that the random variables  $C_{ii}^\uparrow$  and  $C_i^\downarrow$  are normally distributed. Since each of them is the sum of a large number of independent random variables we could suppose that the *Central Limit Theorem* applies. This theorem states that the sum of  $m$  independent random variables tends to be normally distributed for sufficiently large  $m$  if the contribution of each single variable to the total variance is negligible. However, this section shows, that the Central Limit Theorem does not apply in our case. That is, the limiting distributions of our random variables are no normal distributions.

First, we give a formulation of the Central Limit Theorem with the *Lindeberg condition* as well as the *Feller Theorem* according to [3]. The Feller Theorem implies the necessity of the Lindeberg condition. Afterwards, we transform our case to the conditions of these theorems. Then, we prove that the Feller Theorem applies. Thus, the Lindeberg condition is necessary. We show that this condition is not fulfilled. Finally, we give some reasons why the assumption of a normal distribution is justified anyway.

### 4.4.1 The Central Limit Theorem

We introduce briefly the needed theorems based on [3]. In the following, we consider sequences of random variables defined on the same probability space

$$\begin{array}{ccccccc} X_{11} & X_{12} & \dots & X_{1n_1} & & & \\ X_{21} & X_{22} & \dots & \dots & X_{2n_2} & & \\ \vdots & \vdots & & & & \ddots & \end{array} \quad (4.31)$$

Usually, it holds that  $n_1 < n_2 < \dots$ . For this reason, the above array is called a *triangular array*. Throughout this section,  $k \in \mathbb{N}$  denotes a row index of this array. The column index  $p$  ranges from 1 to  $n_k \in \mathbb{N}$ . We define

$$\mu_{kp} := \mathbb{E}[X_{kp}], \quad \sigma_{kp}^2 := \mathbb{V}[X_{kp}], \quad \text{and} \quad X_k := \sum_{p=1}^{n_k} X_{kp}. \quad (4.32)$$

**Theorem 4.1** *Let the sequence  $\{X_{kp}\}$  be independent with  $\mu_{kp} = 0$  for all  $p$  and  $k$  and the variance sequence  $\{\sigma_{kp}^2\}$  satisfying*

$$\mathbb{E}[X_k^2] = \sum_{p=1}^{n_k} \sigma_{kp}^2 = 1. \quad (4.33)$$

Then the limiting distribution of  $X_k$  is the standard normal distribution if

$$\lim_{k \rightarrow \infty} \sum_{p=1}^{n_k} \int_{\{|X_{kp}| > \epsilon\}} X_{kp}^2 d\mathbb{P} = 0, \quad \text{for all } \epsilon > 0. \quad (4.34)$$

Condition (4.34) is called the *Lindeberg condition*. It states that for arbitrarily small  $\epsilon > 0$ , the contribution to the accumulated row variance from those terms with absolute value greater than  $\epsilon$  becomes negligible as the row index approaches infinity.

Generally, the Lindeberg condition is merely sufficient. The *Feller Theorem* characterizes the situation in which the Lindeberg condition is also necessary.

**Theorem 4.2** *Let the sequence  $\{X_{kp}\}$  be independent with  $\mu_{kp} = 0$  for all  $p$  and  $k$  and with variance sequence  $\{\sigma_{kp}^2\}$ . If the limiting distribution of  $X_k$  is the standard normal distribution and*

$$\lim_{k \rightarrow \infty} \max_{1 \leq p \leq n_k} \mathbb{P}(|X_{kp}| > \epsilon) = 0, \quad \text{for all } \epsilon > 0, \quad (4.35)$$

*then the Lindeberg condition holds.*

In the following, we prove that condition (4.35) is satisfied but condition (4.34) is not fulfilled for our random variables. For this reason, they do not converge to a normal distribution when the number of summands approaches infinity.

#### 4.4.2 Transformation

We transform the random variables  $C_{ii}^\uparrow$  and  $C_i^\downarrow$  to random variables meeting the assumptions of Theorem 4.1. That is, each random variable has an expected value of zero and the sum of the variances is one. This transformation as well as the application of the theorems hold for  $C_{ii}^\uparrow$  and  $C_i^\downarrow$  likewise.

We have a random variable for each pixel in the best server area of base station antenna  $i$ . For  $p \in A_i$ , it reads as

$$Y_p := \sum_{s \in S} l_s(p) m_s(p). \quad (4.36)$$

The variable  $m_s(p) \in \mathbb{N}$  denotes the number of mobiles of service  $s$  in position  $p$ . The value  $l_s(p) > 0$  is constant for each  $s \in S$ . We restrict ourselves to considering merely those services with an activity factor and CIR target

greater than zero. That is, in the uplink direction,  $S$  does not include the service “File Download”, for example. The values  $l_s(p)$  are given in the uplink direction by

$$l_s(p) = \frac{\alpha_s^\uparrow \mu_s^\uparrow}{1 + \alpha_s^\uparrow \mu_s^\uparrow}.$$

In the downlink, we have

$$l_s(p) = c_{ip}^\downarrow \frac{\alpha_s^\downarrow \mu_s^\downarrow}{1 + \bar{\omega}_p \alpha_s^\downarrow \mu_s^\downarrow}.$$

The value  $c_{ip}^\downarrow$  is defined by (4.27). The random variables  $Y_p$  are summed up over all pixels in the best server area of base station antenna  $i$ . That is,

$$Y_i := \sum_{p \in A_i} Y_p. \quad (4.37)$$

Each row of the triangular array corresponds to a partition of the cell area  $A_i$  into pixels  $p$ . That is,  $A_i^{(k)} = \{1, \dots, n_k\}$  in the  $k$ th row. This division gets finer in each step or row. Throughout this section, we consider a partition that is constructed in following way. The value  $d \in \{2, 3\}$  denotes the dimension of the given planning area. In step  $k$ , divide each pixel  $p = 1, \dots, n_k$  into  $2^d$  sub-pixels of equal size and distribute  $T_s(p)$  uniformly to each sub-pixel for all  $s \in S$ . In doing so,  $p$  ranges from 1 to  $n_{k+1} = 2^d n_k$  in row  $k + 1$ . It holds that

$$n_k = 2^{dk}. \quad (4.38)$$

As the row index  $k$  goes to infinity, the number of pixels also goes to infinity while the average number of users in each pixel approaches zero.

This problem can be transformed by normalizing the random variables  $Y_p$ , such that Theorem 4.1 is applicable. We set

$$\mu_p := \mathbb{E}[Y_p], \quad \sigma_p^2 := \mathbb{V}[Y_p], \quad \text{and} \quad s_k^2 := \sum_{p=1}^{n_k} \sigma_p^2. \quad (4.39)$$

The traffic intensities in position  $p$  are mutually independent for different services. For this reason, we obtain

$$\mu_p = \sum_{s \in S} l_s(p) T_s(p) \quad \text{and} \quad \sigma_p^2 = \sum_{s \in S} l_s(p)^2 T_s(p). \quad (4.40)$$

We define

$$X_{kp} := \frac{Y_p - \mu_p}{s_k}. \quad (4.41)$$

These random variables are mutually independent. As stated in Section 2.5.2, the traffic intensities in pairwise distinct locations are independent random variables. The weighted summation of such variables does not change this characteristic. Hence, the random variables  $Y_p$  defined in (4.36) are independent. This property is not affected by the division and subtraction of a constant as done in (4.39). For the expected value of  $X_{kp}$ , we obtain

$$\mu_{kp} = \frac{1}{s_k} \mathbb{E}[Y_p - \mu_p] = 0.$$

Furthermore, equation (4.33) is met because the variables  $Y_p$  are mutually independent. It holds:

$$\begin{aligned} \mathbb{E}[X_k^2] &= \mathbb{V}[X_k] = \frac{1}{s_k^2} \mathbb{E} \left[ \left( \sum_{p=1}^{n_k} (Y_p - \mu_p) \right)^2 \right] = \frac{1}{s_k^2} \mathbb{E} \left[ \left( \sum_{p=1}^{n_k} Y_p - \sum_{p=1}^{n_k} \mu_p \right)^2 \right] \\ &= \frac{1}{s_k^2} \mathbb{E} \left[ \left( \sum_{p=1}^{n_k} Y_p - \mathbb{E} \left[ \sum_{p=1}^{n_k} Y_p \right] \right)^2 \right] = \frac{1}{s_k^2} \mathbb{V} \left[ \sum_{p=1}^{n_k} Y_p \right] \\ &= \frac{1}{s_k^2} \sum_{p=1}^{n_k} \mathbb{V}[Y_p] = \sum_{p=1}^{n_k} \frac{1}{s_k^2} \sigma_p^2 = \sum_{p=1}^{n_k} \sigma_{kp}^2 = 1. \end{aligned}$$

Consequently, the conditions of Theorem 4.1 are fulfilled with this transformation.

### 4.4.3 Proof

Now, we prove that condition (4.35) is met for the transformed random variables but (4.34) does not hold. Hence follows, that the limiting distribution of the transformed random variables  $X_k$  is not the standard normal distribution. In order to prove this, we first need the following:

**Proposition 4.1** *For each row index  $k$  of the triangular array (4.31), the value  $s_k^2$  defined in (4.39) is bounded above and below by constants within the open interval  $(0, \infty)$ , which are independent of  $k$ .*

**Proof.** The expected traffic intensity in the entire region  $A_i^{(k)}$  is constant in every step  $k$ . That is, for all  $k$  holds

$$T_i := \sum_{p \in A_i^{(k)}} \sum_{s \in S} T_s(p) \in (0, \infty). \quad (4.42)$$

The values  $l_s(p)$  are bounded by constants for all partitions of the cell area, that is, for all steps  $k$ . We denote by  $\hat{l}_i$  the upper bound and by  $\check{l}_i$  the lower bound of  $l_s(p)$  in cell  $i$ . Hence,

$$\check{l}_i \leq l_s(p) \quad \text{and} \quad \hat{l}_i \geq l_s(p) \quad \forall p \in A_i^{(k)}, k \in \mathbb{N}, s \in S.$$

In the uplink direction, such bounds are given by

$$\check{l}_i = \frac{1}{2} \min_{s \in S} \alpha_s^\uparrow \mu_s^\uparrow \quad \text{and} \quad \hat{l}_i = 1,$$

for example, since  $0 < \alpha_s^\uparrow \mu_s^\uparrow \leq 1$  for all  $s \in S$ . In the downlink, we can set the lower bound to

$$\check{l}_i = \frac{1}{2} \check{\omega}_i p_i^{\max\downarrow} \min_{s \in S} \alpha_s^\downarrow \mu_s^\downarrow.$$

The value  $\check{\omega}_i$  denotes the lower bound of  $\bar{\omega}_p$  for all partitions. This constant exists because for sufficiently large  $k$ , the sub-pixels in which we refine a pixel have the same orthogonality factor as the original pixel. The sub-pixels are that small that the propagation characteristics of the radiowaves are equal in each sub-pixel and thus the orthogonality factors. It holds that  $\check{\omega}_i > 0$  since we do not have perfect orthogonality in the whole area. Moreover,  $0 < \alpha_s^\downarrow \mu_s^\downarrow \leq 1$  applies for all  $s \in S$ . An upper bound in downlink is given by

$$\hat{l}_i = p_i^{\max\downarrow} + \sum_{j \neq i} p_j^{\max\downarrow} + \frac{\hat{\eta}_i}{\check{\gamma}_i^\downarrow}.$$

Here,  $\check{\gamma}_i^\downarrow$  denotes the lower bound of  $\gamma_{ip}^\downarrow$  for all partitions of  $A_i$ . The best server area of antenna  $i$  does not contain pixels that are not covered. For a pixel to be covered, the received power from the antenna has to be sufficiently high (cf. Section 2.2). Therefore,  $\check{\gamma}_i^\downarrow$  exists and it holds that  $\check{\gamma}_i^\downarrow > 0$ . The value  $\hat{\eta}_i$  is the upper bound of  $\eta_p$  for all  $k$ . It is clear that the noise in the cell area does not rise infinitely by refining the partition of the region. It applies that  $\frac{\eta_p}{\gamma_{ip}^\downarrow} \leq \frac{\hat{\eta}_i}{\check{\gamma}_i^\downarrow}$  for every division of  $A_i$ . Because of  $\frac{\gamma_{jp}^\downarrow}{\gamma_{ip}^\downarrow} \leq 1$ , an upper bound of  $\frac{\gamma_{jp}^\downarrow}{\gamma_{ip}^\downarrow} p_j^{\max\downarrow}$  is given by  $p_j^{\max\downarrow}$  for all  $j \neq i$ . Furthermore,  $\bar{\omega}_p \in (0, 1]$  for all  $p$ . Hence, we obtain  $\bar{\omega}_p p_i^{\max\downarrow} \leq p_i^{\max\downarrow}$  and  $\frac{\alpha_s^\downarrow \mu_s^\downarrow}{1 + \bar{\omega}_p \alpha_s^\downarrow \mu_s^\downarrow} \leq \alpha_s^\downarrow \mu_s^\downarrow \leq 1$  for all  $s \in S$ .

It holds that

$$0 < \check{l}_i \leq \hat{l}_i < \infty \quad \text{for all } k \in \mathbb{N}. \quad (4.43)$$

The following expression is satisfied for all  $k$ :

$$\begin{aligned} s_k^2 &= \sum_{p=1}^{n_k} \sum_{s \in S} l_s(p)^2 T_s(p) \\ &\leq \hat{l}_i^2 \sum_{p=1}^{n_k} \sum_{s \in S} T_s(p) = \hat{l}_i^2 T_i. \end{aligned}$$

The same can be applied in the reverse direction with  $\check{l}_i$ . Consequently, we obtain

$$\check{l}_i^2 T_i \leq s_k^2 \leq \hat{l}_i^2 T_i.$$

□

Next, we prove the following proposition:

**Proposition 4.2** *The random variables  $X_{kp}$  defined by (4.41) satisfy condition (4.35).*

**Proof.** According to the way we refine the pixel grid, the user intensity in each position approaches zero for every service as the number of pixels  $n_k = |A_i^{(k)}|$  goes to infinity. That is,

$$k \rightarrow \infty \Rightarrow T_s(p) \rightarrow 0 \quad \forall p \in A_i^{(k)}, s \in S. \quad (4.44)$$

From equation (4.44) we obtain for all  $\tau > 0$ :

$$\begin{aligned} \mathbb{P}(m_s(p) > \tau) &= 1 - \mathbb{P}(m_s(p) \leq \tau) \\ &\leq 1 - \mathbb{P}(m_s(p) = 0) \\ &= 1 - e^{-T_s(p)} \frac{(T_s(p))^0}{0!} \\ &= 1 - e^{-T_s(p)} \\ &\xrightarrow[k \rightarrow \infty]{} 1 - 1 = 0 \quad \forall p \in A_i^{(k)}, s \in S. \end{aligned}$$

Because of  $\mathbb{P}(m_s(p) > \tau) \geq 0$ , above formulation expresses that

$$\lim_{k \rightarrow \infty} \mathbb{P}(m_s(p) > \tau) = 0 \quad \forall p \in A_i^{(k)}, s \in S, \tau > 0. \quad (4.45)$$

For all  $p = 1, \dots, n_k$  and  $\epsilon > 0$  we consider:

$$\mathbb{P}(|X_{kp}| > \epsilon) = \mathbb{P}\left(\frac{|\sum_{s \in S} l_s(p)[m_s(p) - T_s(p)]|}{s_k} > \epsilon\right)$$

We define  $\delta := \epsilon s_k$ . Due to Proposition 4.1,  $\delta \in (0, \infty)$  holds. It applies

$$\begin{aligned} \mathbb{P}\left(\frac{\left|\sum_{s \in S} l_s(p) [m_s(p) - T_s(p)]\right|}{s_k} > \epsilon\right) &= \mathbb{P}\left(\left|\sum_{s \in S} l_s(p) [m_s(p) - T_s(p)]\right| > \delta\right) \\ &\leq \mathbb{P}\left(\sum_{s \in S} l_s(p) |m_s(p) - T_s(p)| > \delta\right) \\ &\leq \mathbb{P}\left(|S| \hat{l}_i \max_{s \in S} |m_s(p) - T_s(p)| > \delta\right). \end{aligned}$$

We set  $\tau := \frac{\delta}{|S| \hat{l}_i}$ . Because of  $|S|, \hat{l}_i \in (0, \infty)$  (cf. (4.43)), it holds that  $\tau \in (0, \infty)$ . For ease of notation, we denote by 1 the index  $s \in S$  for which the maximum value of  $|m_s(p) - T_s(p)|$  is attained. We obtain

$$\mathbb{P}\left(|S| \hat{l}_i \max_{s \in S} |m_s(p) - T_s(p)| > \delta\right) = \mathbb{P}\left(|m_1(p) - T_1(p)| > \tau\right).$$

Because of (4.44) and (4.45), it holds for all  $\tau > 0$  that

$$\lim_{k \rightarrow \infty} \mathbb{P}\left(|m_1(p) - T_1(p)| > \tau\right) = \lim_{k \rightarrow \infty} \mathbb{P}(m_1(p) > \tau) = 0.$$

In conclusion, for all  $p = 1, \dots, n_k$  it applies that

$$\lim_{k \rightarrow \infty} \mathbb{P}\left(|X_{kp}| > \epsilon\right) = 0 \quad \text{for all } \epsilon > 0.$$

Therefore, the above expression holds for the maximum value of  $X_{kp}$  over all  $p = 1, \dots, n_k$ .  $\square$

Due to Theorem 4.2, the Lindeberg condition (4.34) is necessary for the random variables  $X_k$  to converge against the standard normal distribution. That is, if the condition is not fulfilled the variables  $X_k$  do not approach the standard normal distribution as  $k$  goes to infinity. The non-fulfillment of the Lindeberg condition by the random variables is shown in the next step:

**Proposition 4.3** *The random variables  $X_{kp}$  defined by (4.41) do not satisfy the Lindeberg condition (4.34).*

**Proof.** We substitute  $X_{kp}$  by its definition (4.41) in the Lindeberg condition. This yields the following expression to prove:

$$\lim_{k \rightarrow \infty} \sum_{p=1}^{n_k} \frac{1}{s_k^2} \int_{\{|Y_p - \mu_p| > \epsilon s_k\}} (Y_p - \mu_p)^2 d\mathbb{P} \neq 0, \quad \text{for any } \epsilon > 0.$$

Because of Proposition 4.1, we just need to show that

$$\lim_{k \rightarrow \infty} \sum_{p=1}^{n_k} \int_{\{|Y_p - \mu_p| > \epsilon s_k\}} (Y_p - \mu_p)^2 d\mathbb{P} \neq 0, \quad \text{for any } \epsilon > 0.$$

Due to the boundedness of  $s_k$  and  $l_s(p)$  by constants within  $(0, \infty)$  (cf. Proposition 4.1 and (4.43)), above expression is equivalent to:

$$\lim_{k \rightarrow \infty} \sum_{p=1}^{n_k} \sum_{s \in S} \int_{\{|m_s(p) - T_s(p)| > \delta\}} l_s(p)^2 (m_s(p) - T_s(p))^2 d\mathbb{P} \neq 0, \quad \text{for any } \delta > 0.$$

Since  $T_i > 0$  applies, there exist at least one pixel  $p \in A_i^{(k)}$  and one service  $s \in S$  with  $T_s(p) > 0$ . In the case that  $T_s(p) = 0$  for any tuple  $(p, s)$ , it holds that  $m_s(p) = 0$  with probability one. Hence, such tuples  $(p, s)$  are not taken into account in the above integral. Without loss of generality, we thus assume that

$$T_s(p) > 0 \quad \forall p \in A_i^{(k)}, k \in \mathbb{N}, s \in S. \quad (4.46)$$

Following formulation applies for all  $\delta > 0$  because of the special refinement we use (cf. (4.38)):

$$\begin{aligned} & \sum_{p=1}^{n_k} \sum_{s \in S} \int_{\{|m_s(p) - T_s(p)| > \delta\}} l_s(p)^2 (m_s(p) - T_s(p))^2 d\mathbb{P} \\ & \geq 2^{dk} |S| \check{l}_i^2 \min_{p \in A_i^{(k)}, s \in S} \int_{\{|m_s(p) - T_s(p)| > \delta\}} (m_s(p) - T_s(p))^2 d\mathbb{P}. \end{aligned}$$

Without loss of generality, let 1 be the index in  $S$  and  $p^*$  be the pixel in  $A_i^{(k)}$  for which the minimum value in the above expression is attained. For sufficiently large  $k$ , it holds that  $T_1(p^*) < \frac{1}{2}$  due to (4.44). Thus, we obtain for  $\delta \leq \frac{1}{2}$

$$\begin{aligned} & 2^{dk} |S| \check{l}_i^2 \int_{\{|m_1(p^*) - T_1(p^*)| > \delta\}} (m_1(p^*) - T_1(p^*))^2 d\mathbb{P} \\ & = 2^{dk} |S| \check{l}_i^2 \int_{\{m_1(p^*) \geq 1\}} (m_1(p^*) - T_1(p^*))^2 d\mathbb{P} \\ & \geq 2^{dk} |S| \check{l}_i^2 \int_{\{m_1(p^*) = 1\}} (m_1(p^*) - T_1(p^*))^2 d\mathbb{P} \\ & = 2^{dk} |S| \check{l}_i^2 (1 - T_1(p^*))^2 e^{-T_1(p^*)} T_1(p^*). \end{aligned}$$

In (2.3), we expressed the expected number of users for one service in a region of the planning area by using a user density. With this equation, we receive

$$\begin{aligned} & 2^{dk} |S| \check{l}_i^2 (1 - T_1(p^*))^2 e^{-T_1(p^*)} T_1(p^*) \\ & = 2^{dk} |S| \check{l}_i^2 (1 - T_1(p^*))^2 e^{-T_1(p^*)} \int_{p^*} f_1(p) dp. \end{aligned}$$

We define

$$c := f_1(p^*).$$

Due to (4.46), it holds that  $c > 0$ . The following expression is satisfied:

$$\int_{p^*} f_1(p) dp = f_1(p^*) \lambda^d(p^*) = c \lambda^d(A_i) 2^{-dk} > 0.$$

For this reason, we obtain

$$\begin{aligned} & 2^{dk} |S| \check{l}_i^2 (1 - T_1(p^*))^2 e^{-T_1(p^*)} \int_{p^*} f_1(x) dx \\ &= 2^{dk} |S| \check{l}_i^2 (1 - T_1(p^*))^2 e^{-T_1(p^*)} c \lambda^d(A_i) 2^{-dk} \\ &= |S| \check{l}_i^2 (1 - T_1(p^*))^2 e^{-T_1(p^*)} c \lambda^d(A_i). \end{aligned}$$

Because of (4.44), it holds that

$$\lim_{k \rightarrow \infty} (1 - T_1(p^*))^2 = 1 \quad \text{and} \quad \lim_{k \rightarrow \infty} e^{-T_1(p^*)} = 1.$$

Hence follows

$$\lim_{k \rightarrow \infty} |S| \check{l}_i^2 (1 - T_1(p^*))^2 e^{-T_1(p^*)} c \lambda^d(A_i) = |S| \check{l}_i^2 c \lambda^d(A_i) > 0.$$

□

We proved that the random variables  $C_{ii}^\uparrow$  and  $C_i^\downarrow$ , respectively, do not converge against a normal distribution with expected value  $\mathbb{E}[C_{ii}^\uparrow]$  and  $\mathbb{E}[C_i^\downarrow]$ , respectively, and variance  $\mathbb{V}[C_{ii}^\uparrow]$  and  $\mathbb{V}[C_i^\downarrow]$ , respectively.

#### 4.4.4 Discussion

We know that the assumption of  $C_{ii}^\uparrow$  and  $C_i^\downarrow$  being normally distributed does not hold. However, it is reasonable to approximate the distribution of these random variables by a normal distribution. Their exact distribution is a sum of weighted Poisson distributions. This is difficult to handle. A probability for each possible value in the range of the particular random variable has to be computed. This is considerably more complex than using the known quantiles of the normal distribution. Hence, we would have the same problem as with Monte Carlo simulation. The method would be precise but too computationally expensive for some purposes. For this reason, we have to make a compromise and take systematical estimation errors.

The accuracy we get with the approximation by a normal distribution seems to be acceptable. Figures 4.1 and 4.2 illustrate this. The figures depict the exact distribution of  $C_{ii}^\uparrow$  and  $C_i^\downarrow$  for one cell, each described by a histogram arising from the evaluation of 1000 traffic snapshots. The red curve represents a normal distribution with expected value  $\mathbb{E}[C_{ii}^\uparrow]$  and  $\mathbb{E}[C_i^\downarrow]$ , respectively, and variance  $\mathbb{V}[C_{ii}^\uparrow]$  and  $\mathbb{V}[C_i^\downarrow]$ , respectively. Particularly in the downlink direction, there are errors we make with this approximation. This is due to the higher variance in downlink that causes higher deviations from the expected value. However, these errors are acceptable in exchange for a quick and simple way to determine the probability density of the random variables.

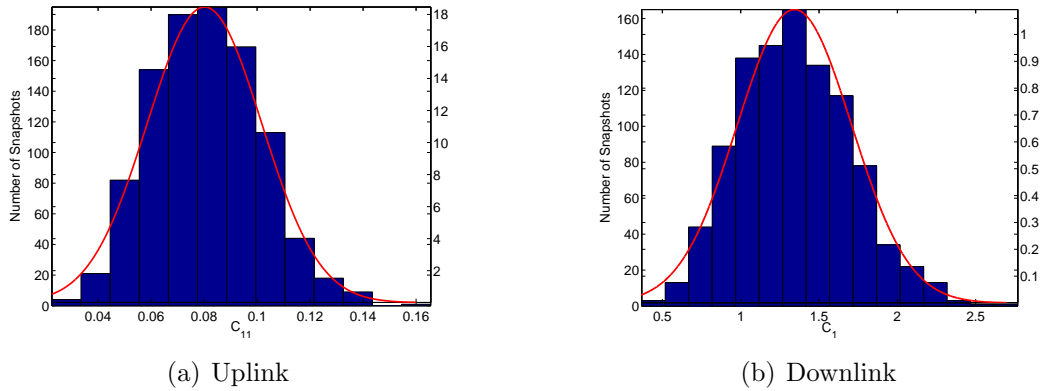


Figure 4.1: Distribution of the random variable for service speech telephony

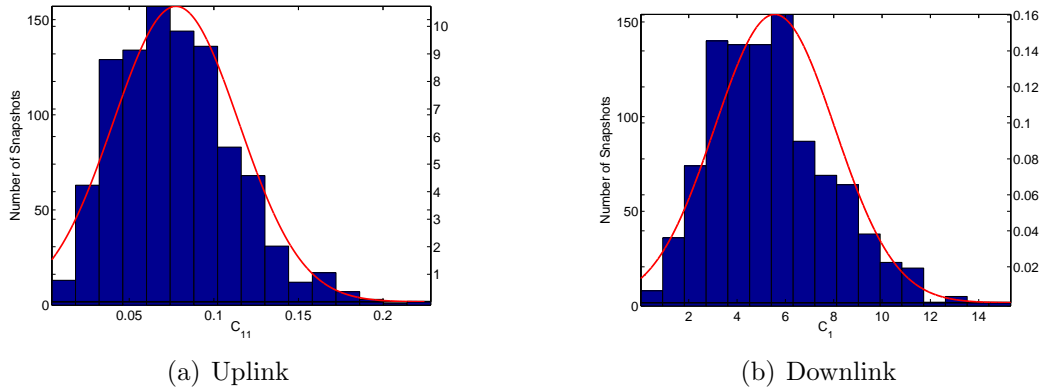


Figure 4.2: Distribution of the random variable for a service mix

## 5 Power Knapsack

An alternative approach of approximating the blocking rates of the cells in a UMTS radio network is discussed in this chapter. We understand the given task as a *Knapsack problem*. In such a problem, we are given a set of elements, each with a certain weight and value. The task is to find a subset out of the given set in a way that its total weight does not exceed a certain bound and that its accumulated value is at maximum.

In our case, we have a kind of fractional power knapsack. We make two central assumptions in this model:

- (1) The power of the own antenna is at its maximum.
- (2) We use constant estimates for the powers of the other antennas.

With these conditions, we are able to assign a specified weight to each mobile in our sector. This weight represents the power that would be received from or consumed by the user if it was served under the above assumptions. The bound in our Knapsack problem is the maximum power the antenna is able to receive from or transmit on the dedicated channels. Due to the assumption of compressible user demand (cf. Section 3.1.3) it is possible to “fill” our power knapsack until the bound is met exactly. The surplus is not served. Hence, the ratio of unserved user weight to the total weight of all mobiles in the sector represents the blocking rate. In our basic model, we assume the power level of the considered antenna to be at its maximum if blocking occurs. From this point of view, condition (1) is reasonable. We use the expected coupling approach from Section 3.1.2 to assess the powers of the other base station antennas.

First, the method is introduced at a set of mobile stations given by a traffic snapshot. Afterwards, we consider the distribution of the accumulated weight of all mobiles in the cell. This random variable is assumed to be normally distributed as sum of many independent random variables. We determine the expected value of the average blocking rate depending on the total weight of all users in the cell.

## 5.1 Snapshot Based Derivation

This section derives the approach for a traffic snapshot. The basic idea can be found in [1], where it was introduced merely for the downlink direction. This thesis also covers the uplink afterwards and enhances the proposed model.

### 5.1.1 Downlink

For a base station antenna  $i \in \mathcal{N}$ , the size of the power knapsack  $\kappa_i^\downarrow$  is defined as

$$\kappa_i^\downarrow := p_i^{\max\downarrow} - p_i^{(c)}. \quad (5.1)$$

This value represents the mentioned upper bound of our cell. We assume, that the present mobiles in cell  $i$  consume exactly this power. The total average transmission power of antenna  $i$  allocated to the traffic on dedicated channels if all mobile stations in its sector are served reads as  $\sum_{m \in \mathcal{M}_i} \alpha_m^\downarrow p_{im}^\downarrow$ . The value  $p_{im}^\downarrow$  is the transmission power from antenna  $i$  to mobile  $m$  under the condition that the antenna transmits at its maximum power level  $p_i^{\max\downarrow}$  (assumption (1)). The power  $p_{im}^\downarrow$  can be determined using the CIR target equality introduced in (2.8). Due to assumptions (1) and (2), we obtain

$$\mu_m^\downarrow = \frac{\gamma_{im}^\downarrow p_{im}^\downarrow}{\gamma_{im}^\downarrow \bar{\omega}_m \left( p_i^{\max\downarrow} - \alpha_m^\downarrow p_{im}^\downarrow \right) + \sum_{j \neq i} \gamma_{jm}^\downarrow \tilde{p}_j^\downarrow + \eta_m}.$$

The powers  $\tilde{p}_j^\downarrow$  for all  $j \neq i$  are the solutions of the system of equations (3.14) using the expected coupling matrix. Solving the above equation for  $p_{im}^\downarrow$  results in

$$p_{im}^\downarrow = \frac{l_m^\downarrow}{\alpha_m^\downarrow} \left( \bar{\omega}_m p_i^{\max\downarrow} + \sum_{j \neq i} \frac{\gamma_{jm}^\downarrow}{\gamma_{im}^\downarrow} \tilde{p}_j^\downarrow + \frac{\eta_m}{\gamma_{im}^\downarrow} \right). \quad (5.2)$$

The downlink user load  $l_m^\downarrow$  for mobile station  $m$  is defined by (3.6).

In Section 2.5.3, we derived the condition for no blocking to occur in cell  $i$ . With the definition (5.1) of  $\kappa_i^\downarrow$ , the downlink inequality of (2.10) can be transformed into

$$\sum_{m \in \mathcal{M}_i} \alpha_m^\downarrow p_{im}^\downarrow \leq \kappa_i^\downarrow. \quad (5.3)$$

It is convenient to write this as

$$\frac{1}{\kappa_i^\downarrow} \sum_{m \in \mathcal{M}_i} \alpha_m^\downarrow p_{im}^\downarrow \leq 1. \quad (5.4)$$

The values  $\alpha_m^\downarrow p_{im}^\downarrow$  are the weights of our Knapsack problem for each mobile in the sector. We define the left hand side of inequality (5.4) as  $K_i^\downarrow$ , that is,

$$K_i^\downarrow := \frac{1}{\kappa_i^\downarrow} \sum_{m \in \mathcal{M}_i} \alpha_m^\downarrow p_{im}^\downarrow. \quad (5.5)$$

This can be understood as the content that shall fit into the power knapsack. The variable  $K_i^\downarrow$  depends on the set of served mobile stations  $\mathcal{M}_i$  since  $p_{im}^\downarrow$  might be different for different users. The value  $K_i^\downarrow$  approximates the fraction of total available transmission power of antenna  $i$  spent on the traffic on dedicated channels. Inequality (5.4) states that blocking occurs if this fraction is greater than one. That means, we “fill” our power knapsack with mobile weights  $\alpha_m^\downarrow p_{im}^\downarrow$  until the bound of one is reached exactly. In doing so, some of these weights might be taken fractionally. The (fractions of) user weights contributing to the excess are rejected. Therefore, the average down-link blocking rate  $\tilde{b}_i^\downarrow$  of base station antenna  $i$  for the considered snapshot is given by

$$\tilde{b}_i^\downarrow = \begin{cases} 0 & \text{for } K_i^\downarrow \leq 1 \\ \frac{K_i^\downarrow - 1}{K_i^\downarrow} & \text{for } K_i^\downarrow > 1. \end{cases} \quad (5.6)$$

We verify this formula by showing that

$$\tilde{b}_i^\downarrow = 1 - \lambda_i^\downarrow.$$

The scaling factor  $\lambda_i^\downarrow$  – introduced in Section 3.1.3 – is defined by:

$$\lambda_i^\downarrow = \min \left\{ 1, \frac{p_i^{\max\downarrow} - p_i^{(c)}}{C_{ii}^\downarrow p_i^{\max\downarrow} + \sum_{j \neq i} C_{ij}^\downarrow \tilde{p}_j^\downarrow + p_i^{(\eta)}} \right\}. \quad (5.7)$$

This formulation can be derived from (3.14) since we estimate the other antennas’ powers  $\tilde{p}_j^\downarrow$ ,  $j \neq i$  (assumption (2)).

- (i) In the case that  $K_i^\downarrow \leq 1$ , equation (5.3) holds. Substituting  $p_{im}^\downarrow$  according to (5.2) yields

$$\sum_{m \in \mathcal{M}_i} l_m^\downarrow \left( \bar{\omega}_m p_i^{\max\downarrow} + \sum_{j \neq i} \frac{\gamma_{jm}^\downarrow}{\gamma_{im}^\downarrow} \tilde{p}_j^\downarrow + \frac{\eta_m}{\gamma_{im}^\downarrow} \right) \leq \kappa_i^\downarrow.$$

This is equivalent to

$$C_{ii}^\downarrow p_i^{\max\downarrow} + \sum_{j \neq i} C_{ij}^\downarrow \tilde{p}_j^\downarrow + p_i^{(\eta)} \leq p_i^{\max\downarrow} - p_i^{(c)}.$$

Hence follows, that  $\lambda_i^\downarrow = 1$  and thus  $\tilde{b}_i^\downarrow = 1 - \lambda_i^\downarrow$ .

(ii) In the case that  $K_i^\downarrow > 1$ , it holds that

$$C_{ii}^\downarrow p_i^{\max\downarrow} + \sum_{j \neq i} C_{ij}^\downarrow \tilde{p}_j^\downarrow + p_i^{(\eta)} > p_i^{\max\downarrow} - p_i^{(c)}.$$

Therefore,  $\lambda_i^\downarrow$  is assessed by

$$\lambda_i^\downarrow = \frac{p_i^{\max\downarrow} - p_i^{(c)}}{C_{ii}^\downarrow p_i^{\max\downarrow} + \sum_{j \neq i} C_{ij}^\downarrow \tilde{p}_j^\downarrow + p_i^{(\eta)}}.$$

For  $\tilde{b}_i^\downarrow$ , we obtain

$$\begin{aligned} \tilde{b}_i^\downarrow &= \frac{K_i^\downarrow - 1}{K_i^\downarrow} = 1 - \frac{1}{\frac{1}{\kappa_i^\downarrow} \sum_{m \in \mathcal{M}_i} \alpha_m^\downarrow p_{im}^\downarrow} \\ &= 1 - \frac{\kappa_i^\downarrow}{\sum_{m \in \mathcal{M}_i} l_m^\downarrow (\bar{\omega}_m p_i^{\max\downarrow} + \sum_{j \neq i} \frac{\gamma_{jm}^\downarrow}{\gamma_{im}^\downarrow} \tilde{p}_j^\downarrow + \frac{\eta_m}{\gamma_{im}^\downarrow})} \\ &= 1 - \frac{p_i^{\max\downarrow} - p_i^{(c)}}{C_{ii}^\downarrow p_i^{\max\downarrow} + \sum_{j \neq i} C_{ij}^\downarrow \tilde{p}_j^\downarrow + p_i^{(\eta)}} = 1 - \lambda_i^\downarrow. \end{aligned}$$

□

## 5.1.2 Uplink

In the uplink direction, a base station antenna does not only receive signals from the mobile stations in the own sector. Instead, the reception power of an antenna is composed of the received powers of all users in the entire planning area. Depending on the attenuation factor from a mobile station to the considered antenna, the strength of the incoming power varies. We assume that the contributions of the other cells  $j \neq i$  are constant at their expected average values. That is,

$$\sum_{j \neq i} \tilde{C}_{ij}^\uparrow \tilde{p}_j^\uparrow = \text{constant}.$$

The matrix  $\tilde{C}^\uparrow$  is the scaled, expected cell load coupling matrix. The scaling describes the blocking behavior of a cell. An antenna rejects users exceeding its power limits. In order to represent this functionality, the scaling has to be involved. The maximum power antenna  $i$  can receive from the mobiles in the own cell reads as

$$\kappa_i^\uparrow = p_i^{\max\uparrow} - \sum_{j \neq i} \tilde{C}_{ij}^\uparrow \tilde{p}_j^\uparrow - \eta_i. \quad (5.8)$$

This is the upper bound or size of our power knapsack.

The total average reception power arising from all present users in the cell if none of them is blocked is given by  $\sum_{m \in \mathcal{M}_i} \gamma_{mi}^\uparrow \alpha_m^\uparrow p_m^\uparrow$ . With condition (1), we obtain from the CIR target equality (2.6):

$$p_m^\uparrow = \frac{l_m^\uparrow}{\gamma_{mi}^\uparrow \alpha_m^\uparrow} p_i^{\max\uparrow}. \quad (5.9)$$

The situation that there is enough capacity to serve all users in cell  $i$  in uplink is characterized by

$$\sum_{m \in \mathcal{M}_i} \gamma_{mi}^\uparrow \alpha_m^\uparrow p_m^\uparrow \leq \kappa_i^\uparrow. \quad (5.10)$$

We transform this inequality into

$$\frac{1}{\kappa_i^\uparrow} \sum_{m \in \mathcal{M}_i} \gamma_{mi}^\uparrow \alpha_m^\uparrow p_m^\uparrow \leq 1. \quad (5.11)$$

The weights of our knapsack are the values  $\gamma_{mi}^\uparrow \alpha_m^\uparrow p_m^\uparrow$  for each mobile station in cell  $i$ . We define the fraction of total possible reception power at antenna  $i$  stemming from the traffic on dedicated channels of the own cell by

$$K_i^\uparrow := \frac{1}{\kappa_i^\uparrow} \sum_{m \in \mathcal{M}_i} \gamma_{mi}^\uparrow \alpha_m^\uparrow p_m^\uparrow. \quad (5.12)$$

Due to inequality (5.11), we can “put” mobile powers into the power knapsack until we meet the upper bound of one exactly. That part of the total offered mobile reception power  $K_i^\uparrow$  greater than one is rejected. Thus, for the average blocking rate  $\tilde{b}_i^\uparrow$  at base station antenna  $i$  in the given traffic snapshot holds:

$$\tilde{b}_i^\uparrow = \begin{cases} 0 & \text{for } K_i^\uparrow \leq 1 \\ \frac{K_i^\uparrow - 1}{K_i^\uparrow} & \text{for } K_i^\uparrow > 1. \end{cases} \quad (5.13)$$

We prove this formula by deriving that

$$\tilde{b}_i^\uparrow = 1 - \lambda_i^\uparrow.$$

If blocking occurs in cell  $i$ , that is,  $\lambda_i^\uparrow < 1$ , it holds that

$$p_i^{\max\uparrow} = C_{ii}^\uparrow \lambda_i^\uparrow p_i^{\max\uparrow} + \sum_{j \neq i} \tilde{C}_{ij}^\uparrow \tilde{p}_j^\uparrow + \eta_i$$

due to (3.16). Hence, the scaling factor  $\lambda_i^\uparrow$  is given by

$$\lambda_i^\uparrow = \min \left\{ 1, \frac{p_i^{\max\uparrow} - \sum_{j \neq i} \tilde{C}_{ij}^\uparrow \tilde{p}_j^\uparrow - \eta_i}{C_{ii}^\uparrow p_i^{\max\uparrow}} \right\}. \quad (5.14)$$

- (i) Let  $K_i^\uparrow \leq 1$  hold. That is, inequality (5.10) is satisfied. If we replace  $p_m^\uparrow$  according to (5.9), this results in

$$\sum_{m \in \mathcal{M}_i} l_m^\uparrow p_i^{\max\uparrow} \leq \kappa_i^\uparrow.$$

This can be written as

$$C_{ii}^\uparrow p_i^{\max\uparrow} \leq p_i^{\max\uparrow} - \sum_{j \neq i} \tilde{C}_{ij}^\uparrow \tilde{p}_j^\uparrow - \eta_i.$$

Therefore,  $\lambda_i^\uparrow = 1$  and  $\tilde{b}_i^\uparrow = 1 - \lambda_i^\uparrow$ .

- (ii) In the case that  $K_i^\uparrow > 1$ , it holds that

$$C_{ii}^\uparrow p_i^{\max\uparrow} > p_i^{\max\uparrow} - \sum_{j \neq i} \tilde{C}_{ij}^\uparrow \tilde{p}_j^\uparrow - \eta_i.$$

Hence follows, that

$$\lambda_i^\uparrow = \frac{p_i^{\max\uparrow} - \sum_{j \neq i} \tilde{C}_{ij}^\uparrow \tilde{p}_j^\uparrow - \eta_i}{C_{ii}^\uparrow p_i^{\max\uparrow}}.$$

For the average blocking rate  $\tilde{b}_i^\uparrow$ , we receive

$$\begin{aligned} \tilde{b}_i^\uparrow &= \frac{K_i^\uparrow - 1}{K_i^\uparrow} = 1 - \frac{1}{\frac{1}{\kappa_i^\uparrow} \sum_{m \in \mathcal{M}_i} \gamma_{mi}^\uparrow \alpha_m^\uparrow p_m^\uparrow} \\ &= 1 - \frac{\kappa_i^\uparrow}{\sum_{m \in \mathcal{M}_i} l_m^\uparrow p_i^{\max\uparrow}} \\ &= 1 - \frac{p_i^{\max\uparrow} - \sum_{j \neq i} \tilde{C}_{ij}^\uparrow \tilde{p}_j^\uparrow - \eta_i}{C_{ii}^\uparrow p_i^{\max\uparrow}} = 1 - \lambda_i^\uparrow. \end{aligned}$$

□

## 5.2 The Expected Power Knapsack

In this section, we understand the variables  $K_i^\downarrow$  and  $K_i^\uparrow$  as realizations of random variables. In this way, the proposed method can be generalized on the basis of average traffic load distributions. The random variables are supposed to follow a normal distribution because they are the sum of many

independent random variables. We determine the expected value of the average blocking rate depending on the scaled, accumulated user weight  $K_i^\uparrow$  and  $K_i^\downarrow$ , respectively. As in former chapters, we assume representative CIR targets  $\mu_s^\downarrow$ ,  $\mu_s^\uparrow$  and transmit activity factors  $\alpha_s^\downarrow$ ,  $\alpha_s^\uparrow$  for every service  $s \in S$ . Moreover, the orthogonality factors  $\bar{\omega}_p$  and noise  $\eta_p$  in downlink are location-specific as well as the attenuation factors  $\gamma_{ip}^\downarrow$  and  $\gamma_{pi}^\uparrow$ .

### 5.2.1 Downlink

We substitute  $p_{im}^\downarrow$  according to (5.2) in the definition (5.5) of  $K_i^\downarrow$ . This results in

$$K_i^\downarrow = \frac{1}{\kappa_i^\downarrow} \sum_{m \in \mathcal{M}_i} \left( \bar{\omega}_m p_i^{\max \downarrow} + \sum_{j \neq i} \frac{\gamma_{jm}^\downarrow}{\gamma_{im}^\downarrow} \tilde{p}_j^\downarrow + \frac{\eta_m}{\gamma_{im}^\downarrow} \right) l_m^\downarrow.$$

According to (5.4), there is no blocking in downlink at antenna  $i$  if

$$K_i^\downarrow \leq 1$$

holds. For  $K_i^\downarrow > 1$ , the average blocking rate is determined by (5.6). Thus, the expected value of the average blocking rate in cell  $i$  can be obtained by

$$\mathbb{E}[\tilde{b}_i^\downarrow] = \int_1^\infty \frac{x-1}{x} \tilde{f}_i^\downarrow(x) dx. \quad (5.15)$$

Here,  $\tilde{f}_i^\downarrow$  denotes the probability density function of  $K_i^\downarrow$ .

The random variable  $K_i^\downarrow$  can be assumed to follow a normal distribution. In fact, the limiting distribution as the number of pixels in the cell area  $|A_i|$  goes to infinity is not a normal distribution. The proof is the same as given in Section 4.4.3 with

$$l_s(p) = \frac{1}{\kappa_i^\downarrow} \left( \bar{\omega}_p p_i^{\max \downarrow} + \sum_{j \neq i} \frac{\gamma_{jp}^\downarrow}{\gamma_{ip}^\downarrow} \tilde{p}_j^\downarrow + \frac{\eta_p}{\gamma_{ip}^\downarrow} \right) \frac{\alpha_s^\downarrow \mu_s^\downarrow}{1 + \bar{\omega}_p \alpha_s^\downarrow \mu_s^\downarrow}.$$

Nevertheless, the assumption is sensible for the same reasons as discussed in Section 4.4.4. In order to assess the probability density function  $\tilde{f}_i^\downarrow$  of  $K_i^\downarrow$  we need to compute the expected value and variance of this random variable. The expected value of  $K_i^\downarrow$  is determined by

$$\mathbb{E}[K_i^\downarrow] = \frac{1}{\kappa_i^\downarrow} \int_{p \in A_i} \left( \bar{\omega}_p p_i^{\max \downarrow} + \sum_{j \neq i} \frac{\gamma_{jp}^\downarrow}{\gamma_{ip}^\downarrow} \tilde{p}_j^\downarrow + \frac{\eta_p}{\gamma_{ip}^\downarrow} \right) l_p^\downarrow dp. \quad (5.16)$$

Remember, that  $l_p^\downarrow$  defined in (3.11) is the expected value of  $l_m^\downarrow$  in position  $p$ . The variance of  $K_i^\downarrow$  satisfies

$$\mathbb{V}[K_i^\downarrow] = \frac{1}{(\kappa_i^\downarrow)^2} \int_{p \in A_i} \left( \bar{\omega}_p p_i^{\max\downarrow} + \sum_{j \neq i} \frac{\gamma_{jp}^\downarrow}{\gamma_{ip}^\downarrow} \tilde{p}_j^\downarrow + \frac{\eta_p}{\gamma_{ip}^\downarrow} \right)^2 \mathbb{V}[l_m^\downarrow(p)] \, dp. \quad (5.17)$$

The user densities in each pixel follow a Poisson distribution and are independent (cf. Section 2.5.2). Therefore, the variance of the user number is equal to its expected value. The variance of  $l_m^\downarrow$  at location  $p$  is given by

$$\mathbb{V}[l_m^\downarrow(p)] = \sum_{s \in S} \left( \frac{\alpha_s^\downarrow \mu_s^\downarrow}{1 + \bar{\omega}_p \alpha_s^\downarrow \mu_s^\downarrow} \right)^2 T_s(p). \quad (5.18)$$

The effect of coupling can be included as described in Section 4.3 in order to improve the estimates of the other antennas' powers and thus to obtain more accurate results.

## 5.2.2 Uplink

In the uplink direction, the realization of the random variable  $K_i^\uparrow$  for a traffic snapshot reads as

$$K_i^\uparrow = \frac{1}{\kappa_i^\uparrow} \sum_{m \in \mathcal{M}_i} l_m^\uparrow p_i^{\max\uparrow}.$$

There are all users served in cell  $i$  if

$$K_i^\uparrow \leq 1$$

holds (cf. (5.11)). The expected value of the uplink blocking rate can be governed by

$$\mathbb{E}[\tilde{b}_i^\uparrow] = \int_1^\infty \frac{x-1}{x} \tilde{f}_i^\uparrow(x) \, dx \quad (5.19)$$

in which  $\tilde{f}_i^\uparrow$  denotes the probability density function of  $K_i^\uparrow$ .

The random variable  $K_i^\uparrow$  is assumed to be normally distributed. As in the previous chapter, the Central Limit Theorem does not apply. This can be proved in analogy to Section 4.4.3 with

$$l_s(p) = \frac{p_i^{\max\uparrow}}{\kappa_i^\uparrow} \frac{\alpha_s^\uparrow \mu_s^\uparrow}{1 + \alpha_s^\uparrow \mu_s^\uparrow}.$$

However, a justification for this assumption can be found in Section 4.4.4. The expected value of  $K_i^\uparrow$  satisfies the expression

$$\mathbb{E}[K_i^\uparrow] = \frac{p_i^{\max\uparrow}}{\kappa_i^\uparrow} \int_{p \in A_i} l_p^\uparrow dp. \quad (5.20)$$

The variance of this random variable is determined by

$$\mathbb{V}[K_i^\uparrow] = \frac{(p_i^{\max\uparrow})^2}{(\kappa_i^\uparrow)^2} \int_{p \in A_i} V[l_m^\uparrow(p)] dp. \quad (5.21)$$

Here, the variance of  $l_m^\uparrow$  at location  $p$  is given by

$$\mathbb{V}[l_m^\uparrow(p)] = \sum_{s \in S} \left( \frac{\alpha_s^\uparrow \mu_s^\uparrow}{1 + \alpha_s^\uparrow \mu_s^\uparrow} \right)^2 T_s(p). \quad (5.22)$$

With  $\mathbb{E}[K_i^\uparrow]$  and  $\mathbb{V}[K_i^\uparrow]$ , the probability density function  $f_i^\uparrow$  of  $K_i^\uparrow$  is uniquely determined. For the uplink direction, the effect of coupling can be taken into account as pointed out in Section 4.3.



## 6 Comparison of both Methods

A central question now is how both approaches are related with each other. In this chapter, we prove that the results of the introduced methods from the last two chapters are equal. The model from Chapter 4 is considered for the general case of varying user load. As in the past chapters, the subscript  $i$  marks the cell whose blocking rate shall be assessed. The index  $j$  denotes other base station antennas.

### 6.1 Uplink

The first approach deals with the random variable

$$C_{ii}^\uparrow := \sum_{m \in \mathcal{M}_i} l_m^\uparrow.$$

The expected average blocking rate is determined according to

$$\mathbb{E}[\bar{b}_i^\uparrow] = \int_0^\infty [1 - \lambda_i^\uparrow(x)] f_i^\uparrow(x) dx \quad (6.1)$$

with  $\lambda_i^\uparrow$  given by

$$\lambda_i^\uparrow(x) = \begin{cases} \min\left\{1, \frac{p_i^{\max\uparrow} - \sum_{j \neq i} \tilde{C}_{ij}^\uparrow \hat{p}_j^\uparrow - \eta_i}{x p_i^{\max\uparrow}}\right\} & \text{for } x > 0 \\ 1 & \text{for } x = 0. \end{cases}$$

The second model covers the random variable

$$K_i^\uparrow := \frac{p_i^{\max\uparrow}}{\kappa_i^\uparrow} \sum_{m \in \mathcal{M}_i} l_m^\uparrow.$$

The expected average blocking rate reads as

$$\mathbb{E}[\tilde{b}_i^\uparrow] = \int_1^\infty \frac{x-1}{x} \tilde{f}_i^\uparrow(x) dx. \quad (6.2)$$

When comparing both random variables, it is easy to see that

$$K_i^\uparrow = \frac{p_i^{\max\uparrow}}{\kappa_i^\uparrow} C_{ii}^\uparrow \quad (6.3)$$

holds. For this reason, following equality is satisfied for all  $x \in \mathbb{R}$ :

$$f_i^\uparrow(x) = \tilde{f}_i^\uparrow\left(\frac{p_i^{\max\uparrow}}{\kappa_i^\uparrow} x\right). \quad (6.4)$$

The average blocking rate  $\bar{b}_i^\uparrow(x) = 1 - \lambda_i^\uparrow(x)$  is zero for  $\lambda_i^\uparrow(x) = 1$ , that is, for

$$x \leq \frac{p_i^{\max\uparrow} - \sum_{j \neq i} \tilde{C}_{ij}^\uparrow \tilde{p}_j^\uparrow - \eta_i}{p_i^{\max\uparrow}} = \frac{\kappa_i^\uparrow}{p_i^{\max\uparrow}}.$$

Therefore, (6.1) is equal to

$$\mathbb{E}[\bar{b}_i^\uparrow] = \int_{\frac{\kappa_i^\uparrow}{p_i^{\max\uparrow}}}^{\infty} \left[ 1 - \frac{p_i^{\max\uparrow} - \sum_{j \neq i} \tilde{C}_{ij}^\uparrow \tilde{p}_j^\uparrow - \eta_i}{x p_i^{\max\uparrow}} \right] f_i^\uparrow(x) dx. \quad (6.5)$$

We apply (6.4) to (6.5) and define  $y := \frac{p_i^{\max\uparrow}}{\kappa_i^\uparrow} x$ . This yields

$$\begin{aligned} \mathbb{E}[\bar{b}_i^\uparrow] &= \int_{\frac{\kappa_i^\uparrow}{p_i^{\max\uparrow}}}^{\infty} \left[ 1 - \frac{\kappa_i^\uparrow}{x p_i^{\max\uparrow}} \right] \tilde{f}_i^\uparrow\left(\frac{p_i^{\max\uparrow}}{\kappa_i^\uparrow} x\right) dx \\ &= \int_1^{\infty} \left[ 1 - \frac{1}{y} \right] \tilde{f}_i^\uparrow(y) dy = \mathbb{E}[\tilde{b}_i^\uparrow]. \end{aligned}$$

## 6.2 Downlink

In the downlink direction, the first model considers the random variable

$$C_i^\downarrow := \sum_{m \in \mathcal{M}_i} \left( \bar{\omega}_m p_i^{\max\downarrow} + \sum_{j \neq i} \frac{\gamma_{jm}^\downarrow}{\gamma_{im}^\downarrow} \tilde{p}_j^\downarrow + \frac{\eta_m}{\gamma_{im}^\downarrow} \right) l_m^\downarrow$$

The average blocking rate is approximated by its expected value in following way:

$$\mathbb{E}[\bar{b}_i^\downarrow] = \int_0^{\infty} [1 - \lambda_i^\downarrow(x)] f_i^\downarrow(x) dx. \quad (6.6)$$

The scaling factor  $\lambda_i^\downarrow$  is assessed by

$$\lambda_i^\downarrow(x) = \begin{cases} \min\left\{1, \frac{p_i^{\max\downarrow} - p_i^{(c)}}{x}\right\} & \text{for } x > 0 \\ 1 & \text{for } x = 0. \end{cases}$$

In the second approach, we define the random variable

$$K_i^\downarrow := \frac{1}{\kappa_i^\downarrow} \sum_{m \in \mathcal{M}_i} \left( \bar{\omega}_m p_i^{\max\downarrow} + \sum_{j \neq i} \frac{\gamma_{jm}^\downarrow}{\gamma_{im}^\downarrow} \tilde{p}_j^\downarrow + \frac{\eta_m}{\gamma_{im}^\downarrow} \right) l_m^\downarrow.$$

The expected average blocking rate is given by

$$\mathbb{E}[\tilde{b}_i^\downarrow] = \int_1^\infty \frac{x-1}{x} \tilde{f}_i^\downarrow(x) dx. \quad (6.7)$$

From the above representation of  $K_i^\downarrow$  we derive

$$K_i^\downarrow = \frac{1}{\kappa_i^\downarrow} C_i^\downarrow. \quad (6.8)$$

Due to this, it holds that

$$f_i^\downarrow(x) = \tilde{f}_i^\downarrow\left(\frac{x}{\kappa_i^\downarrow}\right) \quad (6.9)$$

for all  $x \in \mathbb{R}$ . Because  $\lambda_i^\downarrow(x) = 1$  for

$$x \leq p_i^{\max\downarrow} - p_i^{(c)} = \kappa_i^\downarrow,$$

$\mathbb{E}[\bar{b}_i^\downarrow]$  can be written as

$$\mathbb{E}[\bar{b}_i^\downarrow] = \int_{\kappa_i^\downarrow}^\infty \left[ 1 - \frac{p_i^{\max\downarrow} - p_i^{(c)}}{x} \right] f_i^\downarrow(x) dx. \quad (6.10)$$

With (6.9) and  $y := \frac{x}{\kappa_i^\downarrow}$ , this can be transformed in following way:

$$\begin{aligned} \mathbb{E}[\bar{b}_i^\downarrow] &= \int_{\kappa_i^\downarrow}^\infty \left[ 1 - \frac{\kappa_i^\downarrow}{x} \right] \tilde{f}_i^\downarrow\left(\frac{x}{\kappa_i^\downarrow}\right) dx \\ &= \int_1^\infty \left[ 1 - \frac{1}{y} \right] \tilde{f}_i^\downarrow(y) dy = \mathbb{E}[\tilde{b}_i^\downarrow]. \end{aligned}$$

□



# 7 Computational Results

In this chapter, the computational results of the mathematical models introduced in this thesis are presented and analyzed. First, we focus on the implementation of the approaches. Then, the test cases are introduced briefly. Afterwards, the results are presented and explained. In doing so, we first show the general behavior of the methods at a synthetic scenario with an isolated cell. In a second step, we consider the same simple scenario with a radio network consisting of two base station antennas. This situation serves to validate the developed models. Many extensive tests on realistic data are conducted. In this chapter, we merely give some selected representative results of them. The complete set of computational results can be found in Appendix B.

## 7.1 Implementation

The presented methods are each implemented in two parts. The first one consists of computing the expected value and variance of the particular random variable. Here, we use Java<sup>TM</sup> 2 Standard Edition version 5.0 for programming. The input data is given in XML-format. After reading this, the program iterates over all pixels in the planning area. In every iteration, it adds the computed values to the expected value and variance respectively of the best server in the current location. The powers of the other antennas are computed using the expected coupling approach from Section 3.1.2. In doing so, the load scaling factors  $\lambda^\uparrow$  and  $\lambda^\downarrow$  have to be assessed. The arising extended linear complementarity problem for the uplink direction is solved by ILOG CPLEX 9.0. In the second part of the implementation, the expected value of the average blocking rate of each cell is determined by numerical integration. This is done by MATLAB<sup>®</sup> version 7.0.1. The tests were run on a computer with an Intel<sup>®</sup> Xeon<sup>®</sup> processor with 2.4 GHz. The computer has a RAM of 3.8 MB.

## 7.2 Test Cases

In order to get a notion of how the methods work, the first test case is a synthetic scenario. We consider very simple network configurations. The first radio network is an isolated cell. The second one consists of two base station antennas. Besides those simple cases, the tests are conducted on realistic datasets from the MOMENTUM project [8, 18]. These scenarios comprise the downtown regions of The Hague, Berlin and Lisbon. Complex propagation data is given as well as non-homogeneous traffic distributions for different services. On each scenario, two different network designs are investigated. The smallest scenario is The Hague with 12 sites. This scenario covers an area of 16 km<sup>2</sup>. The treated network configurations have 19 and 36 cells, respectively. The Berlin scenario extends over 56 km<sup>2</sup> and has 65 sites. The network designs have each 122 sectors. The region covered by the Lisbon scenario is 21 km<sup>2</sup> large. The scenario has 60 sites. One of the networks has 128 cells, the other one 164. Moreover, the realistic Turin scenario developed within the COST 273 MORANS activity [19] is one of our test cases. The complexity and scope of the data is equal to that of the data from the MOMENTUM project. The network considered on the Turin scenario has 34 sites and 103 cells.

In all covered radio networks, the maximum transmission power of a base station antenna is 20 W. The downlink load limit is 70 %. In the uplink direction, a maximum noise rise of around 3 dB is assumed. This corresponds to a load limit of 50 %. We scale the traffic intensity with different factors (traffic scaling factors) in order to vary the amount of traffic. In doing so, we produce some overload. The considered service mixes vary, too. We test the single-service case as well as service mixes. In the multi-service case, we conduct tests when merely circuit-switched (cs) services are included in the scenarios like speech telephony and video telephony. Furthermore, a mix of circuit- and packet-switched services is tested for all scenarios. The essential average parameters for every service class are listed in Table 7.1 for the downlink direction. The abbreviation  $R$  denotes the average bit rate of the service,  $\alpha$  is its transmit activity factor and  $\mu$  its average CIR target.

Service	$R$ [Kbps]	$\alpha$	$\mu$ [dB]
Speech telephony	12.2	0.5	-15.90
Video telephony	64.0	1.0	-11.56
Data transmission	64.0	0.9	-10.95

Table 7.1: Average service parameters in downlink

We test two versions of each model. One takes the effect of coupling into account according to (4.29) and (4.30), respectively (refined version), and one does not (simple version). The results are compared to those of Monte Carlo simulation on traffic snapshots introduced in Section 3.1.1. In [7] it is shown that these results are a good approximation of results obtained by Monte Carlo simulation including a more extensive load analysis in each trial. The errorbars around the points belonging to these results represent the confidence intervals for a confidence level of 95 % (cf. Section 3.2). Furthermore, the results of the approach using the expected coupling matrix from Section 3.1.2 are given. This model is the basis of the developed methods. In this way, the achieved improvement is revealed.

## 7.3 Validation

The synthetic scenario serves to validate the models introduced in this thesis. For this reason, the complete curves of the blocking rate are plotted depending on the different traffic scaling factors. This is done for every cell in logarithmic scale. The synthetic scenario is denoted by “Synth.” in the pictures. We additionally plot two dashed, magenta-colored lines in each illustration marking the region of the blocking rate between 1 and 5 %. This interval is the most important for us. Blocking rates lower than 1 % are negligible. Those higher than 5 % are not probable to occur in the network designs we consider.

### 7.3.1 One Cell

In the case of an isolated cell there is no difference between the simple and the refined version since there are no other antennas whose powers could be estimated. Figure 7.1 depicts the results for the isolated antenna of the synthetic scenario in the case of the single service speech telephony in uplink and downlink, respectively. We recognize, that all obtained values lie inside the confidence intervals. Figure 7.2 illustrates the outcomes for the service mix including merely the circuit-switched services. Figure 7.3 shows the results for a general service mix. In both cases, almost all values lie inside the confidence intervals. That is, the presented approaches deliver reasonable outcomes for our purpose. Furthermore, the strong improvement compared to the expected coupling method is noticeable. For low blocking rates, the results of this method are zero and hence not depicted due to the logarithmic scale. Only in ranges over 5 % the results of the expected coupling method approach the exact blocking rates.

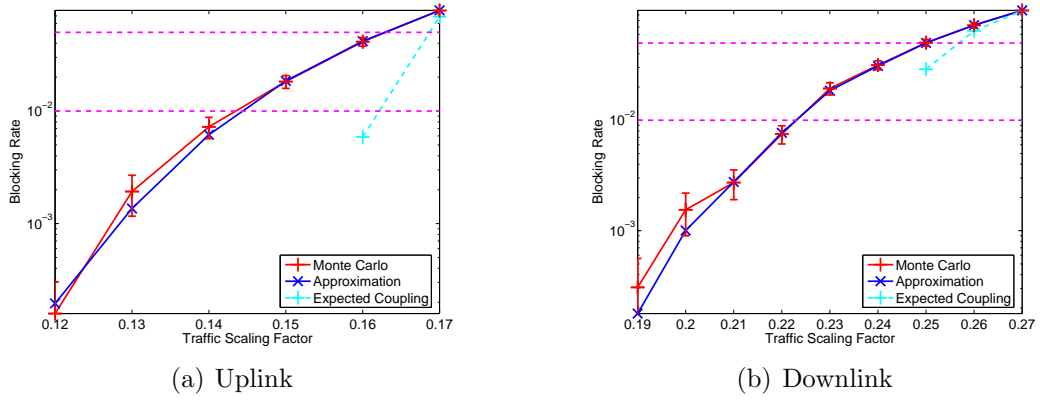


Figure 7.1: Synth.: one cell, speech telephony

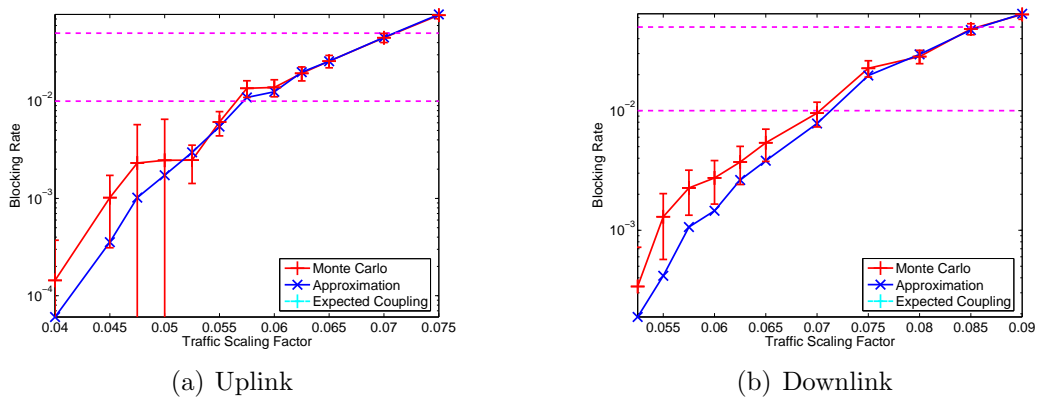


Figure 7.2: Synth.: one cell, cs services

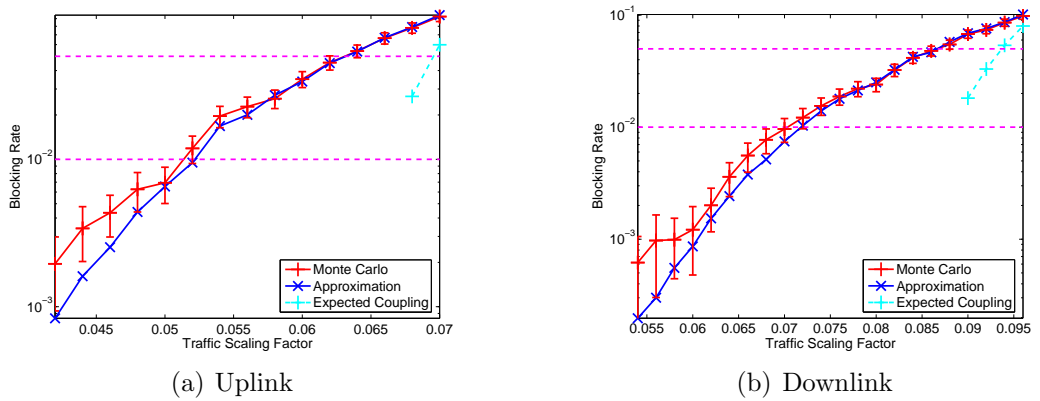


Figure 7.3: Synth.: one cell, service mix

### 7.3.2 Two Cells

For 100% speech telephony users, the results are shown in Figure 7.4 for both cells in the uplink direction. The downlink is depicted in Figure 7.5. Of course, the outcomes of the approaches are not as precise as for an isolated antenna since more sources of estimation errors are involved, now. The Figures 7.6–7.9 depict the results for different service mixes. All figures reveal that the blocking rate is systematically underestimated in low ranges under 2–4%. We note that this underestimation is stronger in the simple version. The curve of the blocking rate of the simple variant approaches the curve of the exact blocking rate later than that of the refined alternative. Particularly in the downlink direction, the results of the precise version are better. The powers of the other base station antennas are estimated higher in this variant and thus the blocking rate. In the uplink, the differences are very small and thus hardly to recognize in the diagrams. In general, the transmission power of a cell is considerably higher than its reception power because the mobile station antennas are much less powerful than the base station antennas. Therefore, the differences between the simple and the refined alternative are higher in downlink.

This systematic estimation error is probably due to the fact that we estimate the powers of the other base station antennas by using the expected coupling model. As pointed out in Section 3.3, this approach tends to underestimate the average power of an antenna in low ranges. If the powers of other antennas are estimated too low, the inter-cell interference in our sector is underestimated. Thus, the blocking rate is underestimated, too. This cannot be compensated for completely by considering the effect of coupling in the refined versions of our methods. This enhancement determines an estimate for the average powers of the other antennas under the assumption that the power level of our antenna is at its maximum. However, the other cells' powers are still underestimated compared to the exact powers conditioned to the situation when the power of our antenna is at its maximum. The reasons are the same as given in Section 3.3. Traffic snapshots with more users than expected contribute above average to the exact power and blocking rate. These snapshots are as probable to occur in reality as traffic snapshots with less users than expected. These effects of randomness are ignored in the expected coupling approach. Furthermore, the assumption of the random variables of our methods being normally distributed is not valid (cf. Section 4.4). Hence, this approximation causes errors, too.

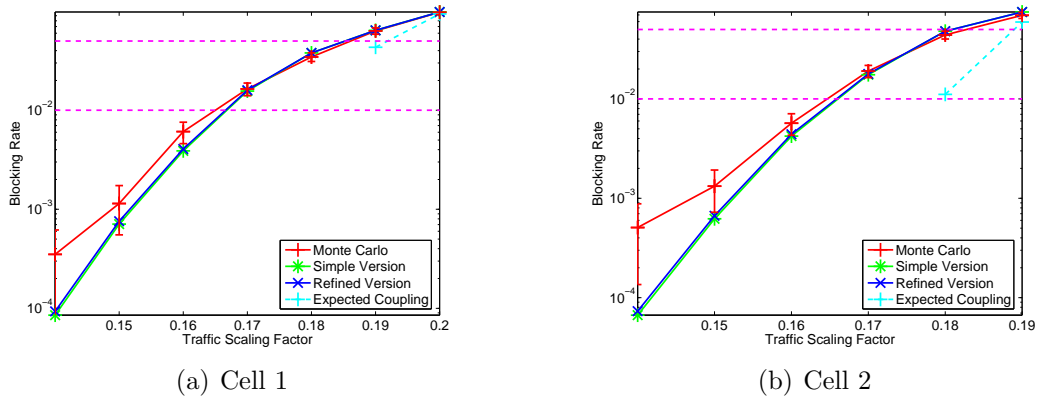


Figure 7.4: Synth.: two cells, speech telephony, uplink

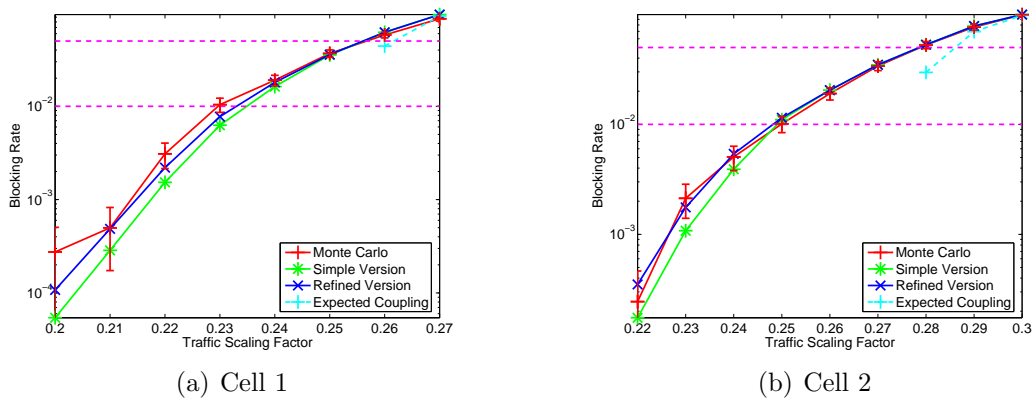


Figure 7.5: Synth.: two cells, speech telephony, downlink

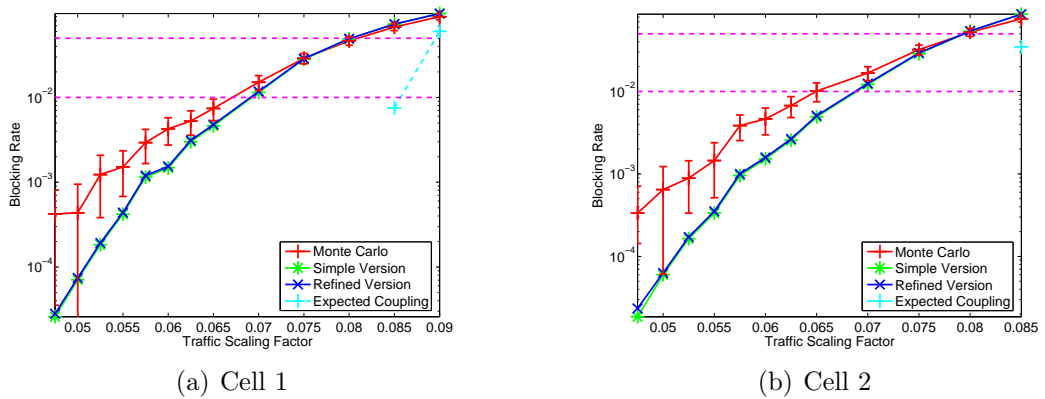
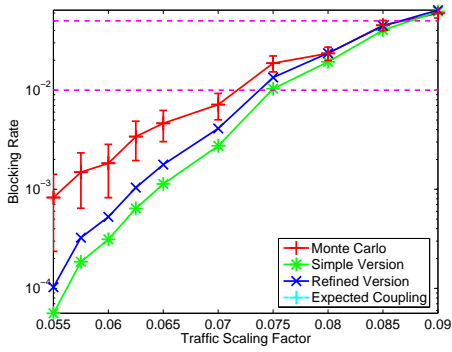
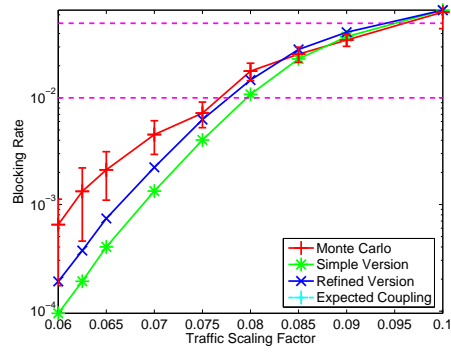


Figure 7.6: Synth.: two cells, cs services, uplink

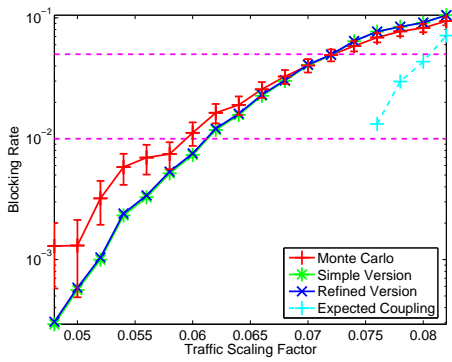


(a) Cell 1

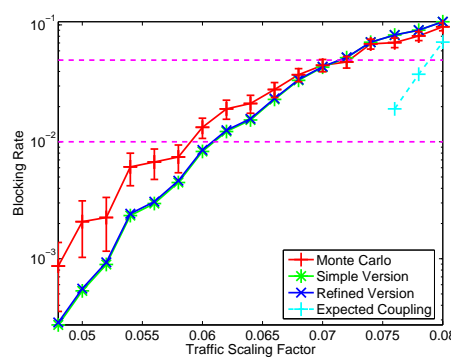


(b) Cell 2

Figure 7.7: Synth.: two cells, cs services, downlink

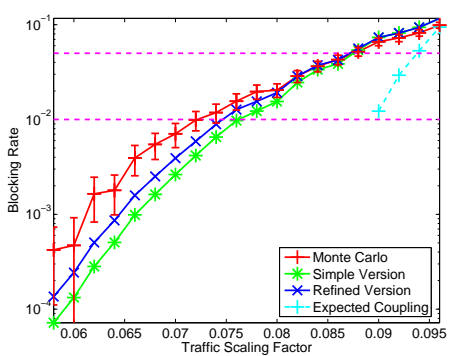


(a) Cell 1

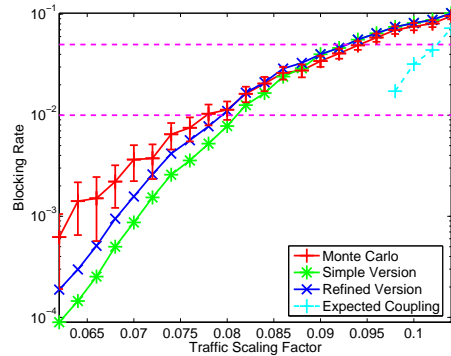


(b) Cell 2

Figure 7.8: Synth.: two cells, service mix, uplink



(a) Cell 1



(b) Cell 2

Figure 7.9: Synth.: two cells, service mix, downlink

## 7.4 Results

We conduct many extensive tests on the described huge real-world scenarios. All these results are given in Appendix B. In this section, we confine ourselves to showing only a few selected ones. In fact, the observations are similar in all cases. In contrast to the synthetic scenario, one diagram is made for one traffic scaling factor. This diagram shows the blocking rate depending on the cell index in logarithmic scale. Only cells with a blocking rate greater than 0.001 are plotted for the sake of clarity. Moreover, a scatter diagram illustrates the difference between the results of our approaches and those of Monte Carlo simulation depending on the exact blocking rate. One such diagram is given for each network design.

In the tests, the traffic scaling factors were chosen such that the maximum blocking rate in the network lies a little above the limit of 2%. Such situations are of most interest since the expected coupling approach fails here completely. The limit is marked in the pictures by a dashed, magenta-colored line. In the depicted regions, the blocking rates obtained by the expected coupling approach lie around zero. For this reason, these blocking rates are not shown in the diagrams due to the logarithmic scale. In all illustrations, the exact blocking rate of a cell is colored red. The approaches introduced in this thesis are colored blue (refined) and green (simple), respectively. This is important since there is no legend due to space limitations. In the caption of the figures, the scenario, the network, the services mix, the traffic scaling factor, and the direction of transmission are given. The abbreviation “UL” stands for “uplink” while “DL” means “downlink”.

Generally, the tests at huge scenarios confirm the observations made at the simple test cases. Our models underestimate the blocking rate in the depicted ranges under 3%. This systematical estimation error is lower for services with a low data rate. Especially for the service speech telephony, the results of our approaches comply well with those of Monte Carlo simulation, see for instance Figure 7.10. Services with a low data rate require a low CIR target and thus have a small user load  $l_p^\uparrow$  and  $l_p^\downarrow$ , respectively. The underlying random variable in our models is the traffic distribution in the planning area. The traffic intensity for a specified service in a certain position is weighted by the average user load for this service. A low user load means, that made estimation errors in the user intensity are weighted lower than for services with a high user load. Furthermore, a high user load causes a high variance of the coupling matrix entries. The variance is a measure for the statistical dispersion of a random variable. That is, a high variance indicates a possibly high difference of the realizations of the random variable from its expected

value. The more the coupling matrix in reality deviates from the expected value we use, the higher are the estimation errors we make.

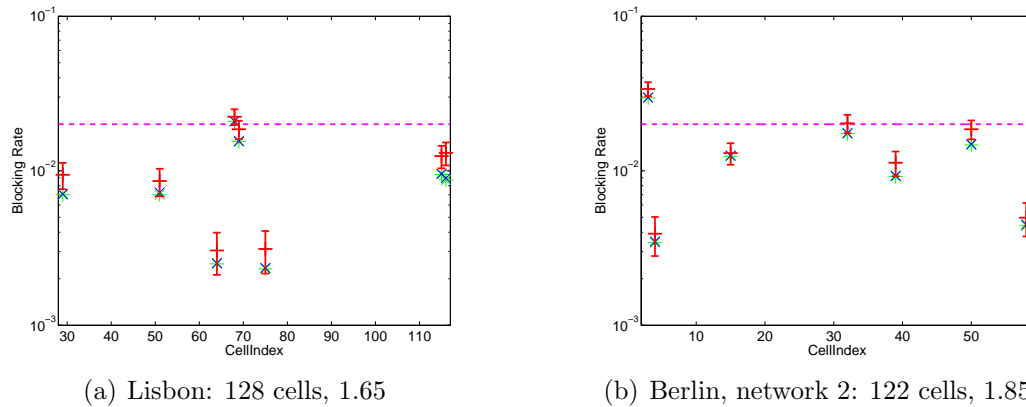


Figure 7.10: Examples for speech telephony, uplink

An example for a service with a relative high user load is depicted in Figure 7.11(a). The diagram illustrates the results in uplink for video telephony. There are fewer cells whose approximated blocking rate lies inside the confidence interval than before. The same applies for packet-switched services. Users of them generally have a high load. An example for the service e-mail is shown in Figure 7.11(b).

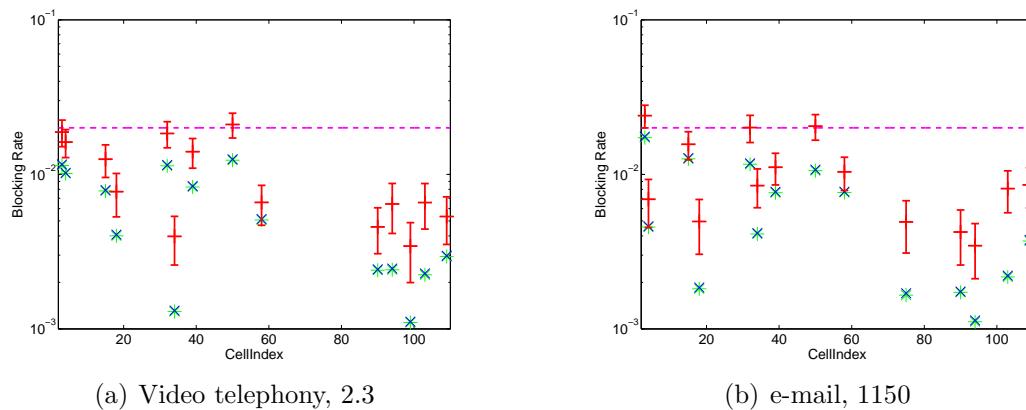


Figure 7.11: Berlin, network 2: 122 cells, uplink

The explained differences between services with different user loads are one reason why the service mixes deliver results with larger differences to the exact blocking rate. The mixes include services with a high user load. Another reason is that in contrast to the single-service case more estimation

errors are involved for several services. The errors made for each service are accumulated in this case. Examples are depicted in Figure 7.12. In all presented figures, we see the difference between the simple and the refined version of our approaches. As in the synthetic scenario, the differences in downlink are much higher than in the uplink direction. In the uplink, the results of both versions are roughly equal.

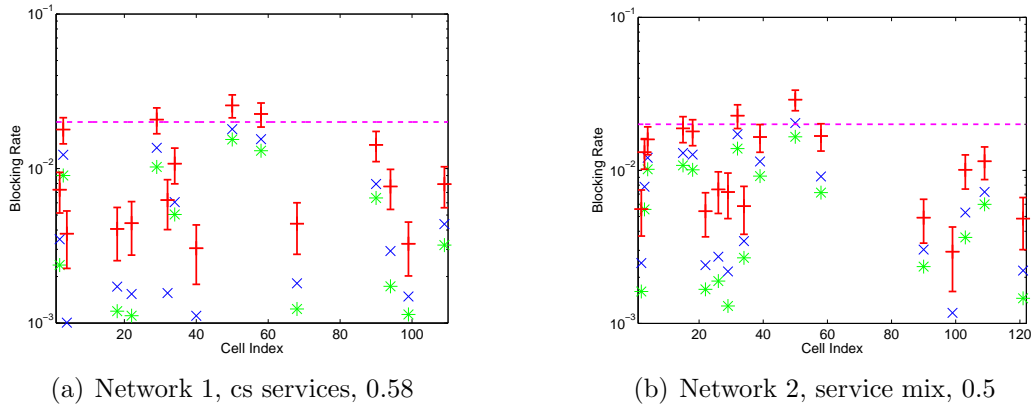


Figure 7.12: Berlin: 122 cells, different service mixes, downlink

Figure 7.13 depicts the scatter diagram for one network of the Berlin scenario in uplink. Figure 7.13(a) shows the entire diagram for all tested traffic scaling factors. Figure 7.13(b) illustrates the extract marked by the black rectangle in Figure 7.13(a). These diagrams visualize the difference between our refined methods and Monte Carlo simulation depending on the exact blocking rate. The values of all cells are plotted for all used traffic scaling factors and services. Each service is marked by a different color. The legend is merely given in Figure 7.13(a) due to space limitations in Figure 7.13(b). The different traffic scaling factors used explain the different heights of the exact blocking rate for different service mixes.

These scatter diagrams show again that our approaches underestimate the blocking rate of most cells in low regions under around 5%. In higher ranges over approximately 10%, they usually overestimate the exact blocking rate. The reason is the same as for the underestimation explained in Section 7.3.2. We miscalculate the powers of the other antennas. The other cells' powers tend to be overestimated by the expected coupling approach in high regions (cf. Section 3.3). Therefore, the inter-cell interference is overestimated and thus the blocking rate in our sector. The described estimation error has more effect on cells with high coupling to their neighbors.

Figure 7.14 shows the scatter diagram for the same network in downlink. We recognize that the blocking rate of most cells is underestimated under

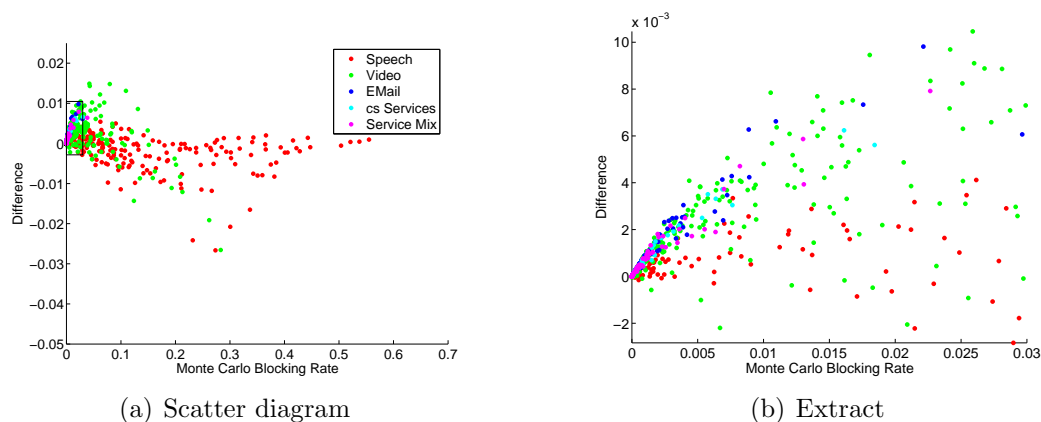


Figure 7.13: Berlin, network 1: 122 cells, scatter diagram, uplink

roughly 3%. The overestimation starts earlier than in uplink. From approximately 5% on, the blocking rate of most sectors is overestimated. This is due to the fact that we vary the off-diagonal entries of the coupling matrix and the traffic noise power, too. Moreover, the differences between our approaches and the exact blocking rates are higher in the downlink direction. This is due to the service mix. In contrast to the uplink, we include more services with a high data rate. Besides, the variance of the random variables is higher in downlink. The scatter diagrams for the other investigated networks can be found in Appendix B.

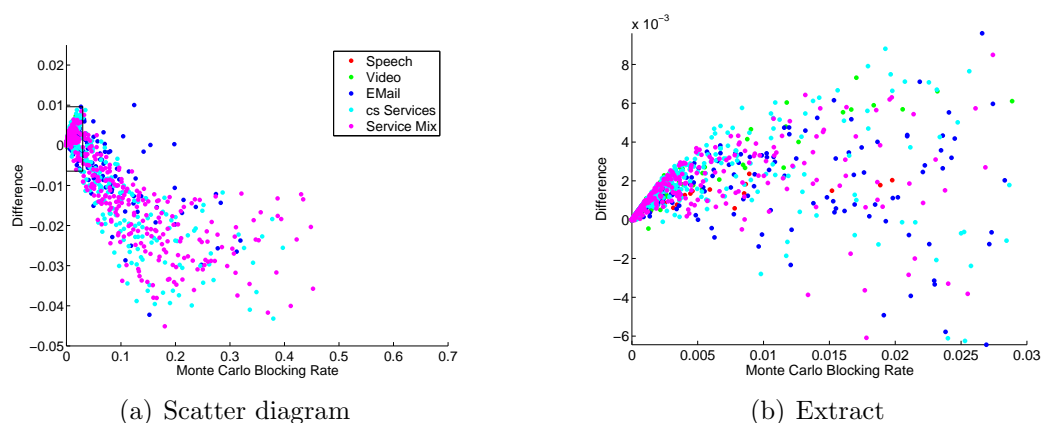
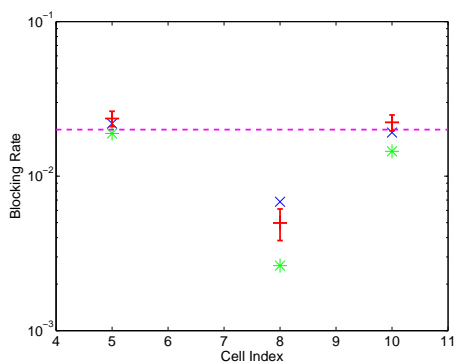


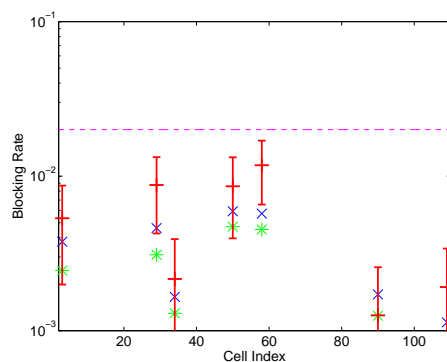
Figure 7.14: Berlin, network 1: 122 cells, scatter diagram, downlink

In Figure 7.15, the overestimation of the blocking rate by our models is illustrated for the downlink direction. In Figure 7.15(a), the result of the refined version of our approaches for the cell with the index 8 lies above the

confidence interval. Actually, such a strong overestimation in these low regions is exceptional. This is the only case of all conducted tests in which the blocking rate lies above the confidence interval for a cell with an exact blocking rate under 2%. In other cases of overestimation in these low regions, the approximation lies inside the confidence interval as shown in Figure 7.15(b) for the cell with the index 90.



(a) The Hague: 19 cells, speech telephony, 6



(b) Berlin, network 1: 122 cells, video telephony, 3.5

Figure 7.15: Examples for overestimation, downlink

### 7.4.1 Running Time

The average running times for the simple versions of our methods are listed in Table 7.2. Those of the refined variants are given in Table 7.3. The total running time is broken down into the two parts of implementation described in Section 7.1. The entries in the column “Part I” specify the time needed to compute the expected value and variance of the random variables including the time for solving the modified equation systems (4.29) and (4.30) in the refined version. The column “Intg” shows the running time for numerical integration in the second part. All the times are given in seconds. The columns with title “I” each refer to the first model introduced in Chapter 4. The heading “II” stands for the second method given in Chapter 5.

The first approach is a few seconds quicker in the first part of the implementation. The reason is the computational complexity of calculating the knapsack size  $\kappa_i^\uparrow$  in uplink in the second model. For assessing this value for every cell, the entries of the coupling matrix are summed up for each row. This causes additional computational effort of quadratic size in the number of cells. However, the first approach takes on average more time for the numerical integration in the second part of the implementation. The reason is

Scenario	Number of Cells	Part I		Intg		Total	
		I [s]	II [s]	I [s]	II [s]	I [s]	II [s]
The Hague	19	34.00	37.46	1.61	0.50	35.16	37.96
	36	32.92	34.26	1.64	0.43	34.56	34.69
Turin	103	53.93	64.90	5.71	1.34	59.64	66.24
Berlin, network 1	122	41.11	47.21	8.27	2.34	49.38	49.55
Berlin, network 2	122	39.79	51.97	7.57	2.08	47.36	54.05
Lisbon	128	67.73	72.65	7.59	2.11	75.32	74.76
	164	61.15	65.16	6.94	1.66	68.09	66.82

Table 7.2: Average running times of the simple versions

that the computation of  $\lambda_i^\dagger$  in the first model is more complex than calculating  $\frac{x-1}{x}$  in the second method. Again, the entries of the uplink coupling matrix are summed up for every row. The relative differences between the models are smaller in the first part of the implementation. This is probably due to the use of a different program for each part. Altogether, the average total running time of both approaches is about the same.

Scenario	Number of Cells	Part I		Intg		Total	
		I [s]	II [s]	I [s]	II [s]	I [s]	II [s]
The Hague	19	35.50	39.05	1.60	0.48	37.10	39.53
	36	38.53	43.04	1.63	0.41	40.16	43.45
Turin	103	71.10	78.35	5.76	1.35	76.86	79.70
Berlin, network 1	122	73.07	75.92	8.31	2.31	81.38	78.23
Berlin, network 2	122	72.81	80.12	7.42	2.10	80.23	82.22
Lisbon	128	102.79	107.87	7.64	2.10	110.43	109.97
	164	156.58	158.44	6.91	1.72	163.49	160.16

Table 7.3: Average running times of the refined versions

For small scenarios, like The Hague, the difference between the simple and the refined versions of our approaches is negligible. By contrast, in larger scenarios solving the modified equation system takes approximately just as long as computing the expected value and variance of the random variables. The time for numerical integration is only a few seconds even for many cells. This time is equal in both versions.

In Table 7.4, the average running times of the refined version of the approach from Chapter 5 are compared to those of Monte Carlo simulation.

The times are given in seconds. During Monte Carlo simulation, we evaluate 1000 traffic snapshots for each scenario by using the method introduced in Section 3.1.1. This analysis is implemented in Java<sup>TM</sup> 2 Standard Edition version 5.0, too. The extended linear complementarity problem arising by the computation of the load scaling factors  $\lambda^\dagger$  in uplink is again solved by ILOG CPLEX 9.0. Besides the given time for computing the blocking rates, the time for creating the traffic snapshots has to be taken into account. This issue is not considered here.

Scenario	Number of Cells	Monte Carlo [s]	Model II [s]
The Hague	19	612	40
	36	765	44
Turin	103	4864	80
Berlin, network 1	122	3680	78
Berlin, network 2	122	3680	82
Lisbon	128	4843	110
	164	9914	160

Table 7.4: Comparison of the average running times

## 7.5 Conclusions

In order to find a compromise between accuracy and complexity, we do not consider the complete underlying system in full detail. The powers of the other antennas in the radio network are estimated by average values. Moreover, we assume the random variables to be normally distributed. These simplifications cause systematical estimation errors.

In general, these errors are similar to those of the basic expected coupling approach but they are considerably lower. In low regions under approximately 3–5%, the developed approaches underestimate the blocking rate. In higher ranges over roughly 5–10%, our methods tend to overestimate the blocking rate. However, these estimation errors lie in an acceptable range. Moreover, the average running times of the developed models are very short. Depending on the frequency of utilization during optimization we can prefer the more precise variant or the simple alternative which is about twice as quick. In the uplink, the results of both versions differ hardly from each other. In the downlink, the refined version yields better results. The total average running times of both proposed approaches are approximately equal.

---

Altogether, we recognize that the developed models approximate the blocking rates in a UMTS radio network very well. The presented computational results confirm this statement. They reveal that we have advanced the basic approach immensely. A further success is that our approaches are very quick compared to the complexity of Monte Carlo simulation. That is, we found a trade-off between accuracy and computational effort. In conclusion, the methods introduced in this thesis are very efficient. We reached the goal to develop a model having about the complexity of the expected coupling approach on the one hand and being about as precise as Monte Carlo simulation on the other hand.



## 8 Summary and Outlook

The goal of this thesis was to develop a mathematical model to efficiently approximate the blocking rates of the cells in a UMTS radio network. The blocking rate denotes the fraction of unserved users due to limited radio resources at a base station antenna. This rate is an important criterion to evaluate the quality of a radio network design. So far, no adequate method was known, however, that is able to predict the average blocking rate quickly and reliably. The difficulty is that the capacity of a UMTS radio cell varies.

In this thesis, two approaches were proposed to approximate the blocking rates in UMTS radio networks. These methods are based on an existing model. In the first method, the inaccuracies of this existing approach were reduced by computing the expected value of the average blocking rate depending on the interference of the own cell. In the second method, the problem was understood as a kind of fractional *Knapsack problem*. We considered the distribution of the total weight of all users in the radio cell. Depending on this accumulated weight, we determined the expected value of the average blocking rate. In both approaches, the interference of the other radio cells was estimated by average values. These estimates were stated more precisely, however, at the cost of complexity. Moreover, we derived analytically that the results of both models are equal.

Extensive computational tests revealed that we found a very good compromise between accuracy and complexity with the developed methods. The characteristics of the basic model are still weakly present. That is, in low ranges the blocking rate is a little underestimated and in higher regions lightly overestimated. However, in contrast to the situation before these systematical estimation errors lie inside acceptable bounds. The computational complexity of both introduced approaches is equal. In contrast to existing methods with comparable accuracy, the average running times are extremely short.

The small estimation errors could be reduced by finding more precise estimates of the other base station antennas' powers. So far, we estimated them by average values, which produce little errors. Another simplification

we made in our methods is that we assumed the considered random variables to be normally distributed. We proved that this assumption does not hold. A more accurate characterization of the distribution of the random variables with low computational effort could improve our results. Furthermore, the proposed model could be enhanced by including soft handover and by combining the uplink and the downlink direction instead of treating them independently.

# A Notation

## Symbol Meaning

$A$	Planning area
$A_i$	Cell area (best server area) of base station antenna $i$
$p$	Location in the planning area
$d$	Dimension of the planning area
$\mathcal{N}$	Set of base station antennas (cells) in the radio network
$i, j$	Base station antennas
$\mathcal{M}$	Set of mobiles
$\mathcal{M}_i$	Set of mobiles served by base station antenna $i$
$m$	Mobile
$S$	Set of services
$s$	Service
$T_s$	Average spatial traffic distribution of service $s$
$T_s(p)$	Average traffic intensity of service $s$ at location $p$
$\lambda^d$	$d$ -dimensional Lebesgue-Measure
$f_s$	User density of service $s$
$p_m^\uparrow$	Uplink transmission power from mobile $m$
$p_{im}^\downarrow$	Downlink transmission power from antenna $i$ to mobile $m$
$p_i^{(c)}$	Constant power of base station antenna $i$
$\bar{p}_i^\uparrow$	Total average reception power at base station antenna $i$
$\bar{p}_i^\downarrow$	Total average transmission power of base station antenna $i$
$p_i^{\max\uparrow}$	Maximum total reception power at base station antenna $i$
$p_i^{\max\downarrow}$	Maximum total transmission power of base station antenna $i$

$\gamma_{mi}^\uparrow$	Uplink attenuation factor between mobile $m$ and antenna $i$
$\gamma_{im}^\downarrow$	Downlink attenuation factor between antenna $i$ and mobile $m$
$\alpha_m^\uparrow, \alpha_m^\downarrow$	Uplink/downlink transmit activity factor of mobile $m$
$\mu_m^\uparrow, \mu_m^\downarrow$	Uplink/downlink CIR target of mobile $m$
$\eta_i, \eta_m$	Noise at base station antenna $i$ /mobile $m$
$\bar{\omega}_m$	Orthogonality factor of mobile $m$
$l_m^\uparrow, l_m^\downarrow$	Uplink/downlink user load of mobile $m$
$\gamma_{pi}^\uparrow$	Uplink attenuation factor between location $p$ and antenna $i$
$\gamma_{ip}^\downarrow$	Downlink attenuation factor between antenna $i$ and location $p$
$\alpha_s^\uparrow, \alpha_s^\downarrow$	Uplink/downlink transmit activity factor of service $s$
$\mu_s^\uparrow, \mu_s^\downarrow$	Uplink/downlink CIR target of service $s$
$\eta_p$	Noise at location $p$
$\bar{\omega}_p$	Orthogonality factor in location $p$
$l_p^\uparrow, l_p^\downarrow$	Expected uplink/downlink user load in location $p$
$C^\uparrow, C^\downarrow$	Uplink/downlink cell load coupling matrix
$\bar{C}^\uparrow, \bar{C}^\downarrow$	Expected uplink/downlink cell load coupling matrix
$\tilde{C}^\uparrow, \tilde{C}^\downarrow$	Scaled uplink/downlink cell load coupling matrix
$p_i^{(n)}$	Traffic noise power at base station antenna $i$
$\bar{p}_i^{(n)}$	Expected traffic noise power at base station antenna $i$
$\tilde{p}_i^{(n)}$	Scaled traffic noise power at base station antenna $i$
$\lambda_i^\uparrow, \lambda_i^\downarrow$	Scaling factor in uplink/downlink for cell $i$
$\tilde{p}_i^\uparrow$	Total average reception power at base station antenna $i$ (solution of the scaled uplink equation system)
$\tilde{p}_i^\downarrow$	Total average transmission power of base station antenna $i$ (solution of the scaled downlink equation system)
$\mathbb{P}(A)$	Probability of event $A$
$\mathbb{E}[X]$	Expected value of random variable $X$
$\mathbb{V}[X]$	Variance of random variable $X$
$T_p$	Average traffic intensity at location $p$ (single service case)
$T_i$	Average traffic intensity in cell $i$
$\mathbb{P}_{T_i}(n)$	Probability for $n$ users in cell $i$
$\bar{b}_i^\uparrow, \bar{b}_i^\downarrow$	Average uplink/downlink blocking rate of cell $i$ (according to Chapter 4)

---

$\bar{n}_i^{\max\uparrow}$	Capacity of cell $i$ in uplink
$\bar{n}_i^{\max\downarrow}$	Capacity of cell $i$ in downlink
$l_i^\uparrow, l_i^\downarrow$	Average uplink/downlink load for a user in cell $i$
$M$	Set of mobility types
$\mathbb{P}_p(m)$	Probability of mobility type $m$ at location $p$
$C_i^\downarrow$	Random variable related to cell $i$ in downlink
$c_{im}^\downarrow/c_{ip}^\downarrow$	Constant factor for mobile $m$ /pixel $p$ in cell $i$ in downlink
$f_i^\uparrow, f_i^\downarrow$	Probability density function of $C_{ii}^\uparrow/C_{ii}^\downarrow$ or $C_i^\downarrow$
$X_{kp}$	Random variable for step $k \in \mathbb{N}$ and pixel $p$ given by a triangular array $\{X_{kp}, p = 1, \dots, n_k : n_k \in \mathbb{N}\}$
$k$	Row index in the triangular array
$n_k$	Number of random variables $X_{kp}$ in the $k$ th row of the triangular array
$\mu_{kp}$	Expected value of the random variable $X_{kp}$
$\sigma_{kp}^2$	Variance of the random variable $X_{kp}$
$X_k$	Sum of the random variables $X_{kp}, p = 1, \dots, n_k$ in the $k$ th step
$A_i^{(k)}$	Set of pixels in the cell area of base station antenna $i$ in the $k$ th step
$l_s(p)$	Constant factor for service $s$ in position $p$
$m_s(p)$	Number of mobile stations of service $s$ in position $p$
$Y_p$	Random variable in pixel $p$
$Y_i$	Sum of the random variables $Y_p$ over all $p \in A_i$
$\mu_p$	Expected value of the random variable $Y_p$
$\sigma_p^2$	Variance of the random variable $Y_p$
$s_k^2$	Sum of the variances $\sigma_p^2$ over all $p = 1, \dots, n_k$
$\hat{l}_i$	Upper bound of $l_s(p)$ in cell $i$
$\bar{l}_i$	Lower bound of $l_s(p)$ in cell $i$
$\tilde{\omega}_i$	Lower bound of $\bar{\omega}_p$ in cell $i$
$\tilde{\gamma}_i^\downarrow$	Lower bound of $\gamma_{ip}^\downarrow$
$\hat{\eta}_i$	Upper bound of $\eta_p$ in cell $i$
$p^*$	Pixel in the cell area of antenna $i$
$\kappa_i^\uparrow, \kappa_i^\downarrow$	Size of the uplink/downlink power knapsack of cell $i$
$\tilde{b}_i^\uparrow, \tilde{b}_i^\downarrow$	Average uplink/downlink blocking rate of cell $i$ (according to Chapter 5)

$K_i^\uparrow, K_i^\downarrow$	Random variable representing the offer for the power knapsack of cell $i$ in uplink/downlink
$\tilde{f}_i^\uparrow, \tilde{f}_i^\downarrow$	Probability density function of $K_i^\uparrow/K_i^\downarrow$

## B Further Results

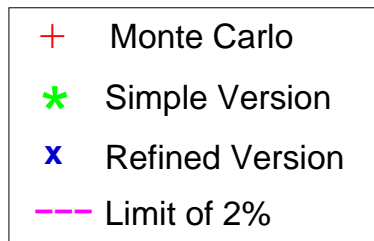


Figure B.1: Legend for all following figures

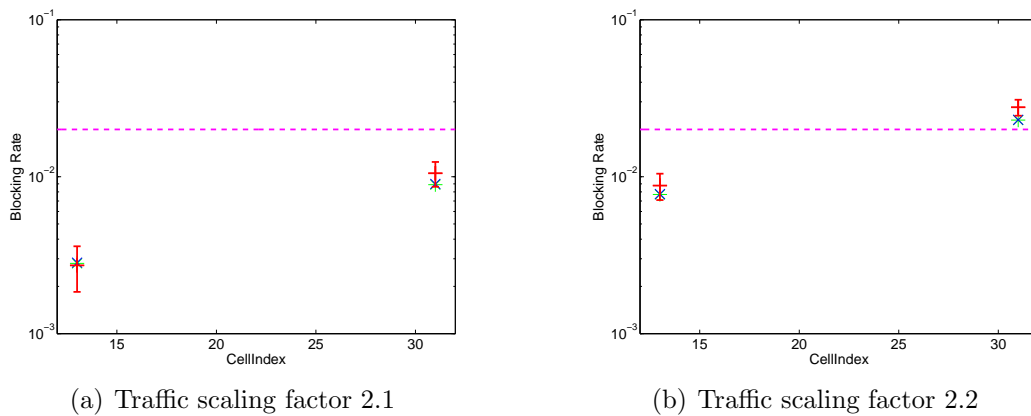
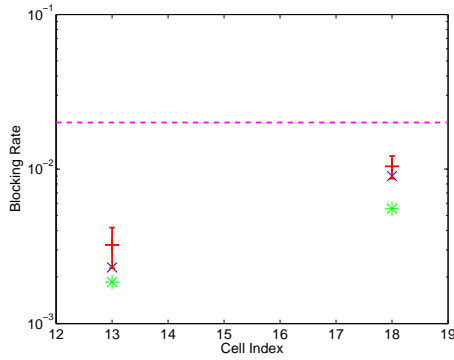
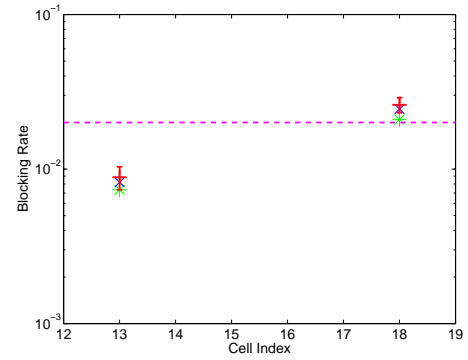


Figure B.2: The Hague: 36 cells, speech telephony, UL

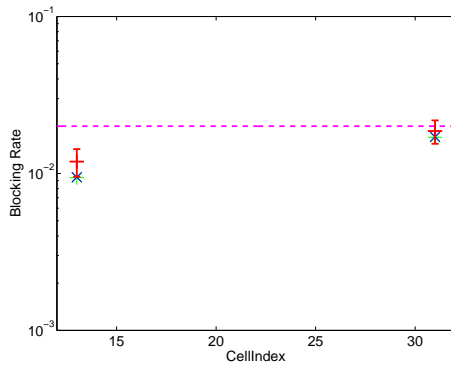


(a) Traffic scaling factor 4.4

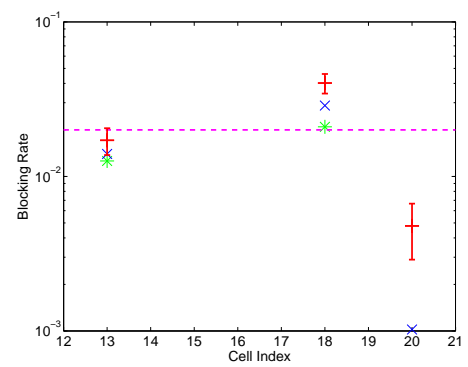


(b) Traffic scaling factor 4.6

Figure B.3: The Hague: 36 cells, speech telephony, DL

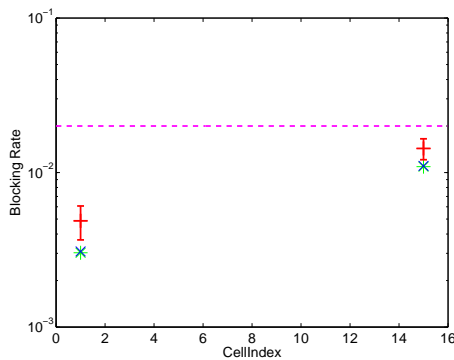


(a) Traffic scaling factor 1.2, UL

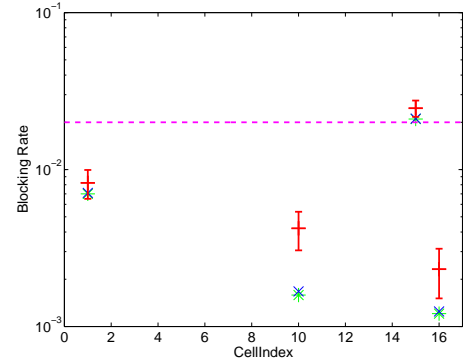


(b) Traffic scaling factor 0.8, DL

Figure B.4: The Hague: 36 cells, cs services



(a) Traffic scaling factor 2.55



(b) Traffic scaling factor 2.65

Figure B.5: The Hague: 19 cells, speech telephony, UL

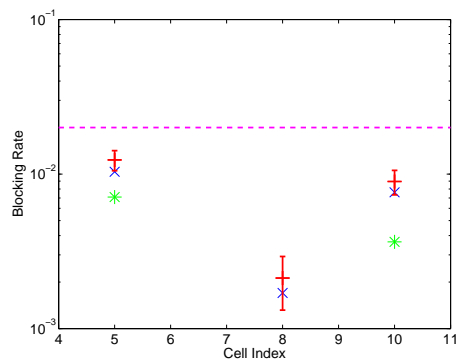
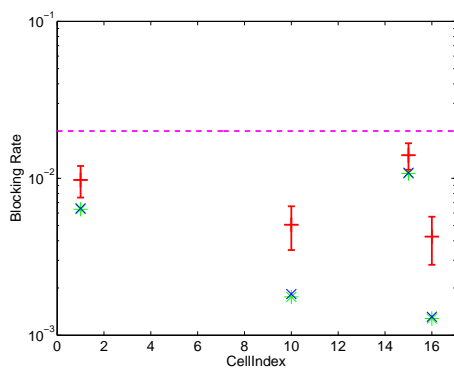
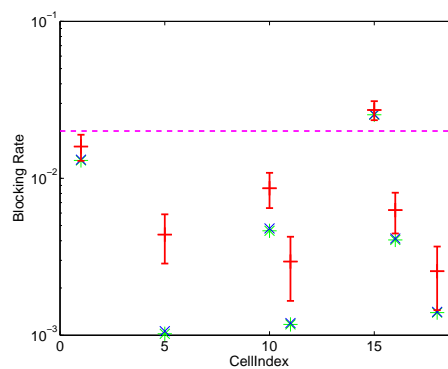


Figure B.6: The Hague: 19 cells, speech telephony, traffic scaling 5.8, DL

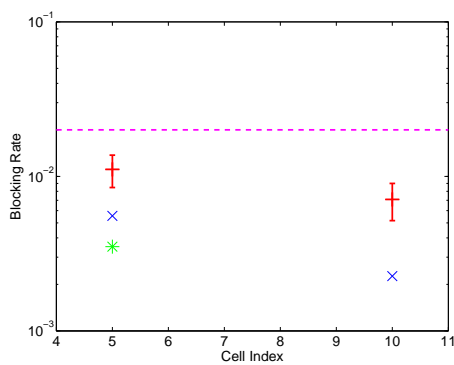


(a) Traffic scaling factor 1.4

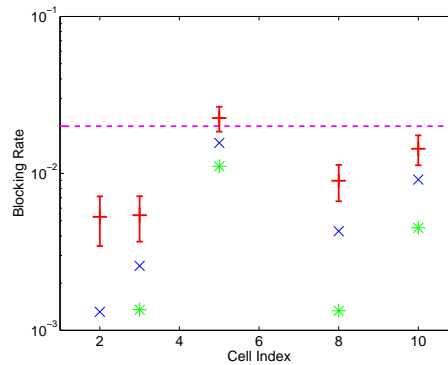


(b) Traffic scaling factor 1.5

Figure B.7: The Hague: 19 cells, cs services, UL

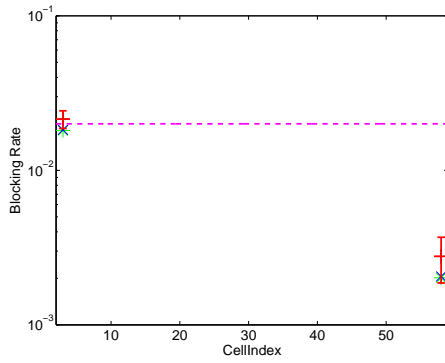


(a) Traffic scaling factor 0.9

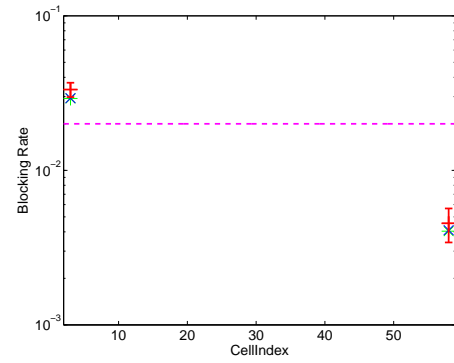


(b) Traffic scaling factor 1.0

Figure B.8: The Hague: 19 cells, cs services, DL

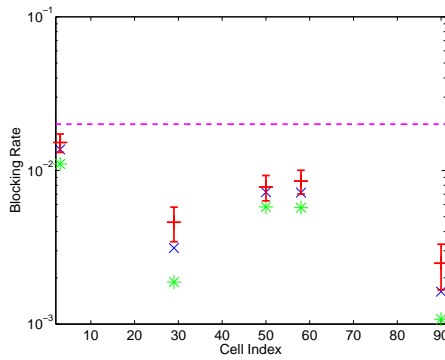


(a) Traffic scaling factor 1.8

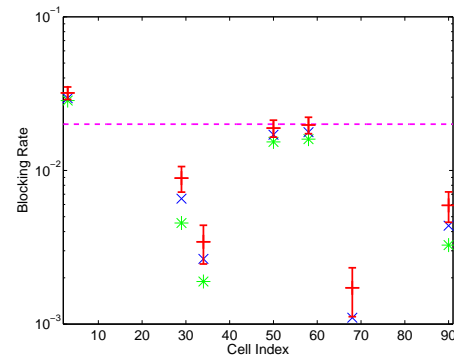


(b) Traffic scaling factor 1.85

Figure B.9: Berlin, network 1: 122 cells, speech telephony, UL

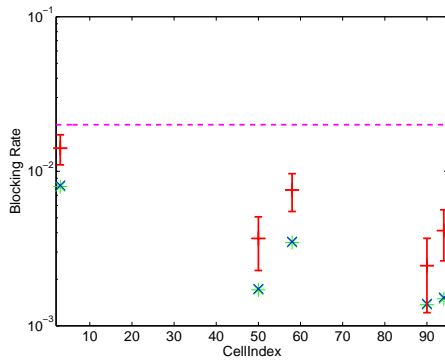


(a) Traffic scaling factor 3.3

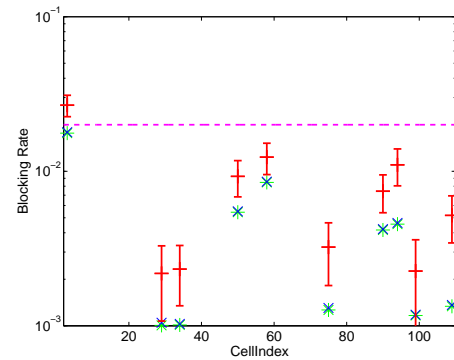


(b) Traffic scaling factor 3.4

Figure B.10: Berlin, network 1: 122 cells speech telephony, DL

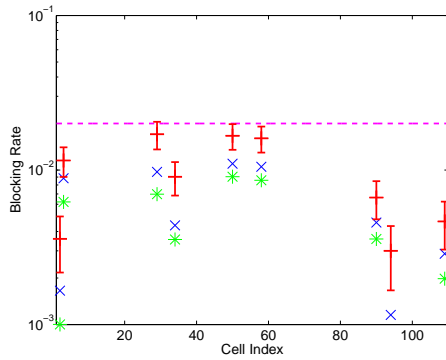


(a) Traffic scaling factor 2.2

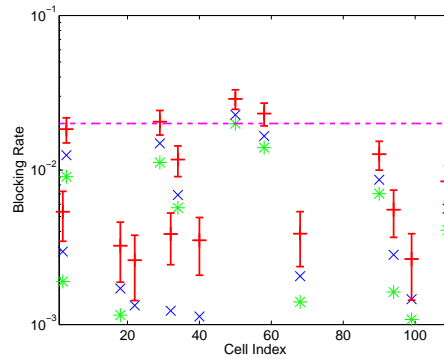


(b) Traffic scaling factor 2.4

Figure B.11: Berlin, network 1: 122 cells, video telephony, UL

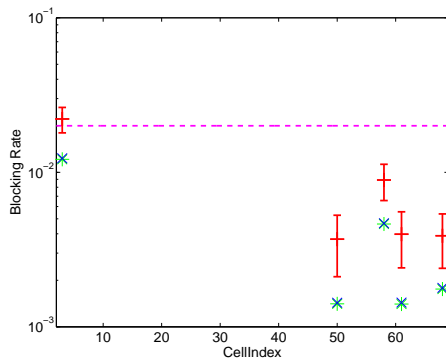


(a) Traffic scaling factor 3.7

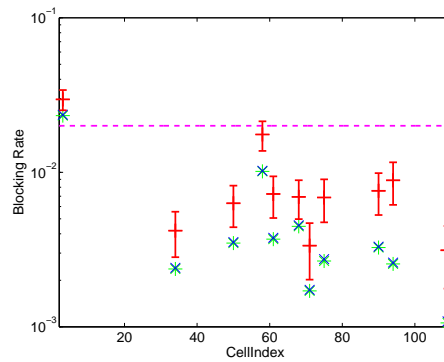


(b) Traffic scaling factor 3.9

Figure B.12: Berlin, network 1: 122 cells, video telephony, DL

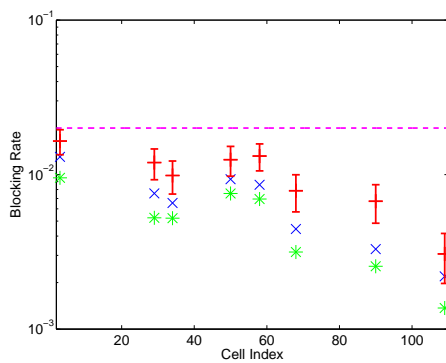


(a) Traffic scaling factor 1100

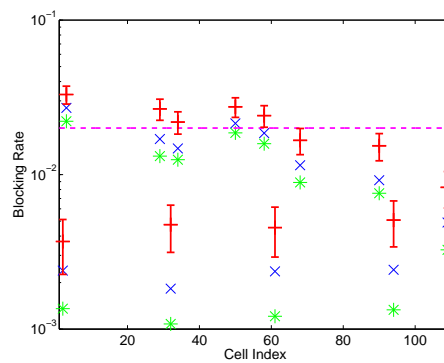


(b) Traffic scaling factor 1200

Figure B.13: Berlin, network 1: 122 cells, e-mail, UL



(a) Traffic scaling factor 750



(b) Traffic scaling factor 800

Figure B.14: Berlin, network 1: 122 cells, e-mail, DL

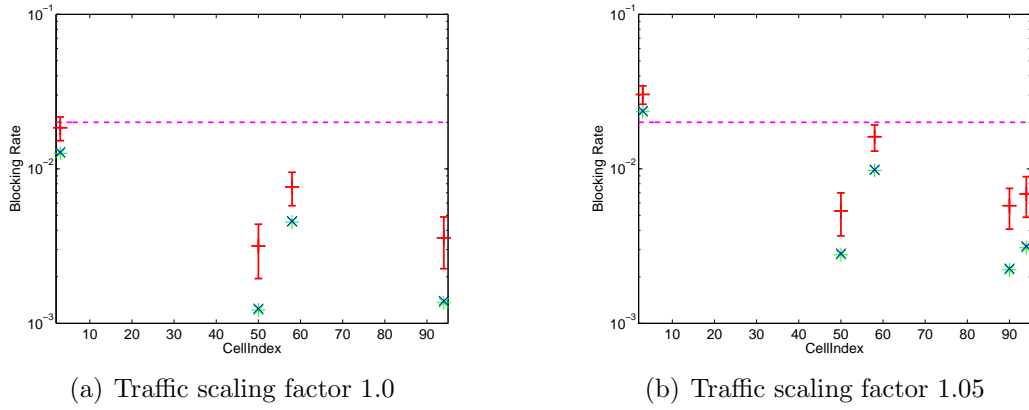


Figure B.15: Berlin, network 1: 122 cells, cs services, UL

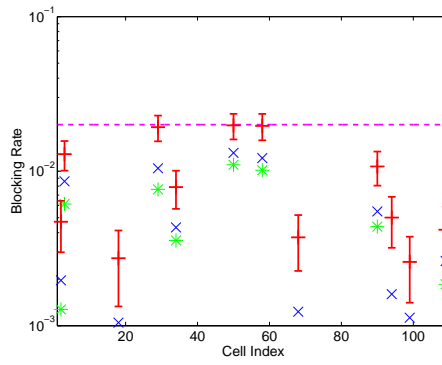


Figure B.16: Berlin, network 1: 122 cells, cs services, 0.56, DL

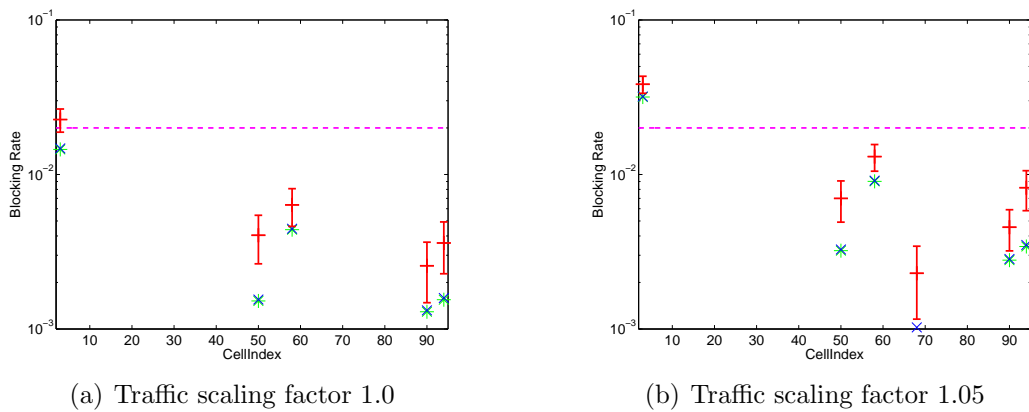
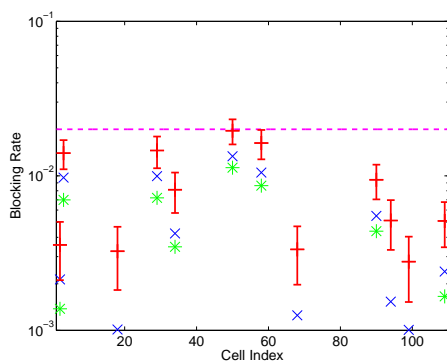
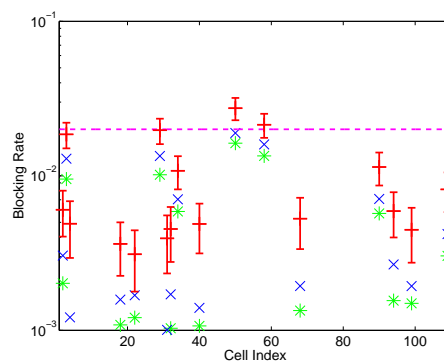


Figure B.17: Berlin, network 1: 122 cells, service mix, UL



(a) Traffic scaling factor 0.52



(b) Traffic scaling factor 0.54

Figure B.18: Berlin, network 1: 122 cells, service mix, DL

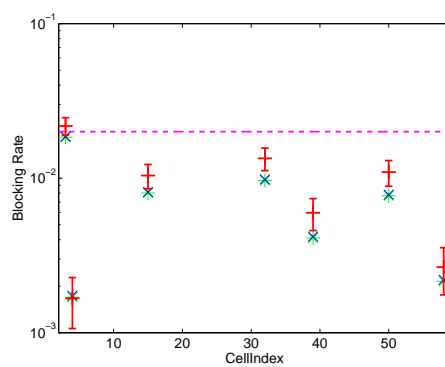
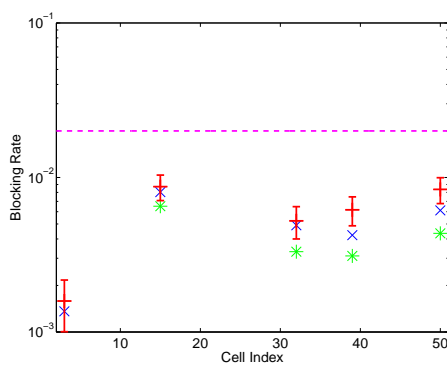
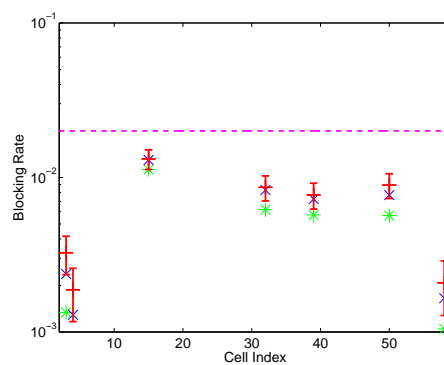


Figure B.19: Berlin, network 2: 122 cells, speech telephony, 1.8, UL



(a) Traffic scaling factor 3.0



(b) Traffic scaling factor 3.05

Figure B.20: Berlin, network 2: 122 cells, speech telephony, DL

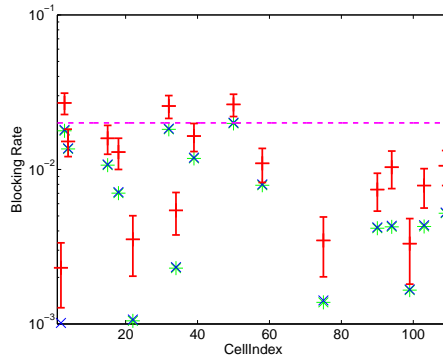
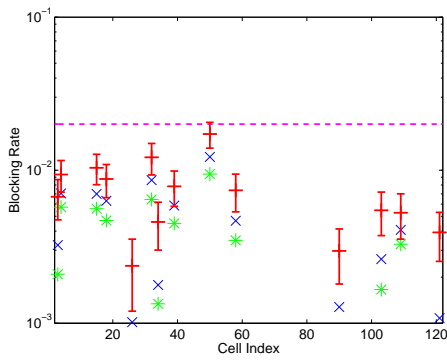
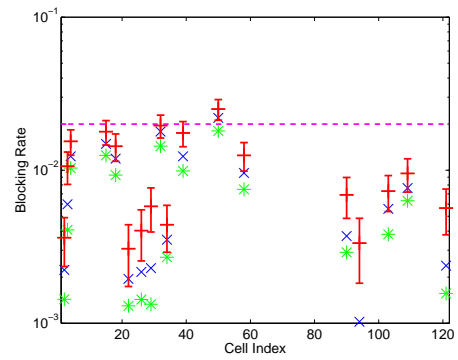


Figure B.21: Berlin, network 2: 122 cells, video telephony, 2.4, UL



(a) Traffic scaling factor 3.4



(b) Traffic scaling factor 3.6

Figure B.22: Berlin, network 2: 122 cells, video telephony, DL

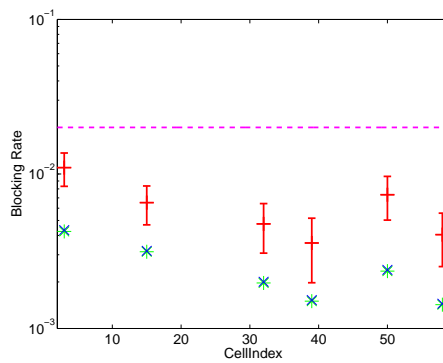
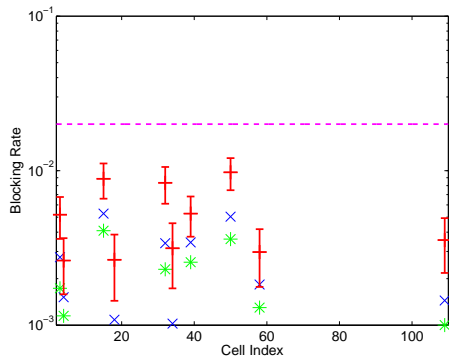
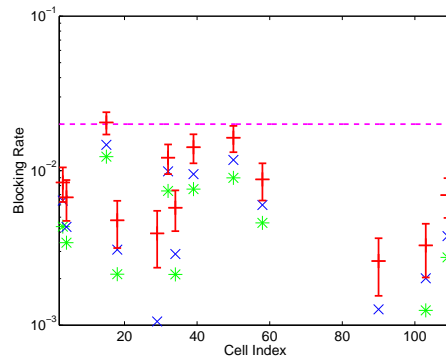


Figure B.23: Berlin, network 2: 122 cells, e-mail, 1000, UL

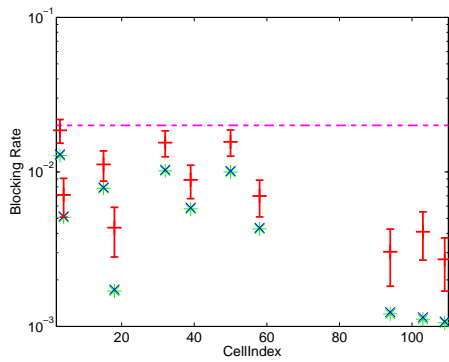


(a) Traffic scaling factor 650

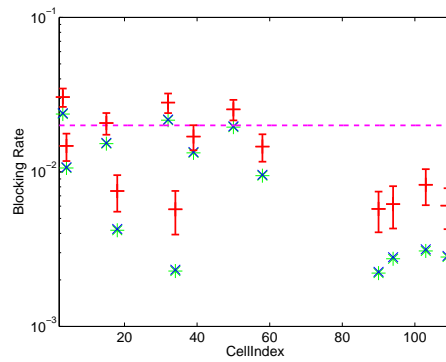


(b) Traffic scaling factor 700

Figure B.24: Berlin, network 2: 122 cells, e-mail, DL

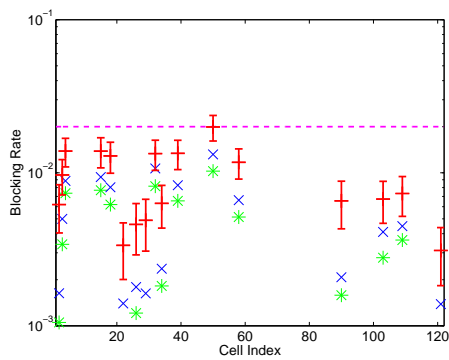


(a) Traffic scaling factor 1.0

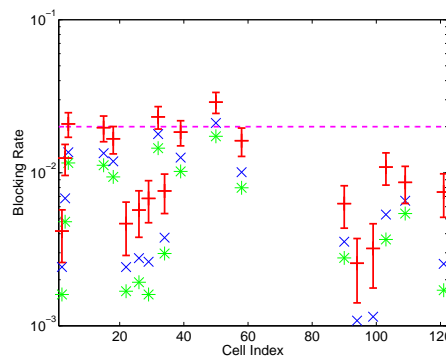


(b) Traffic scaling factor 1.05

Figure B.25: Berlin, network 2: 122 cells, cs services, UL



(a) Traffic scaling factor 0.52



(b) Traffic scaling factor 0.54

Figure B.26: Berlin, network 2: 122 cells, cs services, DL

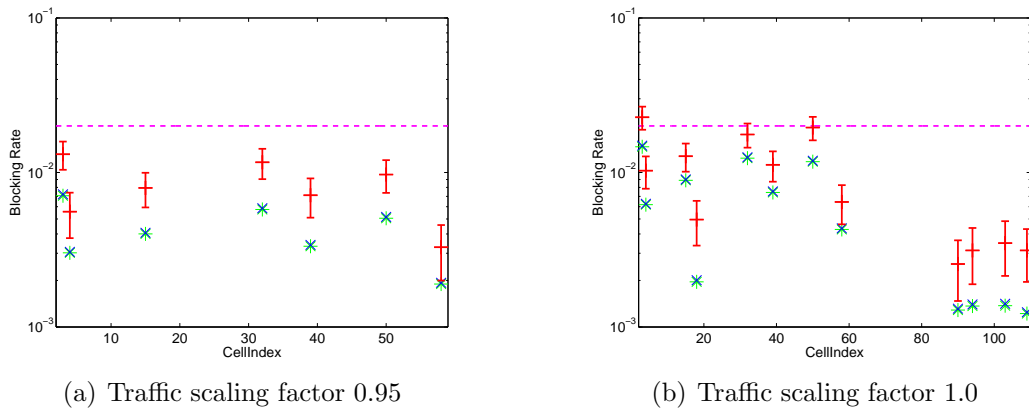


Figure B.27: Berlin, network 2: 122 cells, service mix, UL

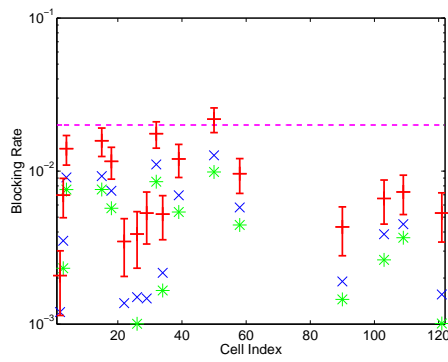


Figure B.28: Berlin, network 2: 122 cells, service mix, 0.48, DL

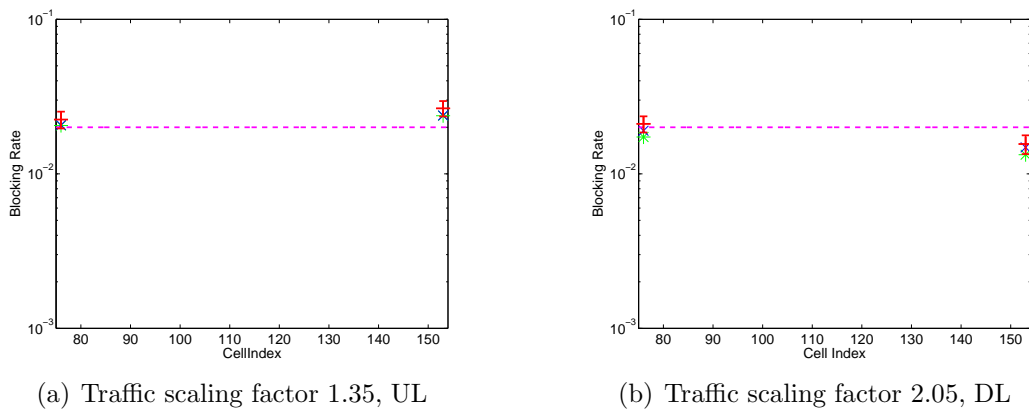
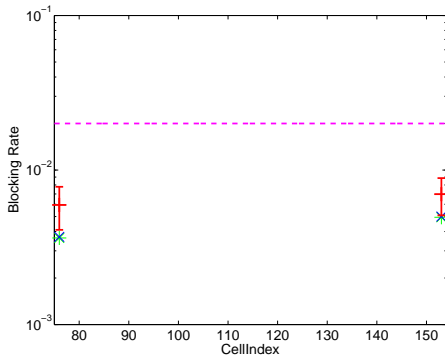
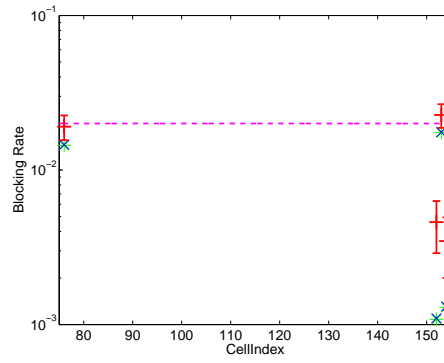


Figure B.29: Lisbon: 164 cells, speech telephony

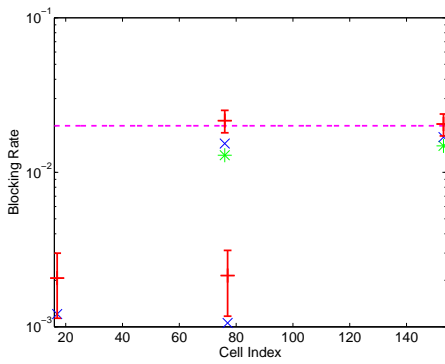


(a) Traffic scaling factor 750

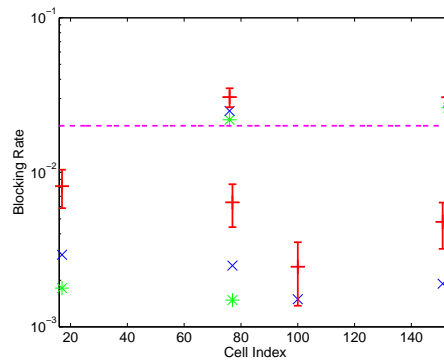


(b) Traffic scaling factor 850

Figure B.30: Lisbon: 164 cells, e-mail, UL

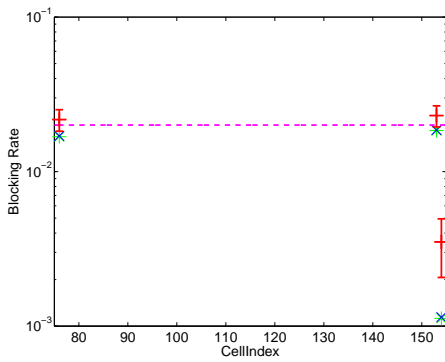


(a) Traffic scaling factor 475

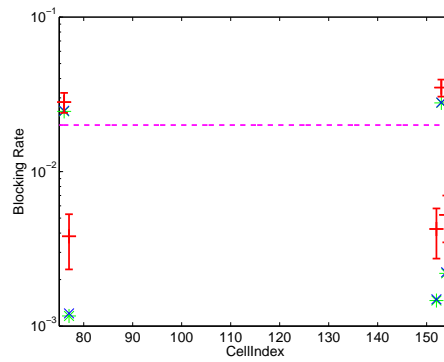


(b) Traffic scaling factor 500

Figure B.31: Lisbon: 164 cells, e-mail, DL

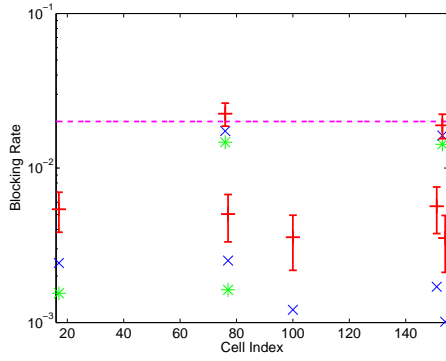


(a) Traffic scaling factor 0.72

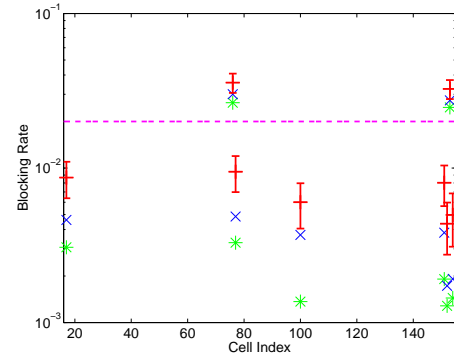


(b) Traffic scaling factor 0.74

Figure B.32: Lisbon: 164 cells, cs services, UL

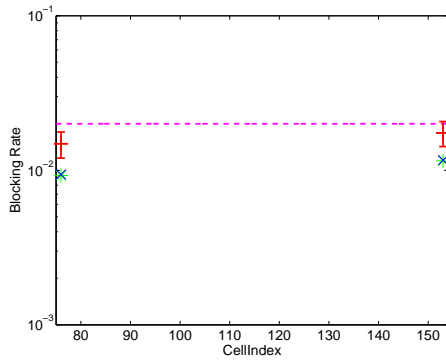


(a) Traffic scaling factor 0.34

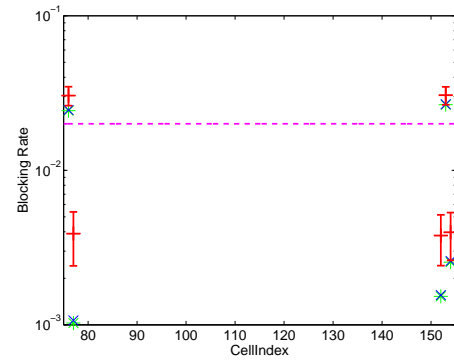


(b) Traffic scaling factor 0.36

Figure B.33: Lisbon: 164 cells, cs services, DL

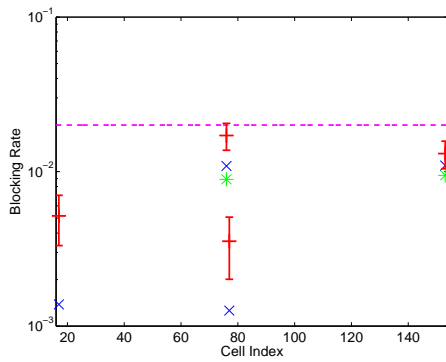


(a) Traffic scaling factor 0.68

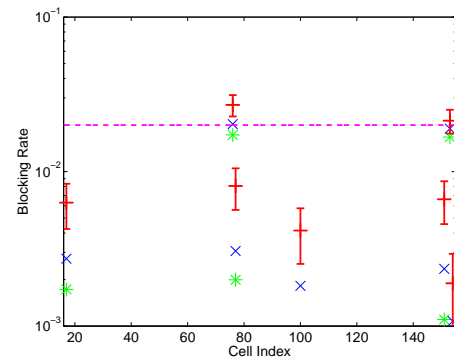


(b) Traffic scaling factor 0.74

Figure B.34: Lisbon: 164 cells, service mix, UL



(a) Traffic scaling factor 0.3



(b) Traffic scaling factor 0.32

Figure B.35: Lisbon: 164 cells, service mix, DL

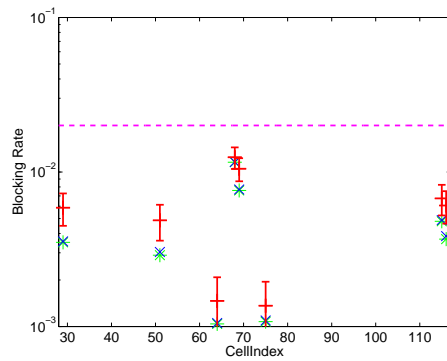
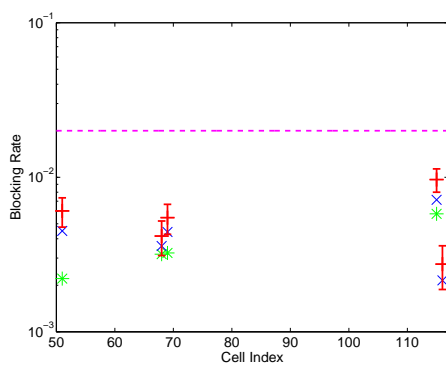
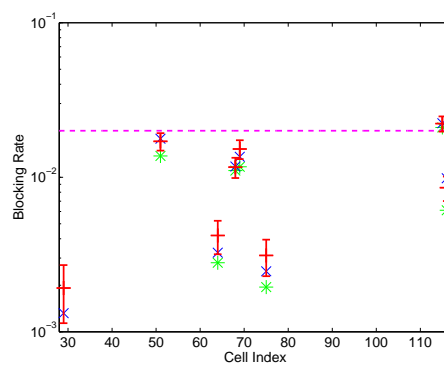


Figure B.36: Lisbon: 128 cells, speech telephony, 1.6, UL

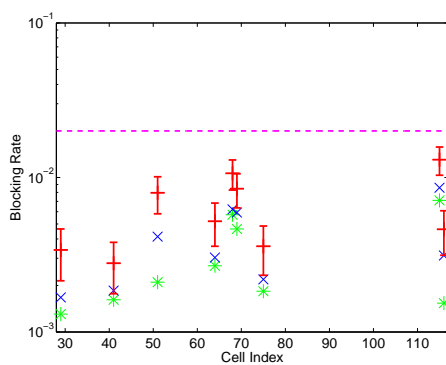


(a) Traffic scaling factor 2.5

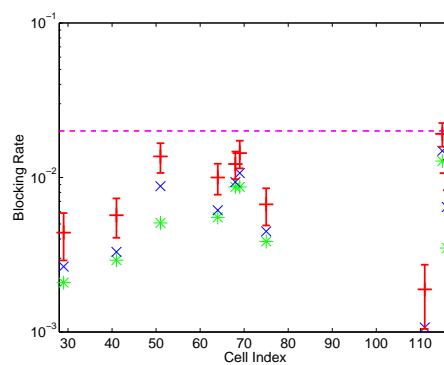


(b) Traffic scaling factor 2.6

Figure B.37: Lisbon: 128 cells, speech telephony, DL

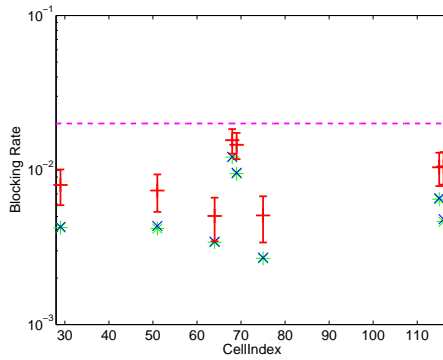


(a) Traffic scaling factor 575

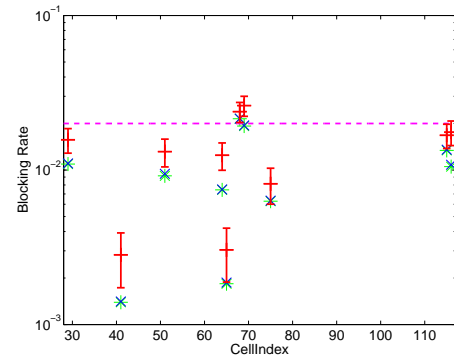


(b) Traffic scaling factor 600

Figure B.38: Lisbon: 128 cells, e-mail, DL

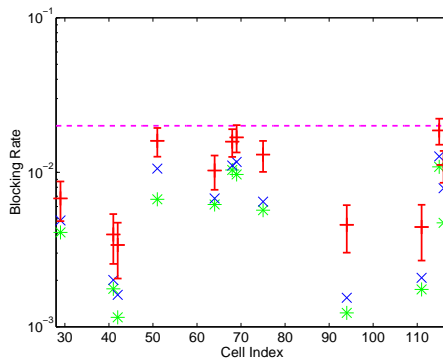


(a) Traffic scaling factor 0.85

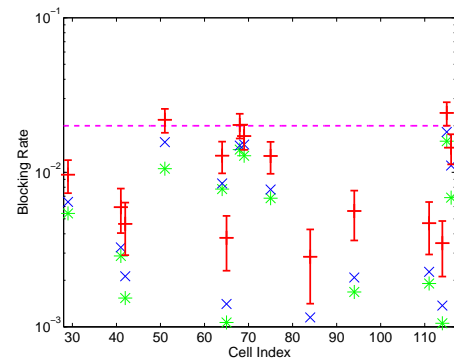


(b) Traffic scaling factor 0.9

Figure B.39: Lisbon: 128 cells, cs services, UL

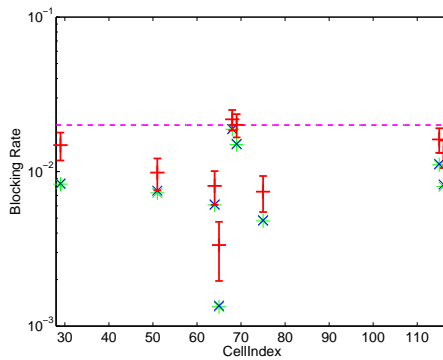


(a) Traffic scaling factor 0.42

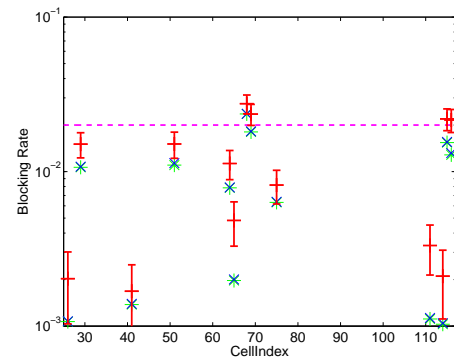


(b) Traffic scaling factor 0.43

Figure B.40: Lisbon: 128 cells, cs services, DL

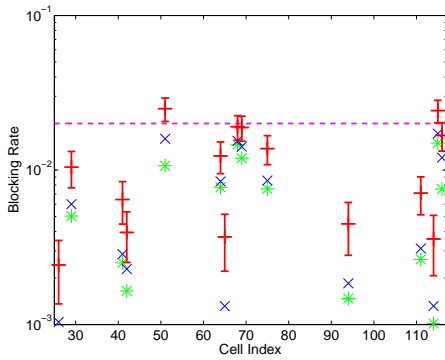


(a) Traffic scaling factor 0.88

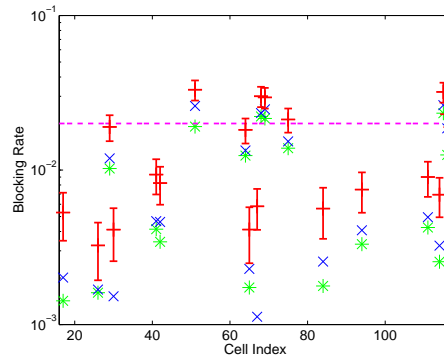


(b) Traffic scaling factor 0.9

Figure B.41: Lisbon: 128 cells, service mix, UL

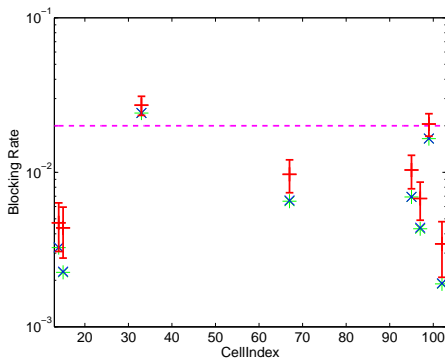


(a) Traffic scaling factor 0.4

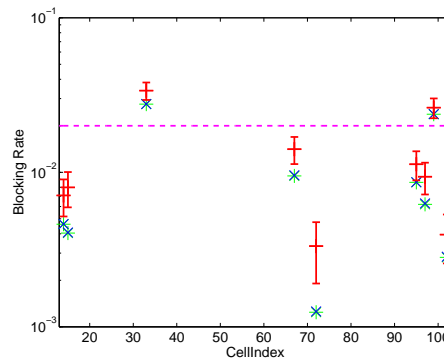


(b) Traffic scaling factor 0.42

Figure B.42: Lisbon: 128 cells, service mix, DL

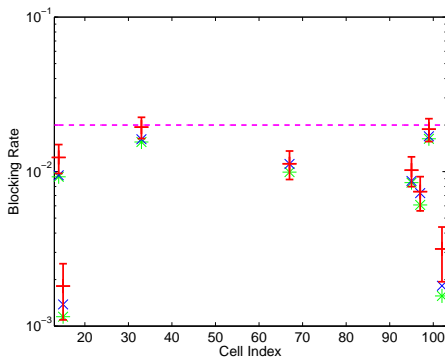


(a) Traffic scaling factor 3.2

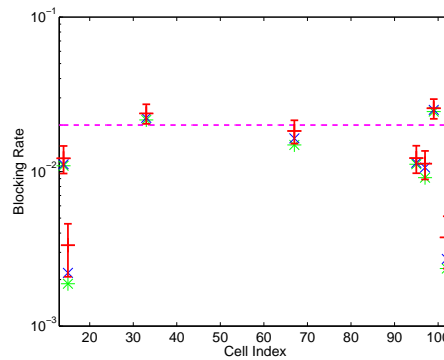


(b) Traffic scaling factor 3.3

Figure B.43: Turin: 103 cells, service mix, UL



(a) Traffic scaling factor 4.4



(b) Traffic scaling factor 4.5

Figure B.44: Turin: 103 cells, service mix, DL

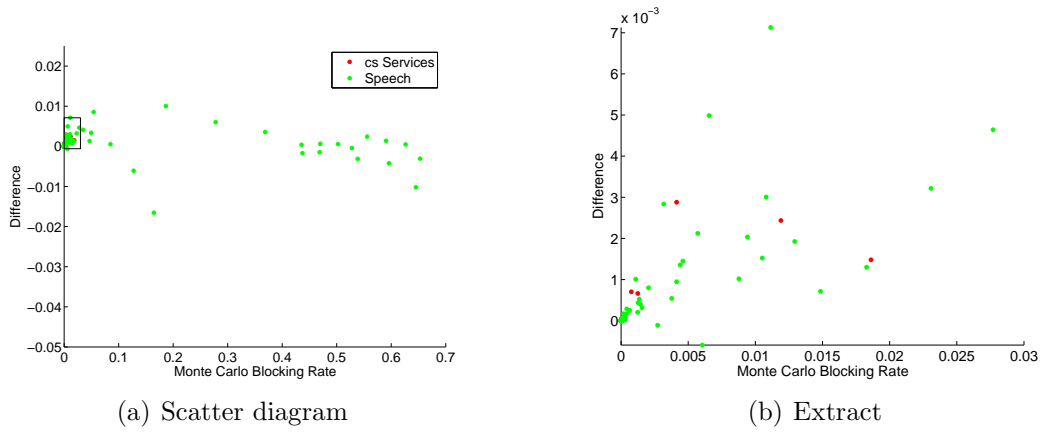


Figure B.45: The Hague: 36 cells, scatter diagram, UL

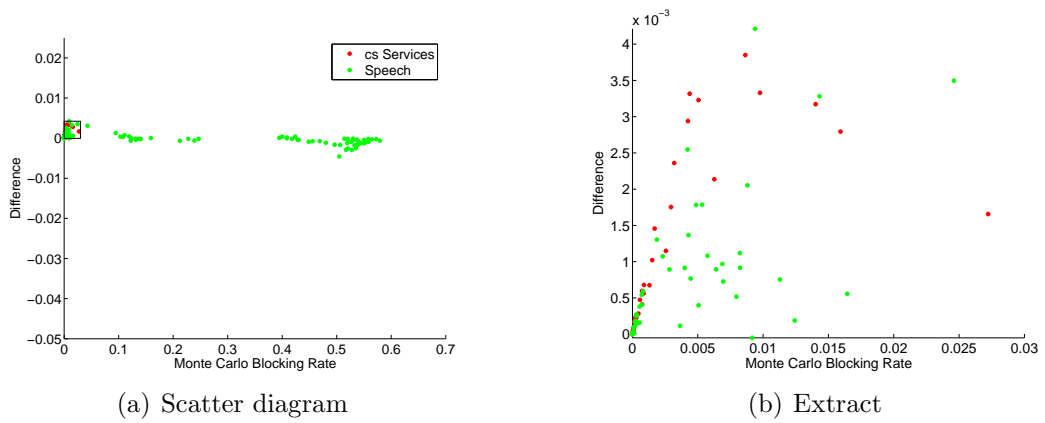


Figure B.46: The Hague: 19 cells, scatter diagram, UL

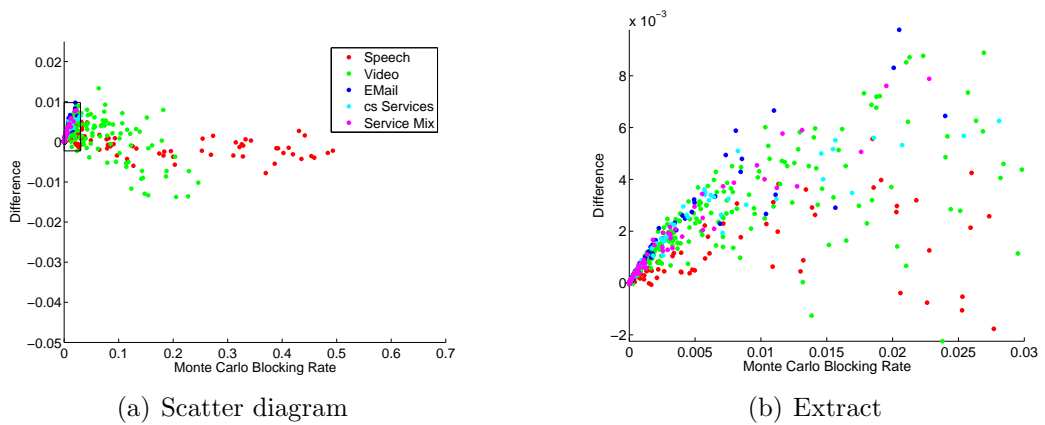


Figure B.47: Berlin, network 2: 122 cells, scatter diagram, UL

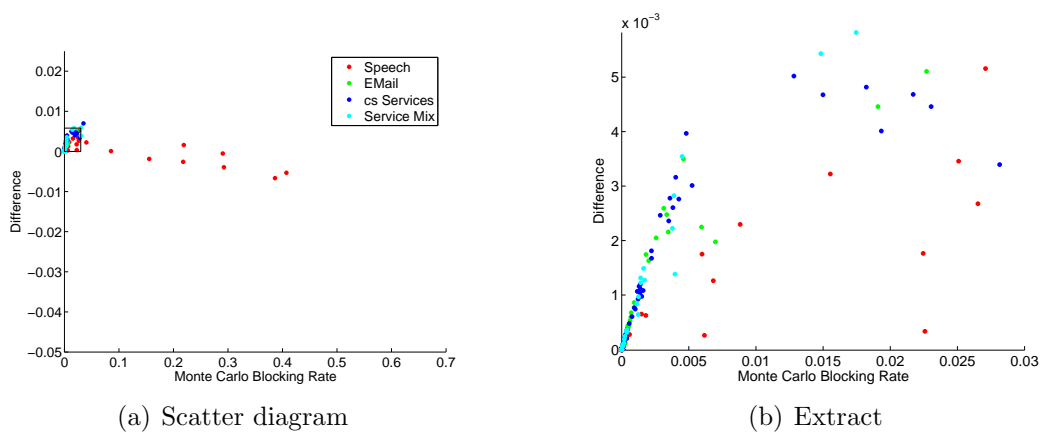


Figure B.48: Lisbon: 164 cells, scatter diagram, UL

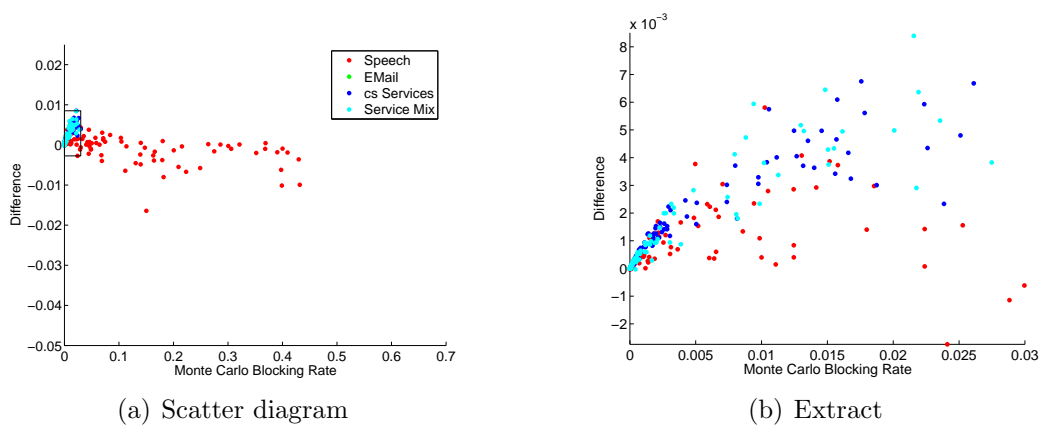


Figure B.49: Lisbon: 128 cells, scatter diagram, UL

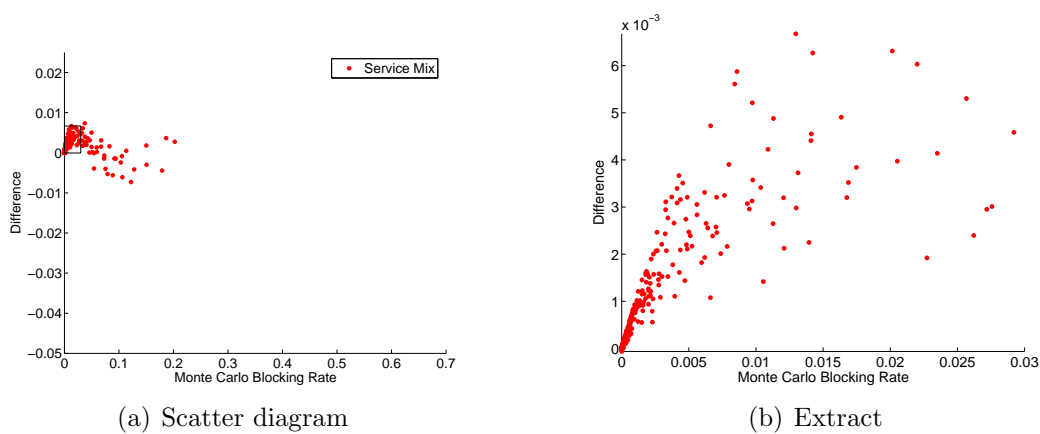


Figure B.50: Turin: 103 cells, scatter diagram, UL

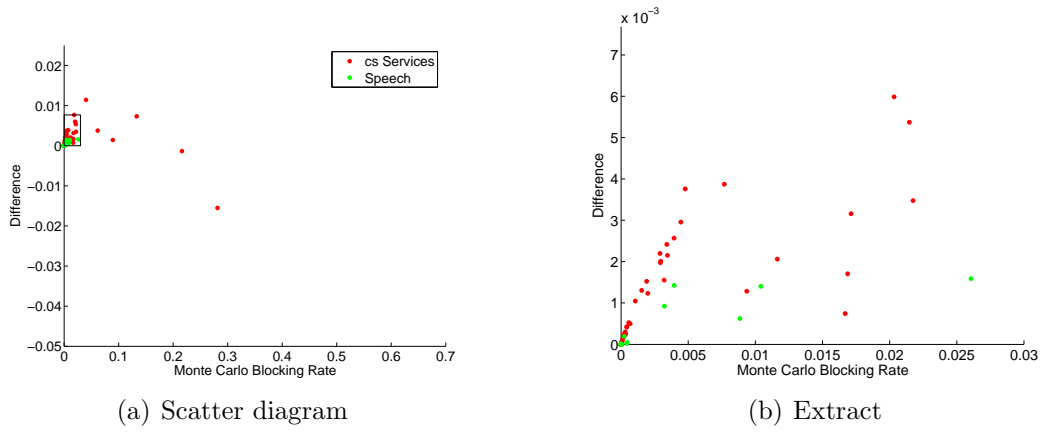


Figure B.51: The Hague: 36 cells, scatter diagram, DL

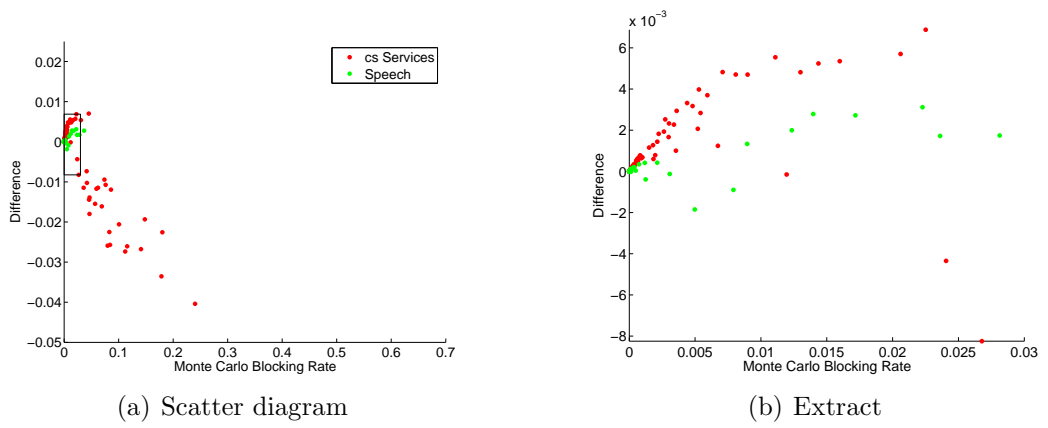


Figure B.52: The Hague: 19 cells, scatter diagram, DL

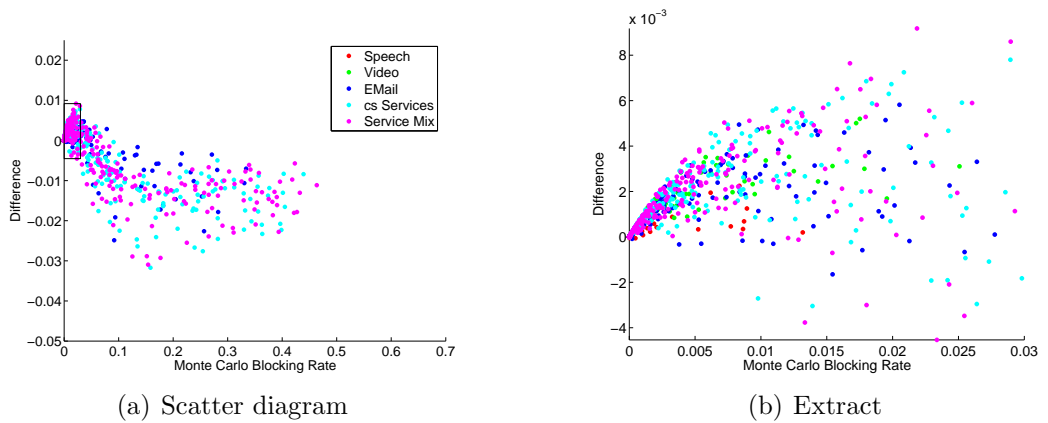
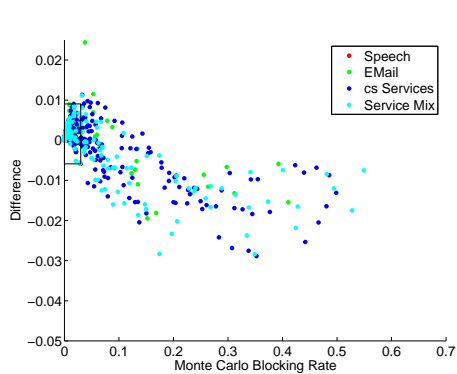
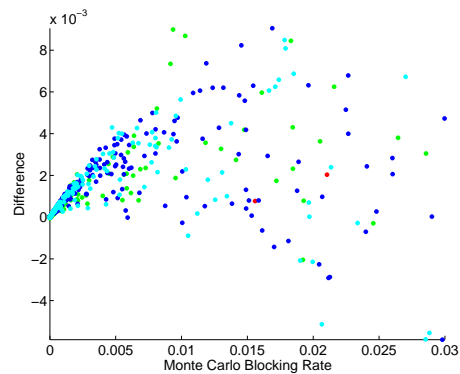


Figure B.53: Berlin, network 2: 122 cells, scatter diagram, DL

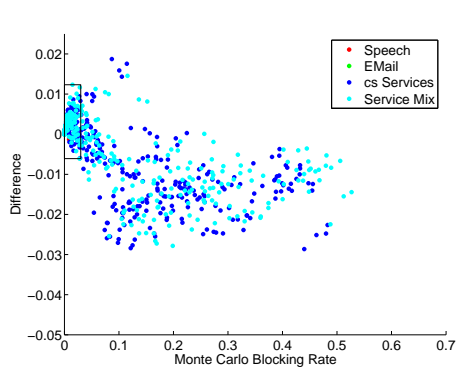


(a) Scatter diagram

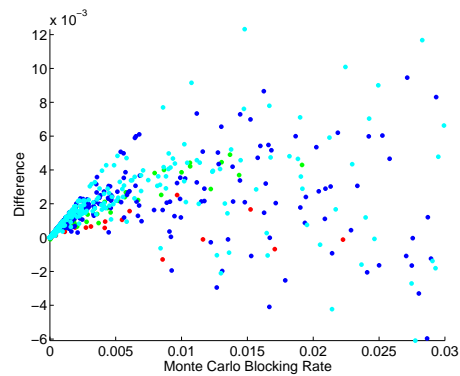


(b) Extract

Figure B.54: Lisbon: 164 cells, scatter diagram, DL

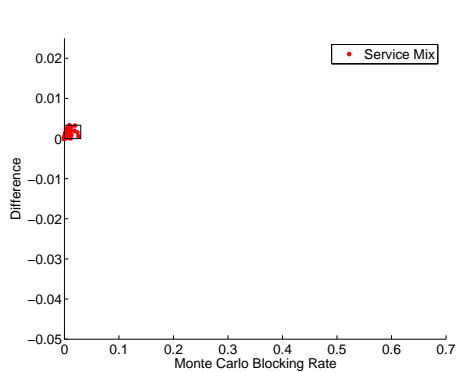


(a) Scatter diagram

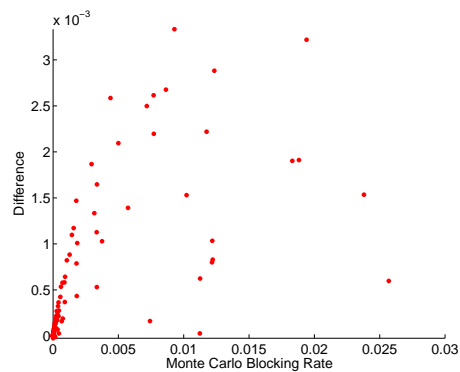


(b) Extract

Figure B.55: Lisbon: 128 cells, scatter diagram, DL



(a) Scatter diagram



(b) Extract

Figure B.56: Turin: 103 cells, scatter diagram, DL



# C Zusammenfassung

Das Ziel der vorliegenden Arbeit ist es, ein mathematisches Modell zu entwickeln, das die Blockier Raten der Zellen in einem UMTS Funknetz effizient approximiert. Die Blockier Rate bezeichnet den Anteil an Teilnehmern, der aufgrund der beschränkten Funkressourcen einer Antenne nicht bedient werden kann. Sie stellt ein wichtiges Kriterium für die Qualitätsbewertung eines Funknetzdesigns dar. Jedoch ist bisher kein Modell bekannt, das die durchschnittliche Blockier Rate schnell und verlässlich vorhersagen kann. Die Schwierigkeit dabei besteht darin, dass die Kapazität einer UMTS Funkzelle schwankt.

In dieser Arbeit werden zwei Ansätze vorgestellt, um die Blockier Raten in UMTS Funknetzen zu approximieren. Diese Methoden basieren auf einem bereits vorhandenen Modell. In der ersten Methode werden dessen Ungenauigkeiten reduziert, indem der Erwartungswert der durchschnittlichen Blockier Rate in Abhängigkeit von der Interferenz aus der eigenen Zelle berechnet wird. In der zweiten Methode wird das vorliegende Problem als eine Art gebrochenes *Rucksack Problem* aufgefasst. Wir betrachten dabei die Verteilung des Gesamtgewichts aller Nutzer in einer Funkzelle. Abhängig von diesem akkumulierten Gewicht bestimmen wir den Erwartungswert der durchschnittlichen Blockier Rate. In beiden Ansätzen wird die Interferenz aus anderen Funkzellen durch Durchschnittswerte abgeschätzt. Diese Schätzungen werden mit zusätzlichem Aufwand präzisiert. Außerdem leiten wir analytisch her, dass die Ergebnisse beider Modelle gleich sind.

Umfangreiche Tests belegen, dass wir mit den entwickelten Methoden einen sehr guten Kompromiss zwischen Genauigkeit und Komplexität gefunden haben. Die Eigenschaften des Basismodells sind in Grundzügen noch vorhanden. D. h., in niedrigen Bereichen wird die Blockier Rate etwas unterschätzt und in höheren leicht überschätzt. Doch im Gegensatz zu vorher liegen diese systematischen Schätzfehler in einem durchaus akzeptablen Bereich. Die Komplexität der beiden vorgestellten Ansätze ist gleich. Im Gegensatz zu existierenden Methoden mit vergleichbarer Genauigkeit sind die durchschnittlichen Laufzeiten extrem kurz.



# List of Figures

2.1	Block diagram of a communications system . . . . .	6
2.2	Cells in a UMTS radio network . . . . .	7
2.3	Operating mode of Code Division Multiplex . . . . .	9
2.4	Wideband spreading . . . . .	10
2.5	Interference attenuation in CDMA . . . . .	11
2.6	Average traffic distribution for one service . . . . .	17
3.1	Power and blocking rate in downlink for an isolated cell . . . . .	29
4.1	Distribution of the random variable for service speech telephony . . . . .	54
4.2	Distribution of the random variable for a service mix . . . . .	54
7.1	Synth.: one cell, speech telephony . . . . .	72
7.2	Synth.: one cell, cs services . . . . .	72
7.3	Synth.: one cell, service mix . . . . .	72
7.4	Synth.: two cells, speech telephony, uplink . . . . .	74
7.5	Synth.: two cells, speech telephony, downlink . . . . .	74
7.6	Synth.: two cells, cs services, uplink . . . . .	74
7.7	Synth.: two cells, cs services, downlink . . . . .	75
7.8	Synth.: two cells, service mix, uplink . . . . .	75
7.9	Synth.: two cells, service mix, downlink . . . . .	75
7.10	Examples for speech telephony, uplink . . . . .	77
7.11	Berlin, network 2: 122 cells, uplink . . . . .	77
7.12	Berlin: 122 cells, different service mixes, downlink . . . . .	78
7.13	Berlin, network 1: 122 cells, scatter diagram, uplink . . . . .	79
7.14	Berlin, network 1: 122 cells, scatter diagram, downlink . . . . .	79
7.15	Examples for overestimation, downlink . . . . .	80
B.1	Legend for all following figures . . . . .	91
B.2	The Hague: 36 cells, speech telephony, UL . . . . .	91
B.3	The Hague: 36 cells, speech telephony, DL . . . . .	92
B.4	The Hague: 36 cells, cs services . . . . .	92

B.5	The Hague: 19 cells, speech telephony, UL . . . . .	92
B.6	The Hague: 19 cells, speech telephony, traffic scaling 5.8, DL . . . . .	93
B.7	The Hague: 19 cells, cs services, UL . . . . .	93
B.8	The Hague: 19 cells, cs services, DL . . . . .	93
B.9	Berlin, network 1: 122 cells, speech telephony, UL . . . . .	94
B.10	Berlin, network 1: 122 cells speech telephony, DL . . . . .	94
B.11	Berlin, network 1: 122 cells, video telephony, UL . . . . .	94
B.12	Berlin, network 1: 122 cells, video telephony, DL . . . . .	95
B.13	Berlin, network 1: 122 cells, e-mail, UL . . . . .	95
B.14	Berlin, network 1: 122 cells, e-mail, DL . . . . .	95
B.15	Berlin, network 1: 122 cells, cs services, UL . . . . .	96
B.16	Berlin, network 1: 122 cells, cs services, 0.56, DL . . . . .	96
B.17	Berlin, network 1: 122 cells, service mix, UL . . . . .	96
B.18	Berlin, network 1: 122 cells, service mix, DL . . . . .	97
B.19	Berlin, network 2: 122 cells, speech telephony, 1.8, UL . . . . .	97
B.20	Berlin, network 2: 122 cells, speech telephony, DL . . . . .	97
B.21	Berlin, network 2: 122 cells, video telephony, 2.4, UL . . . . .	98
B.22	Berlin, network 2: 122 cells, video telephony, DL . . . . .	98
B.23	Berlin, network 2: 122 cells, e-mail, 1000, UL . . . . .	98
B.24	Berlin, network 2: 122 cells, e-mail, DL . . . . .	99
B.25	Berlin, network 2: 122 cells, cs services, UL . . . . .	99
B.26	Berlin, network 2: 122 cells, cs services, DL . . . . .	99
B.27	Berlin, network 2: 122 cells, service mix, UL . . . . .	100
B.28	Berlin, network 2: 122 cells, service mix, 0.48, DL . . . . .	100
B.29	Lisbon: 164 cells, speech telephony . . . . .	100
B.30	Lisbon: 164 cells, e-mail, UL . . . . .	101
B.31	Lisbon: 164 cells, e-mail, DL . . . . .	101
B.32	Lisbon: 164 cells, cs services, UL . . . . .	101
B.33	Lisbon: 164 cells, cs services, DL . . . . .	102
B.34	Lisbon: 164 cells, service mix, UL . . . . .	102
B.35	Lisbon: 164 cells, service mix, DL . . . . .	102
B.36	Lisbon: 128 cells, speech telephony, 1.6, UL . . . . .	103
B.37	Lisbon: 128 cells, speech telephony, DL . . . . .	103
B.38	Lisbon: 128 cells, e-mail, DL . . . . .	103
B.39	Lisbon: 128 cells, cs services, UL . . . . .	104
B.40	Lisbon: 128 cells, cs services, DL . . . . .	104
B.41	Lisbon: 128 cells, service mix, UL . . . . .	104
B.42	Lisbon: 128 cells, service mix, DL . . . . .	105
B.43	Turin: 103 cells, service mix, UL . . . . .	105
B.44	Turin: 103 cells, service mix, DL . . . . .	105
B.45	The Hague: 36 cells, scatter diagram, UL . . . . .	106

---

B.46 The Hague: 19 cells, scatter diagram, UL . . . . .	106
B.47 Berlin, network 2: 122 cells, scatter diagram, UL . . . . .	106
B.48 Lisbon: 164 cells, scatter diagram, UL . . . . .	107
B.49 Lisbon: 128 cells, scatter diagram, UL . . . . .	107
B.50 Turin: 103 cells, scatter diagram, UL . . . . .	107
B.51 The Hague: 36 cells, scatter diagram, DL . . . . .	108
B.52 The Hague: 19 cells, scatter diagram, DL . . . . .	108
B.53 Berlin, network 2: 122 cells, scatter diagram, DL . . . . .	108
B.54 Lisbon: 164 cells, scatter diagram, DL . . . . .	109
B.55 Lisbon: 128 cells, scatter diagram, DL . . . . .	109
B.56 Turin: 103 cells, scatter diagram, DL . . . . .	109



# Bibliography

- [1] C. Balzanelli, A. Munna, and R. Verdone. WCDMA downlink capacity: part 1. In *Proc. of IEEE PIMRC'2003*, Beijing, China, Sept. 2003.
- [2] T. Benkner and C. Stepping. *UMTS: Universal Mobile Telecommunications System*. J. Schlembach Fachverlag, Weil der Stadt, 2002.
- [3] J. Davidson. *Stochastic Limit Theory*. Oxford University Press, 1994.
- [4] B. De Schutter and B. De Moor. The extended linear complementarity problem. *Math. Programming*, 71(3):289–325, Dec. 1995.
- [5] M. Duque-Antón. *Mobilfunknetze: Grundlagen, Dienste und Protokolle*. Vieweg Verlag, Braunschweig/Wiesbaden, 1st edition, May 2002.
- [6] A. Eisenblätter, H.-F. Geerdes, T. Koch, A. Martin, and R. Wessälly. UMTS radio network evaluation and optimization beyond snapshots. *Math. Meth. Oper. Res.*, 63(1), 2006.
- [7] A. Eisenblätter, H.-F. Geerdes, and N. Rochau. Analytical approximate load control in W-CDMA radio networks. In *Proceedings of VTC-2005 Fall*, Dallas, TX, Sept. 2005. IEEE.
- [8] A. Eisenblätter, H.-F. Geerdes, and U. Türke. Public UMTS radio network evaluation and planning scenarios. *Internat. J. on Mobile Network Design and Innovation*, 2005.
- [9] J. Elstrodt. *Maß- und Integrationstheorie*. Springer-Verlag, 2nd edition, 1999.
- [10] G. S. Fishman. *Monte Carlo: Concepts, Algorithms and Applications*. Springer Series in Operations Research. Springer Verlag, New York, USA, 1996.
- [11] H.-O. Georgii. *Stochastik: Einführung in die Wahrscheinlichkeitstheorie und Statistik*. de Gruyter, Berlin, Germany, 2nd edition, 2004.

- 
- [12] S. Haykin and M. Moher. *Modern Wireless Communications*. Pearson Education, Inc., 2005.
- [13] H. Holma and A. Toskala, editors. *WCDMA for UMTS*. John Wiley & Sons, Ltd., revised edition, 2001.
- [14] K.-D. Kammeyer. *Nachrichtenübertragung*. B.G. Teubner Verlag, 3rd edition, 2004.
- [15] U. Krengel. *Einführung in die Wahrscheinlichkeitstheorie und Statistik*. vieweg studium – Aufbaukurs Mathematik. Vieweg Verlag, Braunschweig/Wiesbaden, 6th edition, Feb. 2002.
- [16] J. Laiho, A. Wacker, and T. Novosad, editors. *Radio Network Planning and Optimisation for UMTS*. John Wiley & Sons, Ltd, 2002.
- [17] N. Madras. *Lectures on Monte Carlo Methods*. American Mathematical Society, Providence, Rhode Island, 2002.
- [18] MOMENTUM Project, IST-2000-28088. MOMENTUM public UMTS planning scenarios. Available online at <http://momentum.zib.de/data.php>, 2003.
- [19] COST 273: Mobile Radio Access Network Reference Scenarios (MORANS). <http://www.cost273.org/morans/>, 2004.
- [20] P. E. Pfeiffer and D. A. Schum. *Introduction to Applied Probability*. Academic Press, New York, 1973.
- [21] U. Türke, T. Winter, R. Perera, E. Lamers, E. Meijerink, E. R. Flederus, and A. Serrador. Comparison of different simulation approaches for cell performance evaluation. Technical Report D2.2, IST-2000-28088 MOMENTUM, 2002.
- [22] B. Walke. *Mobilfunknetze und ihre Protokolle*, volume 1. B. G. Teubner Verlag, Stuttgart, 1998.
- [23] B. Walke, M. P. Althoff, and P. Seidenberg. *UMTS–Ein Kurs*. J. Schlembach Fachverlag, Weil der Stadt, 2nd edition, 2002.
- [24] Wikipedia. Universal Mobile Telecommunications System – Wikipedia, Die freie Enzyklopädie. <http://de.wikipedia.org/wiki/UMTS>, 2005. [Online; accessed 09.11.2005].